AFGWC TECHNICAL MEMORANDUM 78-002

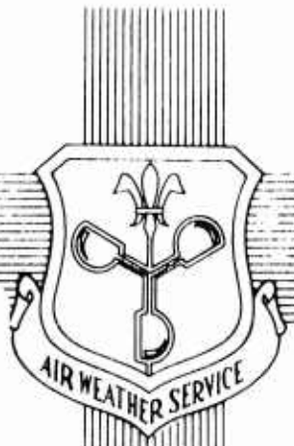

LEVEL

9

THE AFGWC AUTOMATED CLOUD ANALYSIS MODEL

Falko K. Fye, Major, USAF

HQ Air Force Global Weather Central
Offutt AFB, Nebraska 68113

Approved for public release;
Distribution Unlimited

HQ Air Force Global Weather Central
Offutt AFB, Nebraska 68113

June 1978

This report approved for public release. There is no objection to unlimited distribution of this report to the public at large, or by DDC to the National Technical Information Service (NTIS).

This technical report has been reviewed and is approved for publication.

FOR THE COMMANDER

ROBERT C. SABIN, Lt Col, USAF
Chief, Technical Services Division

UNCLASSIFIED

SECURITY CLASSIFICATION OF THIS PAGE *(When Data Entered)*

REPORT DOCUMENTATION PAGE

READ INSTRUCTIONS BEFORE COMPLETING FORM

1. REPORT NUMBER: AFGWC-TM-78-002	2. GOVT ACCESSION NO.
3. RECIPIENT'S CATALOG NUMBER: Technical Memo	
4. TITLE *(and Subtitle)*: The AFGWC Automated Cloud Analysis Model	5. TYPE OF REPORT & PERIOD COVERED
	6. PERFORMING ORG. REPORT NUMBER
7. AUTHOR(s): Falko K. Fye	8. CONTRACT OR GRANT NUMBER(s)
9. PERFORMING ORGANIZATION NAME AND ADDRESS: HQ Air Force Global Weather Central (MAC), Offutt AFB NE 68113	10. PROGRAM ELEMENT, PROJECT, TASK & WORK UNIT NUMBERS
11. CONTROLLING OFFICE NAME AND ADDRESS: HQ Air Force Global Weather Central (MAC), Offutt AFB NE 68113	12. REPORT DATE: June 1978
	13. NUMBER OF PAGES
14. MONITORING AGENCY NAME & ADDRESS *(if different from Controlling Office)*: (Same as Block 9)	15. SECURITY CLASS. *(of this report)*: Unclassified
	15a. DECLASSIFICATION/DOWNGRADING SCHEDULE

16. DISTRIBUTION STATEMENT *(of this Report)*

Approved for public release; distribution unlimited.

17. DISTRIBUTION STATEMENT *(of the abstract entered in Block 20, if different from Report)*

N/A

18. SUPPLEMENTARY NOTES

19. KEY WORDS *(Continue on reverse side if necessary and identify by block number)*

Automated Cloud Analysis
Electro-Optical Weapons System
Multi-Spectral Analysis
Nephanalysis
Objective Analysis
Remote Sensing
Satellite Data Processing
Weather Analysis

20. ABSTRACT *(Continue on reverse side if necessary and identify by block number)*

The Air Force Global Weather Central (AFGWC) automated cloud analysis program (3DNEPH) produces high resolution, three-dimensional analyses of clouds over the entire globe. Up to eight analyses are scheduled per day with additional limited area analyses available on request. Horizontal grid spacing is 25 nautical miles and the vertical grid consists of 15 layers of varying thickness from the earth's surface to 55,000 feet above mean sea level. The program is a string of individual modules which process and integrate meteorological cloud information from surface, pilot, and upper air reports. An additional

DD FORM 1 JAN 73 1473 EDITION OF 1 NOV 65 IS OBSOLETE

UNCLASSIFIED

SECURITY CLASSIFICATION OF THIS PAGE *(When Data Entered)*

403 677

(Block 20 Continued)

capability to interpret and incorporate visual and infrared satellite imagery results in high resolution, worldwide coverage. Many recent advances in the techniques and methodology for interpreting satellite imagery are described. A new manual data input processor, quality control procedures, and applications are also described. A large appendix provides detailed information on the high resolution terrain, geography, temperature, and background brightness (albedo) fields used to support the model. A history of the model is included for the benefit of archive data users and detailed descriptions of the satellite processing algorithms are also provided in the appendix. Numerous samples of displayed data using several display methods are included.

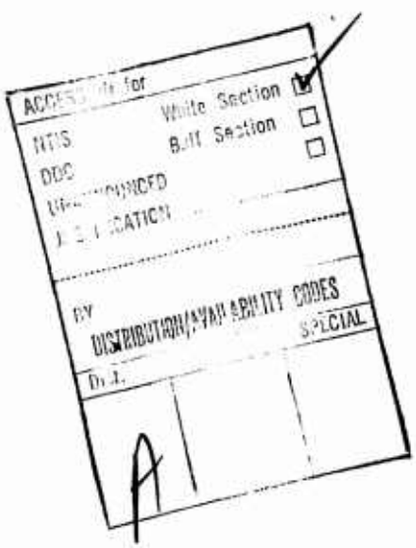

PREFACE

The task of writing a new Technical Memorandum (TM) for the 3DNEPH Program to replace AFGWC TM 71-2 was started on 12 November 1975. Because of its low priority, the project was, for the most part, in a deficit status.

With the transfer of the author from AFGWC to Air Command and Staff College, an opportunity to complete the new TM arose under the school's research program. The school approved the concept in October 1977.

The purpose of the new TM is to provide updated information on 3DNEPH and to document many new programs and concepts developed since AFGWC TM 71-2 was written in 1971. In addition, many auxiliary activities which have generated almost as much interest as the model itself are described for the first time. The new TM was submitted to the faculty of ACSC on 20 April 1978. The final typing for publication was done in May and June 1978 at AFGWC. It was written for the user of 3DNEPH data, the many frustrated programmers who must work with the program, and the meteorological community where 3DNEPH is a truly unique computer model.

The author is indebted to the many people who contributed to the successful completion of the project.

- The Air Command and Staff College, Air University,
  Maxwell AFB AL 36112
  Commandant: B/G Beck
  Chief, Research Division: Lt Col Staley

- Maj Bill Battista, ACSC/EDO-1, Research Advisor

- Capt Bill Klein, AFGWC/TS, for liaison and coordination with AFGWC

- AlC Reynolds Cushing, AFGWC/TS, for his assistance and work on the many graphics used in the TM

- The following reviewers for their advice and comments:

  Lt Col John Dierks, AFGWC/DO
  Lt Col Al Coburn, AFGWC/DO
  Maj Bill Irvine, AFGWC/TS
  Maj Ed Harriman, AFGWC/WS
  Capt Jeff Koenig, AFGWC/TS

- and to Mrs Mary Zimmerman, AFGWC/TS, for her expert typing of the final copy.

Maj Falko K. Fye
1 May 1978

CONTENTS

CONTENTS

CONTENTS

APPENDIX C

APPENDIX D

APPENDIX E

APPENDIX F

APPENDIX G

APPENDIX H

APPENDIX I

FIGURES

TABLES

THE AFGWC AUTOMATED CLOUD

ANALYSIS MODEL

1. INTRODUCTION

The AFGWC automated cloud analysis model has been operational since January, 1970. Known as 3DNEPH (Three-Dimensional Nephanalysis), this computer system was written to gain maximum use of the increasing quantity of meteorological cloud information. Satellite imagery is the heart of the 3DNEPH system and provides high density data over the entire world. The 3DNEPH has been the only known automated system capable of processing and interpreting the tremendous volume of satellite data, integrating these with conventional cloud information, and constructing a high quality, timely data base for multiple users. As a pioneering effort, the 3DNEPH has not had the benefit of experience from other automated cloud analysis models. The result over the past several years was a continuous record of modifications and improvements to support new mission goals and to improve the final product. This Technical Memorandum (TM) describes the 3DNEPH after several years of evolution and is intended for archive and research users as well as operational users.

2. GRID SYSTEM

2.1 Resolutions considerations. The 3DNEPH analysis data base is specified at a horizontal resolution of approximately 25 nautical miles (nm). Selection of this resolution was based on three factors.

(a) The first is the volume of output data which dictates a resolution only fine enough to satisfy operational requirements. Considering the worldwide scope, the resolution becomes critical in terms of the overall system cost.

(b) A second consideration is the accuracy of satellite rectification and mapping programs. While current satellite imagery systems have an optimum sampling resolution of approximately 1.5 nautical miles and an estimated mapping accuracy of 8 to 12 nm, a single sample will not reliably indicate cloud cover over a particular point on the earth. However, a set of samples over a larger area provides a reliable indication of cloud cover for the point.

(c) A third consideration is the 20 to 40 nm areal extent of a typical surface observation.

The 25 nm grid adequately satisfies these three conditions.

Factors bearing on the vertical resolution are system costs, infrared satellite data accuracy, the accuracy of ground based cloud height reports, the accuracy of temperature/moisture soundings, and operational requirements. A vertical grid (described later) with varied layer thickness as a function of height generally satisfies these conditions.

2.2 Horizontal grid. The 3DNEPH grid is a subset of the basic horizontal AFGWC 200 nm macroscale grid. This subset is one-eighth of this 200 nm grid resulting in an average grid spacing of approximately 25 nm. (The terms eighth-mesh and 25 nm gridpoint will be used interchangeably). The grid is based on a polar stereographic projection which is true at a latitude of 60 degrees. Actual grid spacing is variable due to the distortion of the projection. This latitudinal variation in grid spacing is given precisely by:

$$S = 13.780864(1 + \sin(\phi)) \qquad (1)$$

where S is the grid spacing in nautical miles and ϕ is the latitude in degrees. Grid spacing varies from 13.78 nm at the equator to 27.56 nm at the poles according to equation 1.

For each hemisphere, the eighth-mesh AFGWC grid consists of a 512 by 512 array centered at the respective pole and oriented on 80 degrees west longitude. Gridpoints beyond the edge (equator) of the polar stereographic projection are disregarded. The size of this grid array (262,144 total gridpoints) requires partitioning to facilitate automated processing. The 512 by 512 array is therefore divided into 64 equally sized areas called "3DNEPH boxes". Each box contains an array of 64 by 64 gridpoints and thus the grid is reduced to manageable sections. The 3DNEPH boxes are also the basis of special analyses over small areas or windows. Figures 1 and 2 illustrate the 3DNEPH grid system for the Northern and Southern Hemispheres, respectively.

2.3 Vertical grid. The vertical grid consists of 15 layers of varying thickness from the surface to 55,000 feet. These 15 layers are divided into two subsets:

(a) Six terrain-following layers are specified with respect to the local terrain height.
(b) The next nine (9) layers are specified with respect to Mean Sea Level (MSL).

Table 1 provides detailed information on the bases, tops, and thickness of the layers. An important consideration in the application of this vertical grid is the treatment of terrain (the terrain height data base is discussed in the appendices). Since the lower layers are terrain-following, certain layers (layers 7-15) may be "filled" by terrain-following layers. If an MSL layer is completely filled with terrain-following layers, it is appropriately flagged to indicate that data for this height must be retrieved from the terrain-following layers.

3. OPERATING SYSTEM

3.1 Concept. An overriding consideration in the design and modification of the 3DNEPH is the automated environment in which the model must operate. At the same time, cloud analysis algorithms and computer programs are written to obtain the maximum amount of useful information

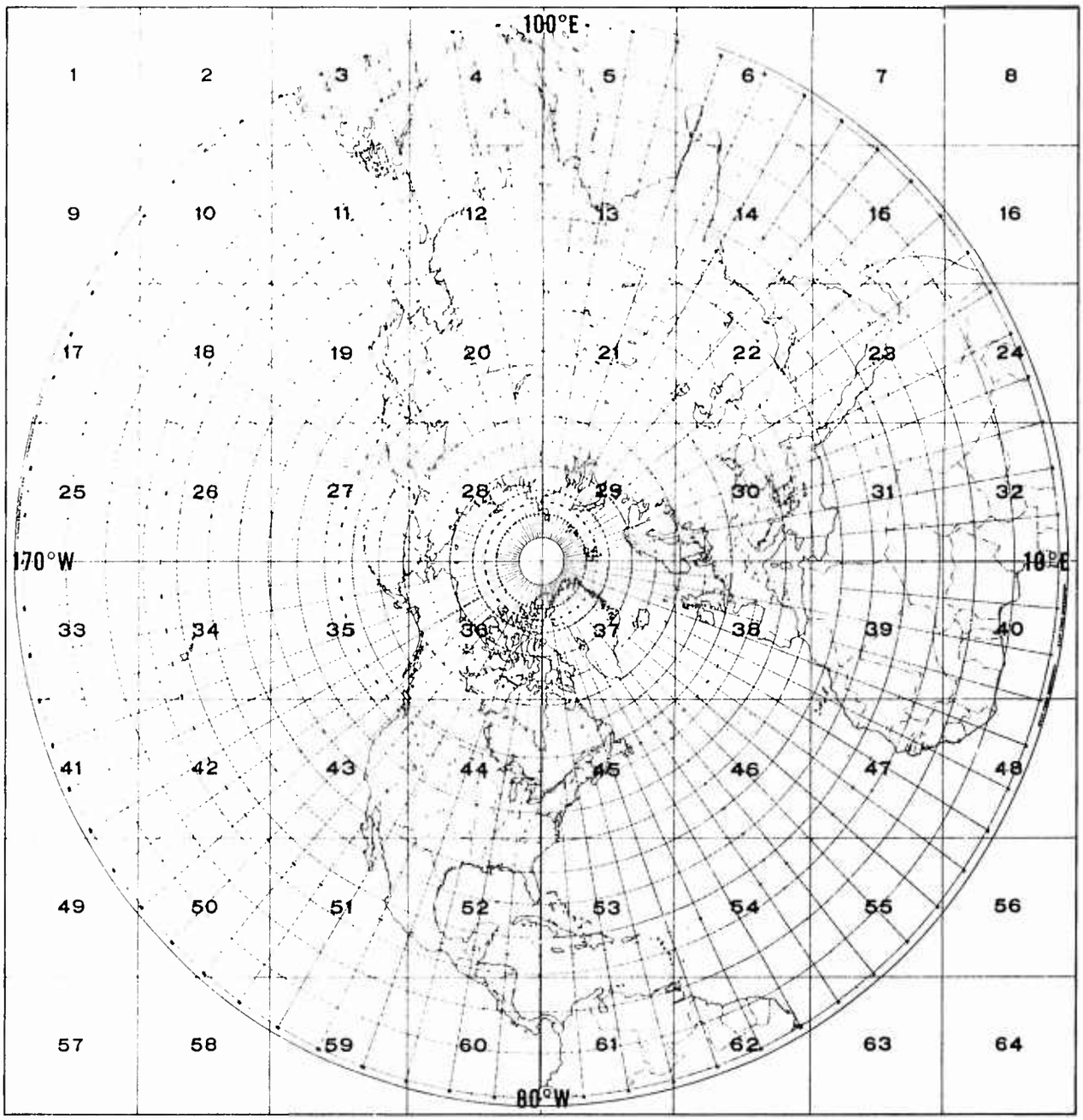

Figure 1. Northern Hemisphere 3DNEPH grid over a polar stereographic projection. Each square partition is a "3DNEPH Box". Corner boxes are not used.

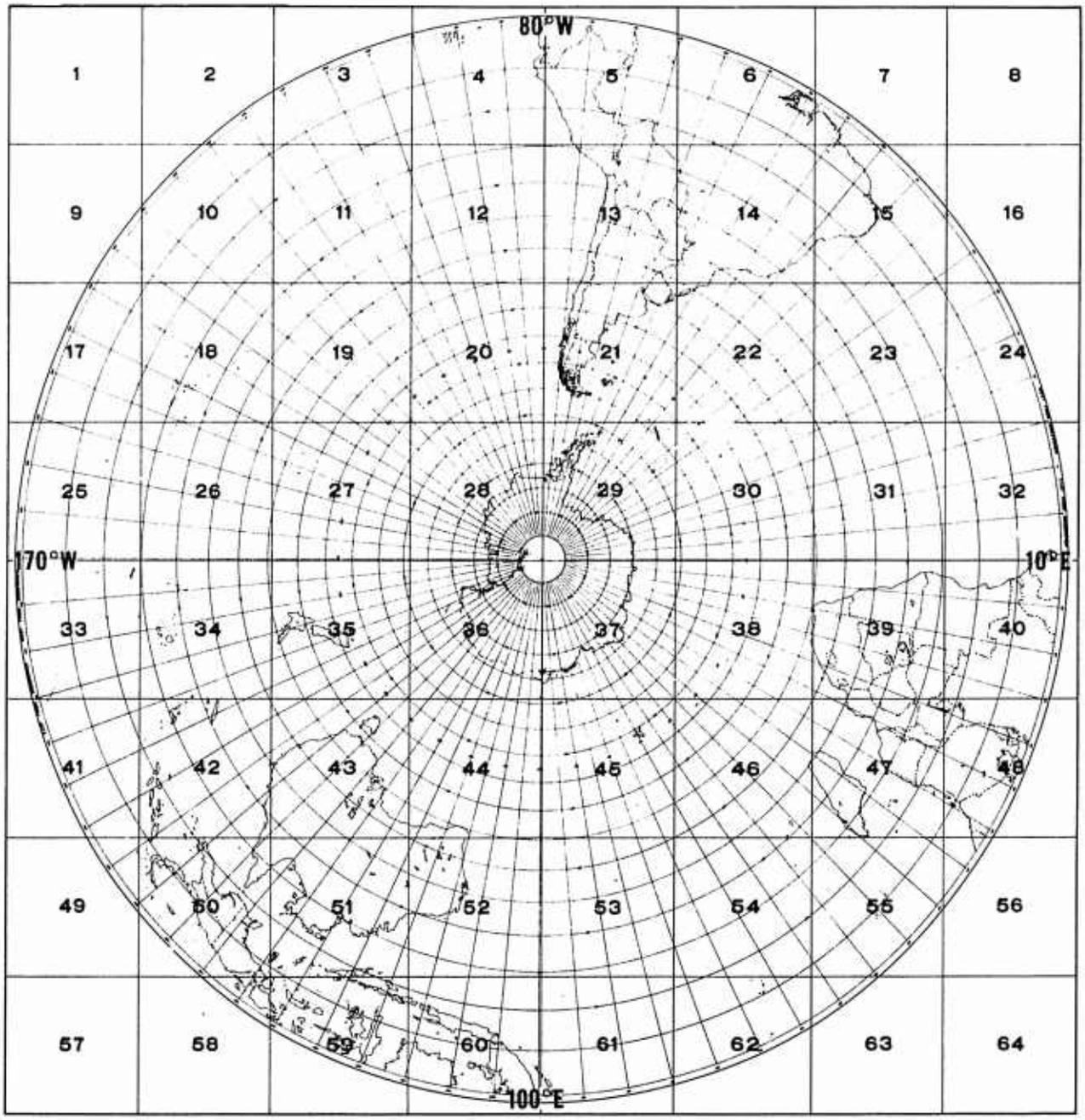

SOUTHERN HEMISPHERE

Figure 2. Southern Hemisphere 3DNEPH grid.

TABLE 1. LAYER HEIGHTS AND THICKNESSES OF THE 3DNEPH GRID.

LAYER	Height ft (m)	Pressure Level mb	Thickness ft (m)
	Surface		
1			150 (46)
	150 (46) AGL		
2			150 (46)
	300 (91) AGL		
3			300 (92)
	600 (183) AGL		
4			400 (122)
	1000 (305) AGL		
5			1000 (305
	2000 (610) AGL		
6			1500 (457)
	3500 (1067) AGL/MSL		
7			1500 (457)
	5000 (1524) MSL	850	
8			1500 (457)
	6500 (1981) MSL	800	
9			3500 (1067)
	10000 (3048) MSL	700	
10			4000 (1219)
	14000 (4267) MSL	600	
11			4000 (1219)
	18000 (5486) MSL	500	
12			4000 (1219)
	22000 (6706) MSL	430	
13			4000 (1219)
	26000 (7925) MSL	360	
14			9000 (2743)
	35000 (10668) MSL	240	
15			20000 (6096)
	55000 (16764) MSL	100	

from the raw cloud information and make it available in an integrated fashion to the various cloud data users as rapidly as possible. The result has been a careful balance between meteorological methodology and computer systems design. The 3DNEPH cannot be viewed as an entity unto itself; it relies heavily on the output from other automated programs. Many activities provide support only to the 3DNEPH and are therefore considered a part of the 3DNEPH system. The following independent automated activities are required to produce the 3DNEPH analyses. Several of these activities are discussed in detail in subsequent sections and the appendices.

(a) Northern and Southern Hemisphere analyses.
(b) Window analyses.
(c) Data base adjustments in response to manual input.
(d) Automated quality control.
(e) Temperature analyses and forecast.
(f) Sea temperature analyses.
(g) Satellite data status check.
(h) Transfer 3DNEPH data to other AFGWC computer systems.
(i) Build archival and recovery tapes.

3.2 Dual mode capability. The 3DNEPH operates in two modes known as the hemispheric mode and the window mode.The former provides frequent routine hemispheric analyses for support to general users of cloud analysis data. The later mode provides very timely analyses over selected areas for special users.

3.2.1 Hemispheric analysis. The hemispheric operating mode consists of complete hemispheric analyses over 60 of the 3DNEPH boxes shown in Figures1 and 2. Typically, the Northern Hemisphere analysis is completed every 3 hours while the Southern Hemisphere is analyzed every 6 hours. Start times are a function of conventional meteorological data arrival times. Each hemispheric analysis is a series of operations involving modular processors. These processors validate, condense, interpret, or integrate raw and pre-processed data. Figure 3 illustrates the flow of the hemispheric analysis and the interaction with various automated data base files. With complete hemispheric coverage of satellite data, such an analysis produces over 5 million unique pieces of data as part of the 3DNEPH data base.

3.2.2 Window analysis. The 3DNEPH program can also function in an unscheduled window mode. The same string of processors are employed as in the hemispheric mode, but the final output is stored in a separate data base. Such window analyses are usually selected based on satellite data arrival times and provide timely analyses over a limited area of interest. Up to 16 3DNEPH boxes (Fig. 1) can be selected in any configuration. Two window analyses can operate simultaneously with a hemispheric analysis. The overall flow for the window mode of operation is given in Figure 4.

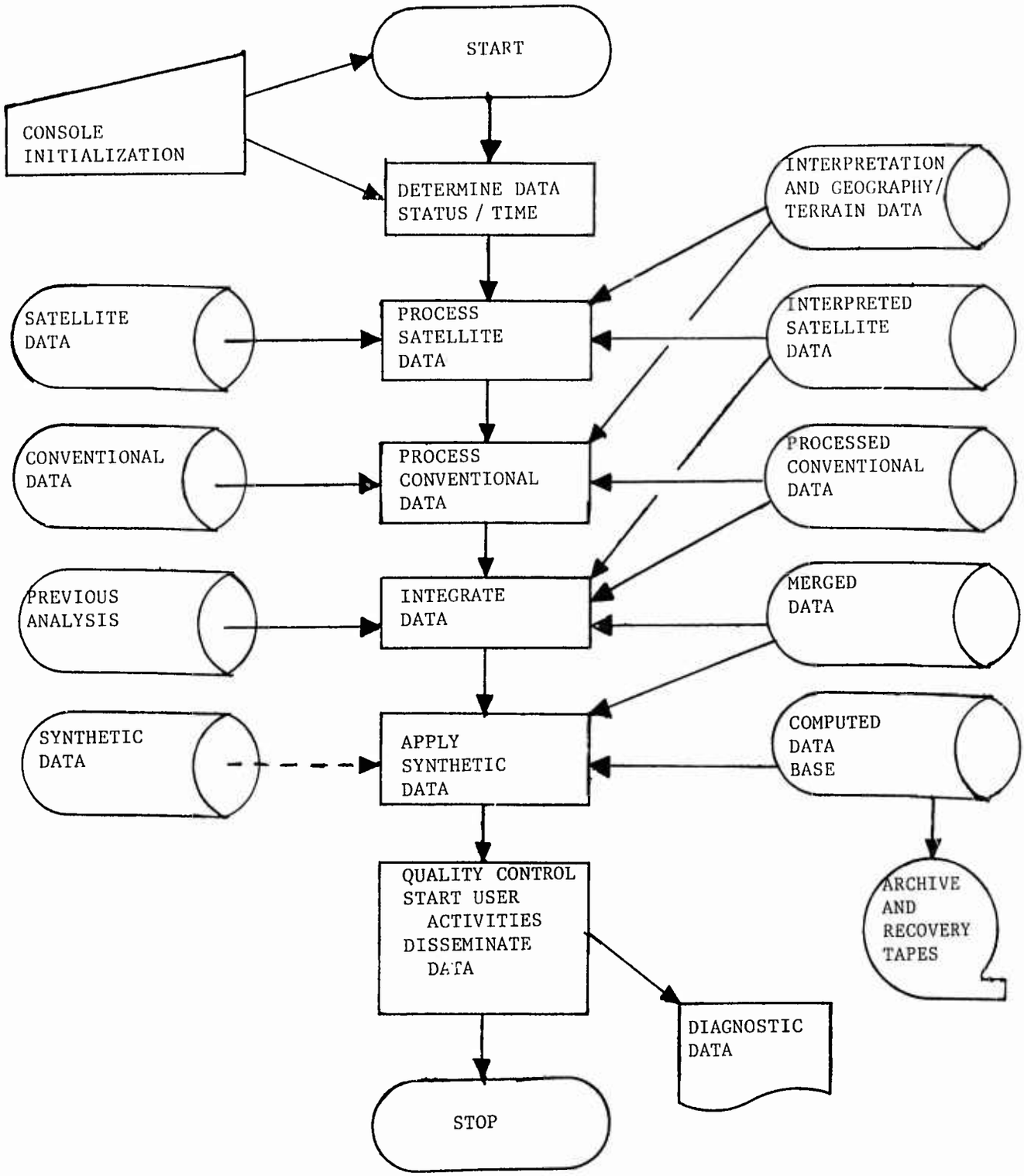

Figure 3. Functional flow chart of the major steps of the 3DNEPH hemispheric operating mode.

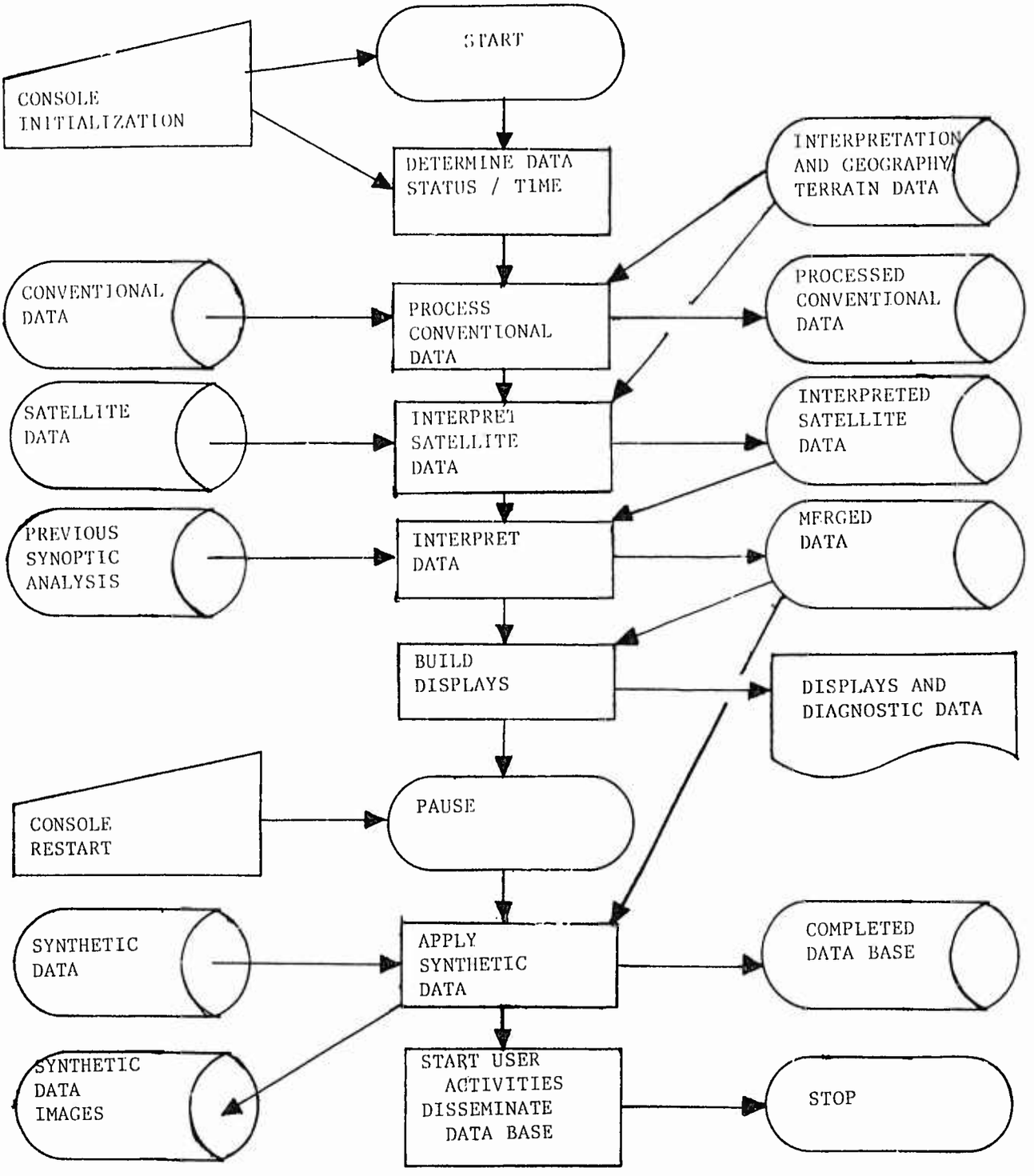

Figure 4. Functional flow chart of the major steps of the 3DNEPH window or off-time operating mode.

4. AUTOMATED SATELLITE DATA PROCESSING

The basis of the 3DNEPH automated analysis system is the timely availability of digital satellite imagery. When viewed as part of the overall data acquisition and processing system, the 3DNEPH occupies a small application portion of a very large and complex program. The Defense Meteorological Satellite Program (DMSP) is a complete system for the acquisition and processing of satellite data and is instrumental in the 3DNEPH production of timely, credible, worldwide cloud analyses. The inclusion of NOAA (National Oceanic and Atmospheric Administration) satellite data into the operating system was a significant augmentation to the DMSP data and demonstrated the flexibility of the overall satellite data processing system.

4.1 Satellite imagery availability. In the normal configuration, digital imagery data are available from two DMSP spacecraft with early morning and noon sun-synchronous polar orbits, respectively. NOAA spacecraft typically are flown in mid-morning orbits. Both NOAA and DMSP sources provide infrared and visual imagery for the daylight side of the earth and infrared imagery in the night portion of each orbit. Nighttime visual imagery are also available from DMSP and processing of these data has been demonstrated, but are not incorporated into the normal production cycles. Figure 5 is a flowchart illustrating the processing steps involved in acquiring DMSP/NOAA data and preparing it for automated processing by the 3DNEPH. Data are handled in units of a quarter orbit such that each revolution around the earth results in four separate entities. Geometric aspects of satellite data are discussed in the appendices.

4.2 Pre-processing satellite data. Aside from conversion of analog to digital data, the DMSP/NOAA imagery must be formatted, rectified, normalized, mapped, and stored onto a computer mass storage device before the 3DNEPH can analyze these data. Each process is described below.

4.2.1 Digitization. Digitization involves conversion of an analog waveform generated by the satellite sensor to a set of discrete quantitative values referred to as grayshades. These grayshades actually correspond to relative voltage levels obtained by sampling the analog waveform produced by the respective sensor. Digitization can be and is performed at various stages of the pre-processing, depending on the data source. A critical aspect of the digitization for 3DNEPH is that it be constant and uniform, i.e., that the hardware which performs the function be accurately calibrated. The digitization process can also be used to enhance imagery by making dark shades brighter, bright shades darker, or other linear or non-linear replacements of the original data (typical replacements are shown in Fig. 6). All such modifications require careful evaluation before automated analyses of the data can be performed. Table 2 shows the infrared grayshade convention used by 3DNEPH and a characterization of the visual grayshades. Note that the grayshade represents approximately 1.6 Celsius degrees in the infrared data.

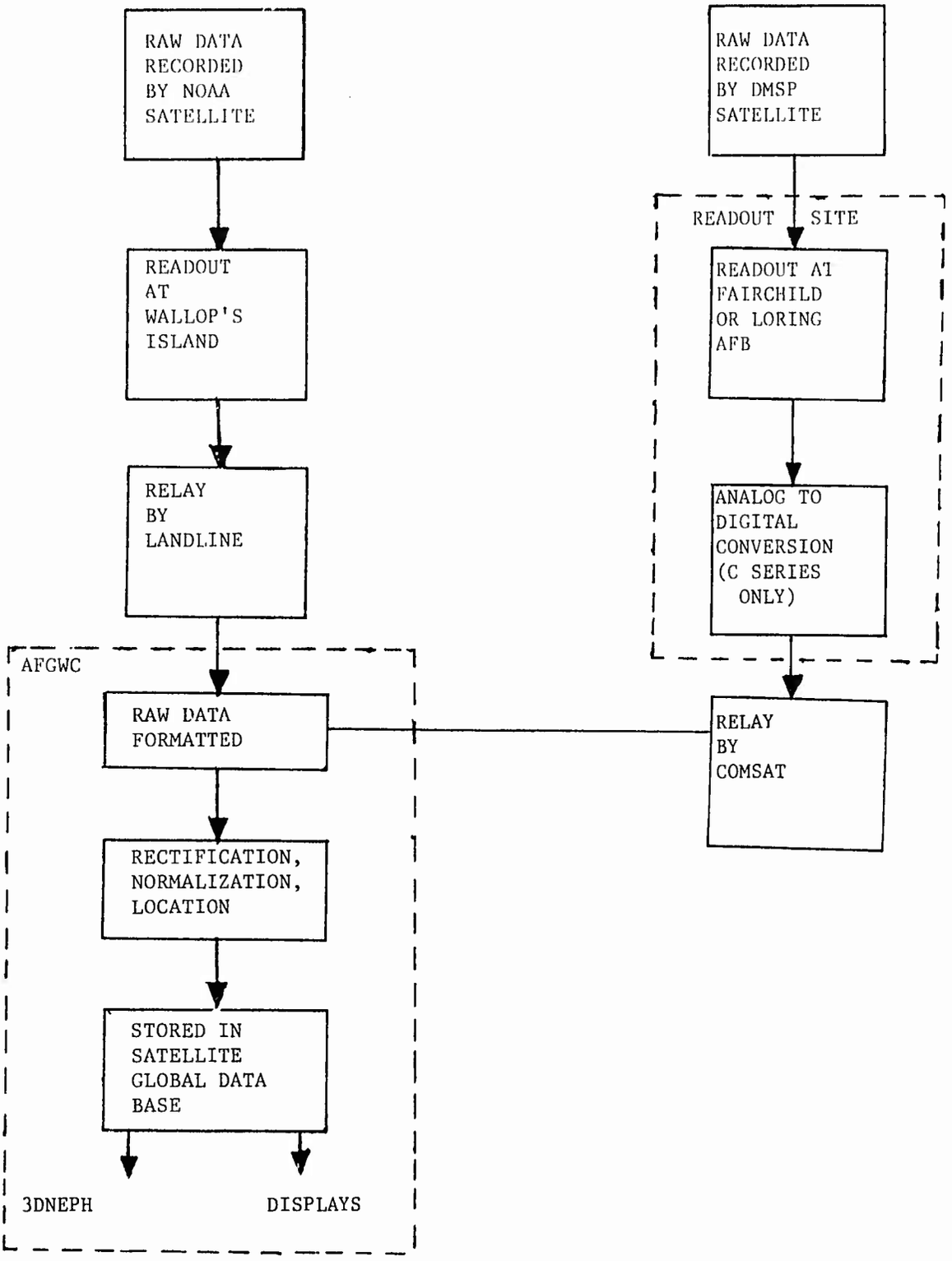

Figure 5. Flow chart of the major steps in the acquisition and processing of NOAA and DMSP satellite data.

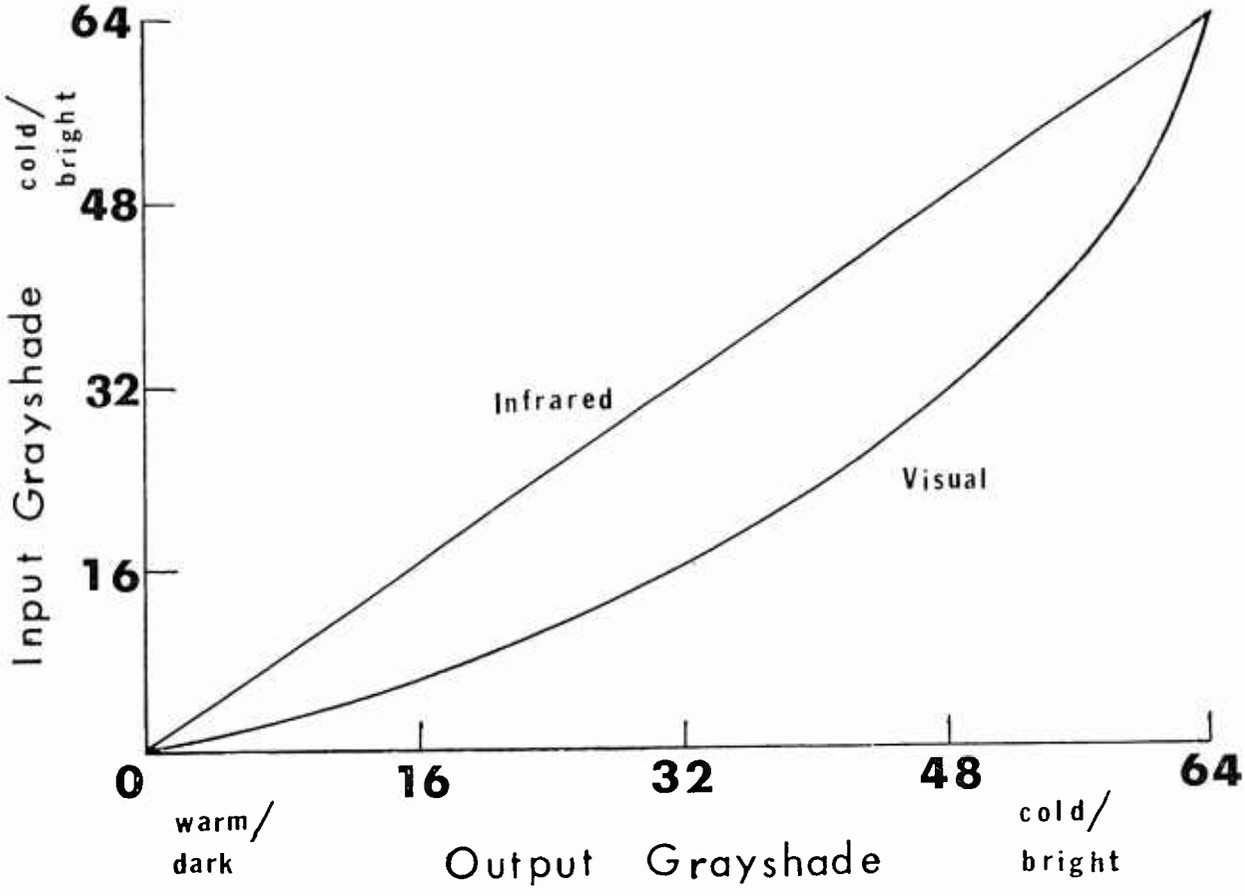

Figure 6. Visual and infrared data replacement curves used to enhance imagery. Infrared data are typically replaced linearly, but various replacement curves can be used.

4.2.2 Formatting, rectification and mapping. Formatting the data is a hardware function which involves the establishment of a bit configuration suitable for subsequent software handling. Rectification and mapping algorithms are described by Cherne (1974) and provide correction for distortion and earth location, respectively. The accuracy of these methods carry strong implications for the 3DNEPH since analyses are made by comparing a satellite data input to fixed, surface derived information. Any mislocation of input data by the pre-processing algorithms can result in erroneous analyses. Mislocation does occur, however, and dictates the application of statistical methods over areas larger than the resolution of the input data. This is part of the motivation for selecting the 25 nm grid as previously discussed.

4.2.3 Normalization. Normalization of the raw grayshade data, or the reduction of the imagery to the same relative gray scale, is not attempted in the pre-processing phase. The lack of normalization of both visual and infrared data results in significant grayshade anomalies which are functions of the time and space variations within each quarter orbit of satellite data. This has profound implications for the 3DNEPH satellite data processors and has been significant in the evolutionary history of the 3DNEPH processing technology. Some typical manifestations of unnormalized data are:

TABLE 2. VISUAL/INFRARED SENSED GRAYSHADES CORRELATED TO EARTH-BASED FEATURES/TEMPERATURES. THE VISUAL CHARACTERIZATIONS SHOWN VARY CONSIDERABLY WITH SATELLITE AND TIME OF YEAR AND DO NOT CORRESPOND WITH THE INFRARED TEMPERATURES.

Visual Characterization	Grayshade	Infrared Temperature		
		K(deg)	C(deg)	F(deg)
	1	310.0	37.0	98.6
Water	2	308.4	35.4	95.7
	3	306.8	33.8	92.9
Farmland	4	305.2	32.2	90.0
	5	303.7	30.7	87.2
	6	302.1	29.1	84.3
	7	300.5	27.5	81.5
	8	298.9	25.9	78.6
Old Scattered	9	297.3	24.3	75.7
Snow Cumulus	10	295.7	22.7	72.9
	11	294.1	21.1	70.0
	12	292.5	19.5	67.2
	13	291.0	18.0	64.3
Desert	14	289.4	16.4	61.5
	15	287.8	14.8	58.6
Snow	16	286.2	13.2	55.7
	17	284.6	11.6	52.9
	18	283.0	10.0	50.0
	19	281.4	8.4	47.2
	20	279.8	6.8	44.3
	21	278.3	5.3	41.5
Sunglint	22	276.7	3.7	38.6
on	23	275.1	2.1	35.7
Water/Snow	24	273.5	.5	32.9
	25	271.9	-1.1	30.0
	26	270.3	-2.7	27.2
	27	268.7	-4.3	24.3
	28	267.1	-5.9	21.5
	29	265.6	-7.4	18.6
	30	264.0	-9.0	15.7
	31	262.4	-10.6	12.9
	32	260.8	-12.2	10.0
	33	259.2	-13.8	7.2
	34	257.6	-15.4	4.3
	35	256.0	-17.0	1.5
Cumulonimbus	40	248.1	-24.9	-12.8
	45	240.2	-32.8	-27.1
Stratus	50	232.2	-40.8	-41.4
	55	224.3	-48.7	-55.7
	60	216.3	-56.7	-70.0
	63	211.6	-61.4	-78.5

(a) Left-right grayshade variations in response to the relative sun location.
(b) Strong seasonal fluctuations in grayshades with illumination changes and temperature trends.
(c) Varying degrees of sunglint.
(d) Sensor and hardware calibration drift and/or degradation.

Several 3DNEPH processors compensate or otherwise treat these grayshade variations to avoid inaccurate cloud analyses. Further discussion is provided in the respective satellite processor sections. A single exception is a correction applied during pre-processing for the so-called "limb-darkening" effect. This essentially provides compensation for attenuation of upwelling infrared radiation. The attenuation is a function of the varying atmospheric mass (optical depth) as the satellite sensor scans to the left or right of its subtrack. The form of the correction is given by equation 2.

$$T = T_o + .0125(T_o - 291.5) + .00156(T_o - 210)^2\phi^2 \qquad (2)$$

where T is the corrected output temperature in Kelvin degrees, T_o is the sensed temperature in Kelvin degrees, and ϕ is the angle in radians between local vertical and the line of sight from the satellite to the local point (scan angle). Details of the angular relationship used in equation 2 are provided in the appendices. The origin of the equation is discussed in detail in AWSTR 74-250 (1974). The last term, which involves the angle ϕ, was added at AFGWC to provide a larger correction as the satellite sensor views points at larger scan angles. Equation 2 provides a correction which essentially normalizes the imagery for optical depth and provides a temperature dependent correction for water vapor in the atmosphere. While adequate for general display purposes, this correction is not adequate for automated processing and more comprehensive corrections are required in the 3DNEPH and are discussed in the appendices.

4.3 The Satellite Global Data Base. Once mapped, rectified and corrected, the digital imagery are stored in a computer mass storage file referred to as Satellite Global Data Base (SGDB) (Figures 7 and 8). The SGDB is a real time data file such that new data are stored immediately after pre-processing and overlie (and erase) older data which were previously mapped into the same area. The result is that only the most recent data are available for any area of the earth. Depending on the satellite mix of local crossing times and data availability, the entire SGDB can be updated every 6 to 12 hours in the case of infrared data and 18 to 24 hours for visual data.

4.3.1 Grid system. The data in the SGDB are gridded onto a polar stereographic projection which coincides with the 3DNEPH grid. This procedure greatly simplifies the analysis process by eliminating the requirement to perform complicated transformations. The SGDB data are contained in a 4096 by 4096 array resulting in a pixel (picture element) resolution of approximately 3 nautical miles. Data which are coarser

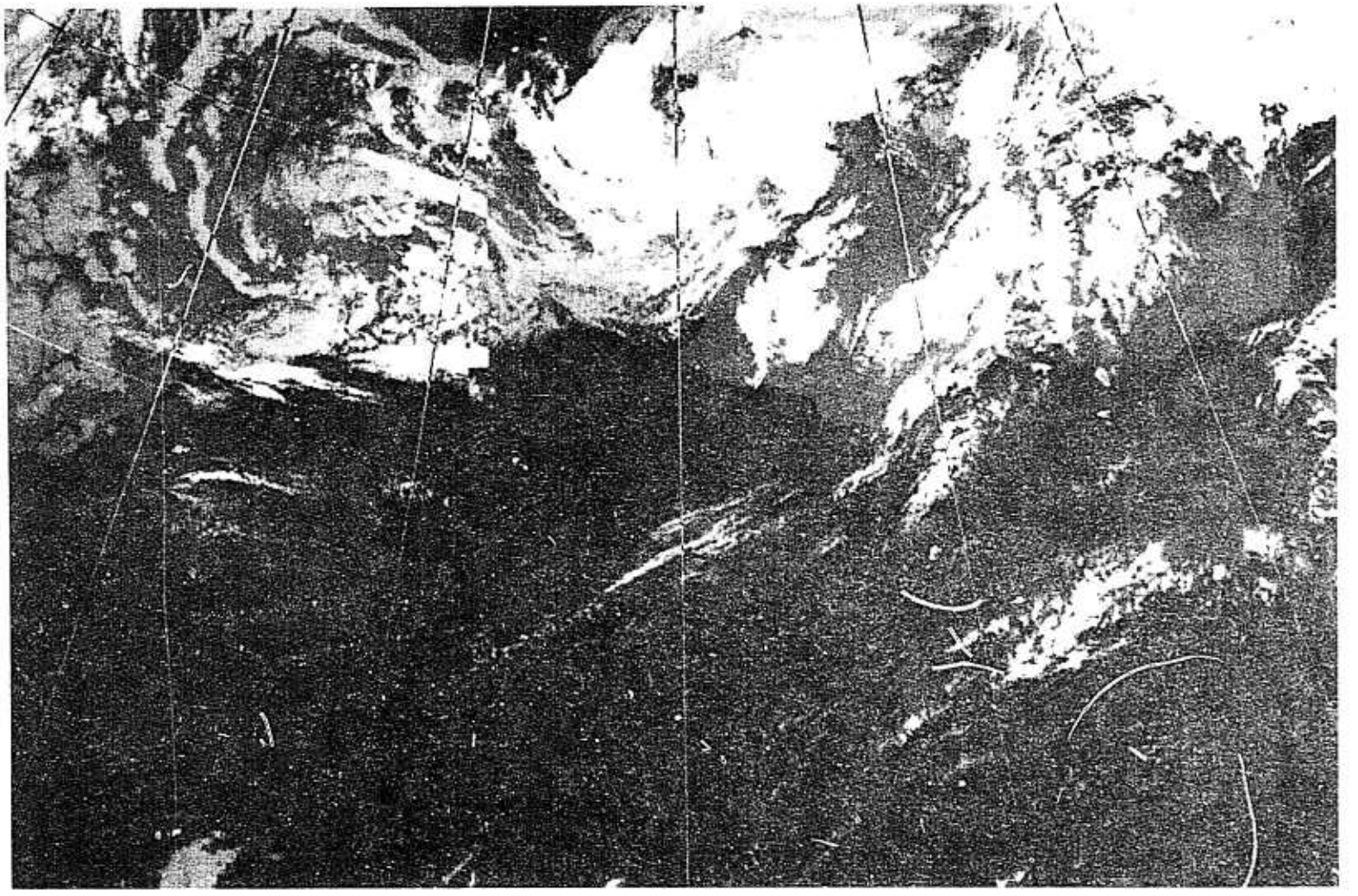

Figure 7. Digital infrared imagery from the Satellite Global Data Base. The data shown are from DMSP satellite number 12535. The area is the Mediterranean and North Africa on 8 April 1978.

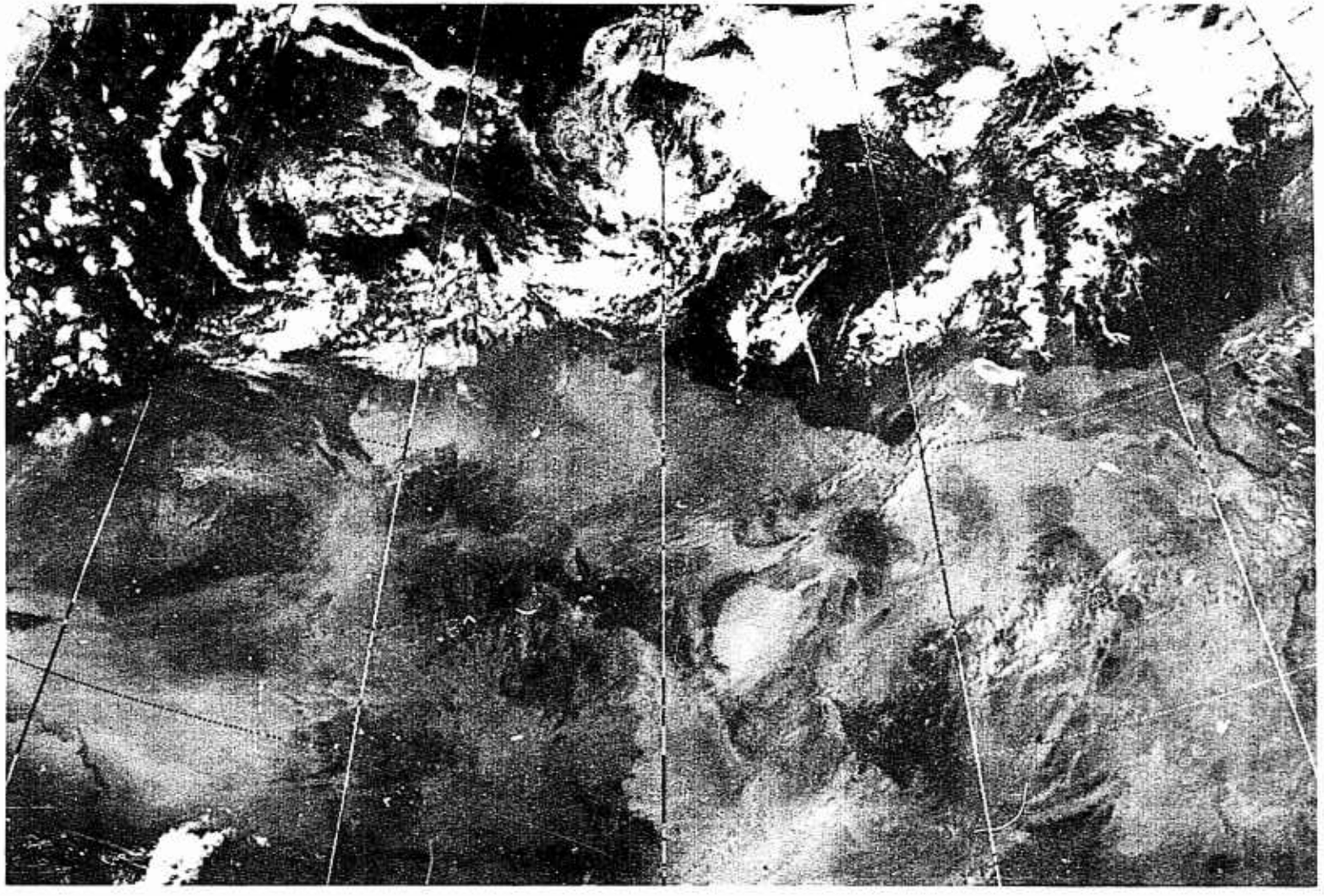

Figure 8. Display of visual imagery from the Satellite Global Data Base. These data are coincident (taken at the same time from the same satellite) with the infrared data in Figure 7.

than the 3 nm resolution are repeated to fill in the appropriate number of SGDB pixels. Each visual or infrared pixel of data is represented by a single grayshade value ranging from 1 to 63. The resolution of the analyzed output of the 3DNEPH satellite data processor is 25 nm. Therefore, statistical methods are employed to reduce the 64 pixels contained in each 25 nm gridpoint to a single output. This relationship is illustrated by Figure 9.

4.3.2 Supplementary data and layout. Additional information is also required to properly identify the data and is provided at a resolution of 50 nm (every 132 x 132, 3 nm pixels). These supplementary data are gridded and interspersed with the raw pixel grayshades. Table 3 lists the supplementary data that are available.

TABLE 3. SUPPLEMENTARY DATA AVAILABLE IN THE SGDB AT THE 50 NM RESOLUTION

Information	Units/Description
1. Satellite source	Last two digits of satellite name.
2. Orbital mode	Quarter orbit number (1,2,3,or 4).
3. Local zenith angle	Whole degrees between sun and local vertical.
4. Satellite view angle (scan angle)	Whole degrees between subpoint and local point.
5. Left-right indicator	Indicator of left or right measurement of scan angle with respect to direction of travel.
6. Data time	Number of ten minute intervals into the current year.
7. Satellite orbit number	Number of revolutions around the earth since launch.
8. Data disposition indicator	Arbitrary numbers as currently defined.

The SGDB is actually four files - a file for each hemisphere and each data type (visual or infrared). However, to avoid unnecessary processing complications, the visual and infrared data are interleaved, making it possible to process and compare these data types for the same geographical location. This capability is very significant since it permits simultaneous applications of visual and infrared data in 3DNEPH.

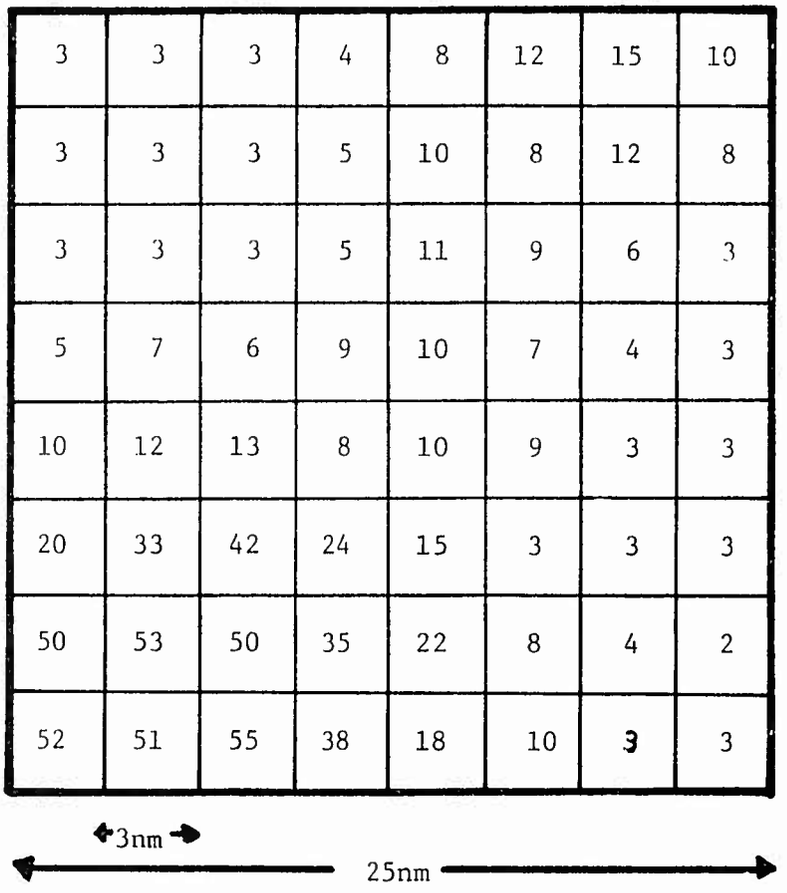

Figure 9. Relationship between a 3DNEPH 25 nm gridpoint and the 3 nm data in the SGDB. Each small square is a picture element (pixel) with a single grayshade from 1 to 64. Note the probable existence of clouds in the lower left and possible existence of scattered clouds, snow, or sand in the upper right.

4.4 Preliminary satellite data processing. Satellite data processing in the 3DNEPH satellite processors employs procedures which are efficient and uncomplicated. This design is essential if a real-time operating mode is to be realized. The basic procedure which is common to both the infrared and visual data processors involves calculation of certain first-order statistics followed by comparison of these statistics to certain temperature and albedo background field statistics. Figure 10 is a flow chart depicting the overall data processing procedure. Statistics and other processing decisions derived from the 64 pixels centered around each eighth-mesh gridpoint are described in the following paragraphs.

4.4.1 Average. Average eighth-mesh grayshade is obtained from:

$$\bar{G} = N^{-1} \sum_{i=1}^{N} G_i \quad , \; G>0, \; N>0 \tag{3}$$

where G_i is a unique pixel grayshade (range 1 to 63) and N is the total number of available pixel grayshades (usually 64).

4.4.2 Variability. Variability (V) of the pixel grayshades with respect to the eighth-mesh average grayshade is provided by:

$$V = N^{-1} \sum_{i=1}^{N} |G_i - G| \quad , \; G>0, \; N>0 \tag{4}$$

where G_i is the unique pixel grayshade (range 1 to 63), N is the total number of available pixel grayshades, and G is the average grayshade as defined above.

4.4.3 Missing data. Missing data pose an important problem for 3DNEPH. Failure to recognize missing data or mark degraded data as missing can result in discontinuous or "speckled" cloud analyses. Sources of missing data are:

(a) An insufficient number of pixels with grayshades ranging from 1 to 63 for each eighth-mesh gridpoint. This is a criteria levied on N in equations 3 and 4.
(b) Data which lie near or beyond the terminator of a particular quarter orbit of visual data.
(c) Any data which exceed preset thresholds of look or zenith angles (explained in the appendices) of visual or infrared data established for the purpose of eliminating data of poor resolution, illumination, or other uncompensated anomalies. This procedure is referred to as "trimming" the data.

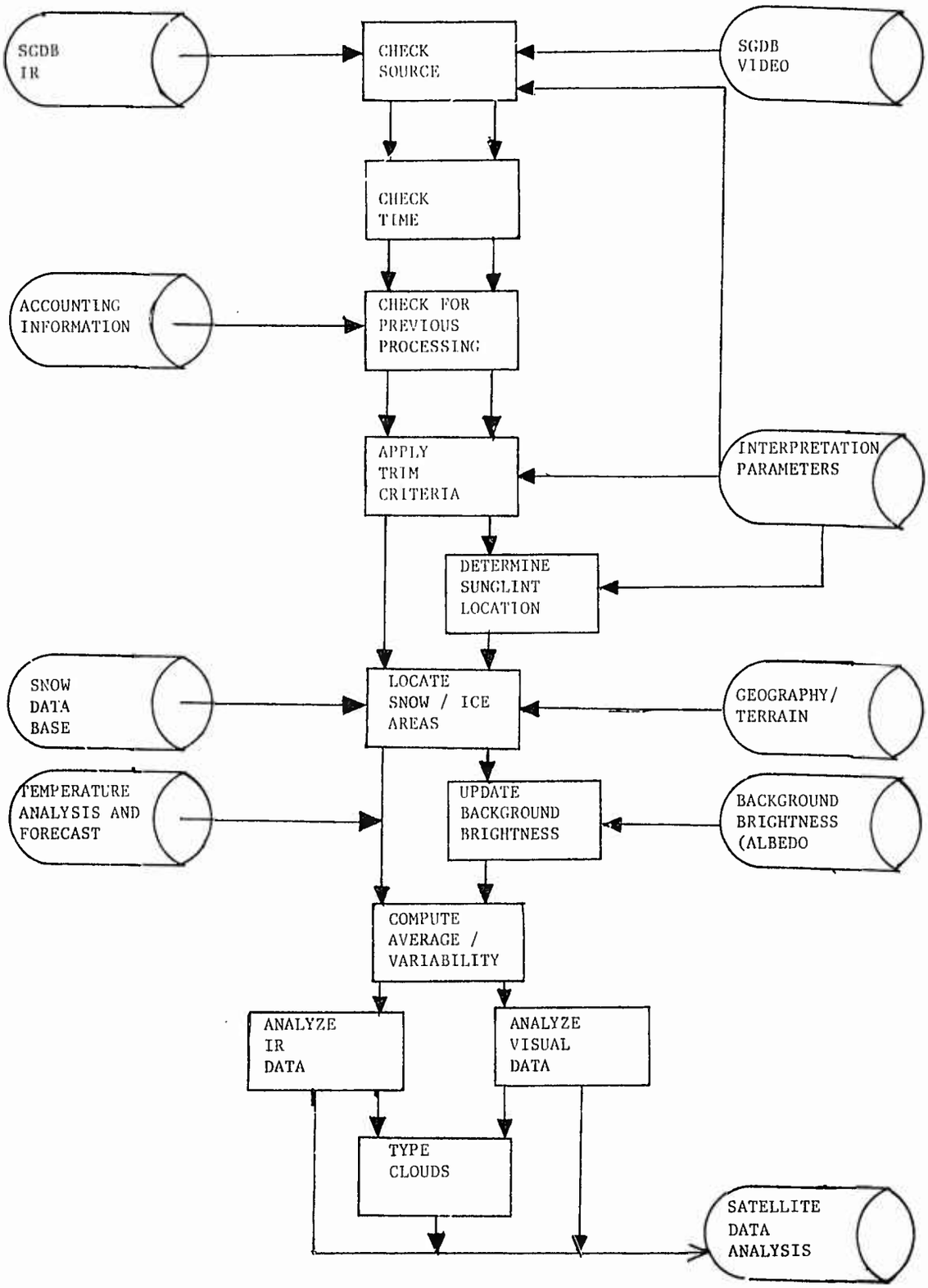

Figure 10. Functional flow chart of the major steps in the preliminary satellite data processing of the 3DNEPH. The dual paths depict separate but similar procedures for both visual and infrared data types.

(d) Unreasonably bright grayshades in areas of sunlight are marked as missing in visual data.

(e) Snow areas are considered missing for visual data processing because a cloud analysis is not feasible for gridpoints involving such bright backgrounds.

By identifying missing and unuseable data, the 3DNEPH can provide analyses which incorporate only reasonable data.

4.4.4 Data time. Data time is a major consideration in the satellite processors. Generally, all data in the SGDB which are unprocessed by a previous 3DNEPH are processed, thus limiting the age of the data to three hours (six hours in the Southern Hemisphere). All data are subjected to a time check before processing is allowed. The time criteria can be varied, but are generally four and seven hours for the respective hemispheres. An account of processed data is maintained to preclude redundant processing.

4.4.5 Data source. Data source is checked to screen out data which are not designated for automated processing. Many normalization and "tuning" procedures rely on this information.

5. INFRARED DATA PROCESSOR

The infrared data processor of the 3DNEPH combines information from the SGDB, temperature data base, background brightness data base, and the geography/terrain fields in the production of an independent cloud analysis data base. This processor produces cloud top height information as well as total cloud amount for each 25 nm gridpoint where satellite data are available. Figure 11 is a flow chart depicting the major steps involved in processing infrared data and the input and output of the processor. Procedures shown in Figure 11 are discussed in the following paragraphs.

5.1 Modal specification. The first step in infrared data processing is the separation of the 64 grayshade pixels associated with a 3DNEPH gridpoint into "modes." This is necessary to identify the significant features within the 25 nm gridpoint so that an independent height can be determined for each feature. It would not be practical to determine a height for each independent pixel. The modal specification procedure permits the identification of one or two cloud layers or one cloud layer in a partly cloudy situation. Certain adjustments for independent pixels which are themselves partly cloudy can also be made and will be described later.

The modal specification procedure begins by building a frequency distribution (histogram) for the 64 grayshade pixels as illustrated in Figure 12. This conveniently groups together pixels of similar temperatures despite the fact that they may not be adjacent to one another. A mode is then defined from the histogram based on the following empirically determined criteria:

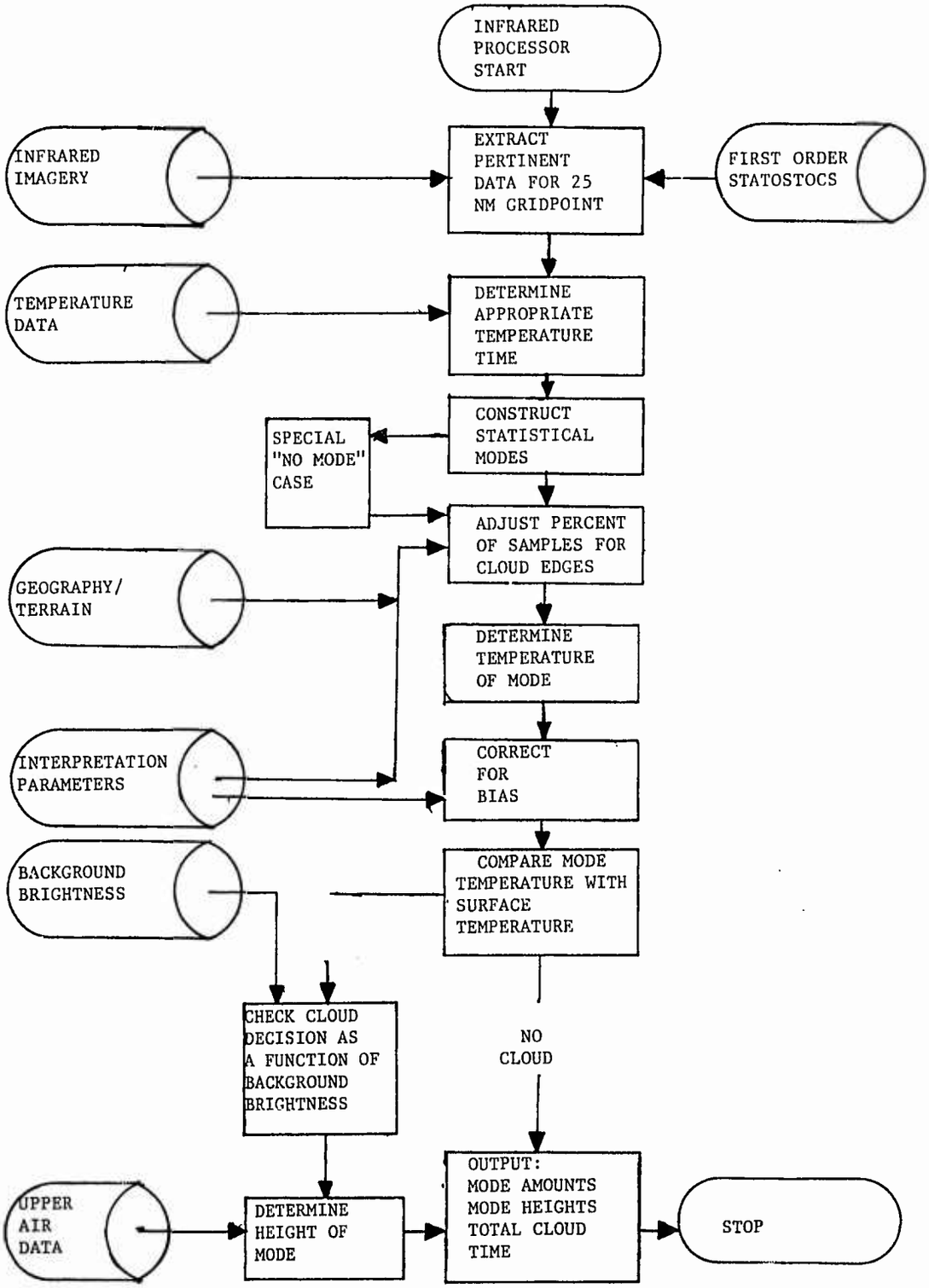

Figure 11. Functional flow chart of the major steps in the infrared satellite data processor.

(a) A single grayshade which contains six (6) or more samples.
(b) A group of adjacent grayshades containing 12 or more samples.

When more than two modes are identified, modes are combined on the basis of relative amplitude (stronger modes are retained) and the grayshade difference between modes (an indication of significance). In cases where a mode cannot be defined according to the above criteria, the procedure defaults to the specification of a cloud threshold temperature which is determined from the appropriate surface temperature.

5.2 Resolution compensation. The 3 nm imagery is incapable of resolving fine cloud detail or discerning cloud edges in a partly cloudy situation. A 3 nm pixel which is coincident with a cloud edge, for example, will have a grayshade which is quantitatively between the background temperature and the cloud top temperature. This rationale can be expanded to the larger spacial domain of the 3DNEPH. The variability of pixel grayshades within a 25 nm gridpoint mode is a measure of the number of pixels which are partially filled by clouds. Thus, a no-mode case would probably represent a scattered cloud field containing small cloud elements. An overcast area would appear as a strong mode (high amplitude) with a very small range, as would a clear area.

Following modal specification, an empirical correction based on the above discussion is made to arrive at a more accurate cloud amount. The correction consists of reduction of the area (or number of pixels) within the domain of each mode. The amount of the reduction is a function of the distance, in terms of grayshades, between the peak of the mode and the warm end of the mode. This is illustrated in Figure 12 by the dash-dot curve. Thus, the overall reduction is negligible for a strong mode case and larger for a no-mode case. The revised "mode amount" ultimately becomes the cloud amount if subsequent processing determines that a particular mode represents clouds.

5.3 Bias correction. Before cloud decisions can be made, the infrared temperatures must be corrected for absorption of the infrared energy as it passed through the atmosphere to the sensor and for a host of other systematic anomalies which tend to bias the infrared temperature. Part of this bias is introduced by anomalies in the surface temperature field which is used in the basic cloud/no cloud decision. Procedures have been developed which automatically correct the infrared temperature. The goal of these procedures is to correct the infrared temperature such that no temperature difference exists when the infrared and surface temperatures are compared for a clear sky situation. A detailed discussion of the biasing procedure is provided in the appendices.

5.4 Cloud decision. With the mode amounts specified, a representative temperature must be selected for comparison with a surface temperature to determine if clouds are present. A representative temperature can be defined in a number of ways. The grayshade with the maximum number of samples (the peak) within the mode, an average value, or maximum and minimum values could all be used to represent the temperature of the mode. After careful investigation, the coldest temperature within a

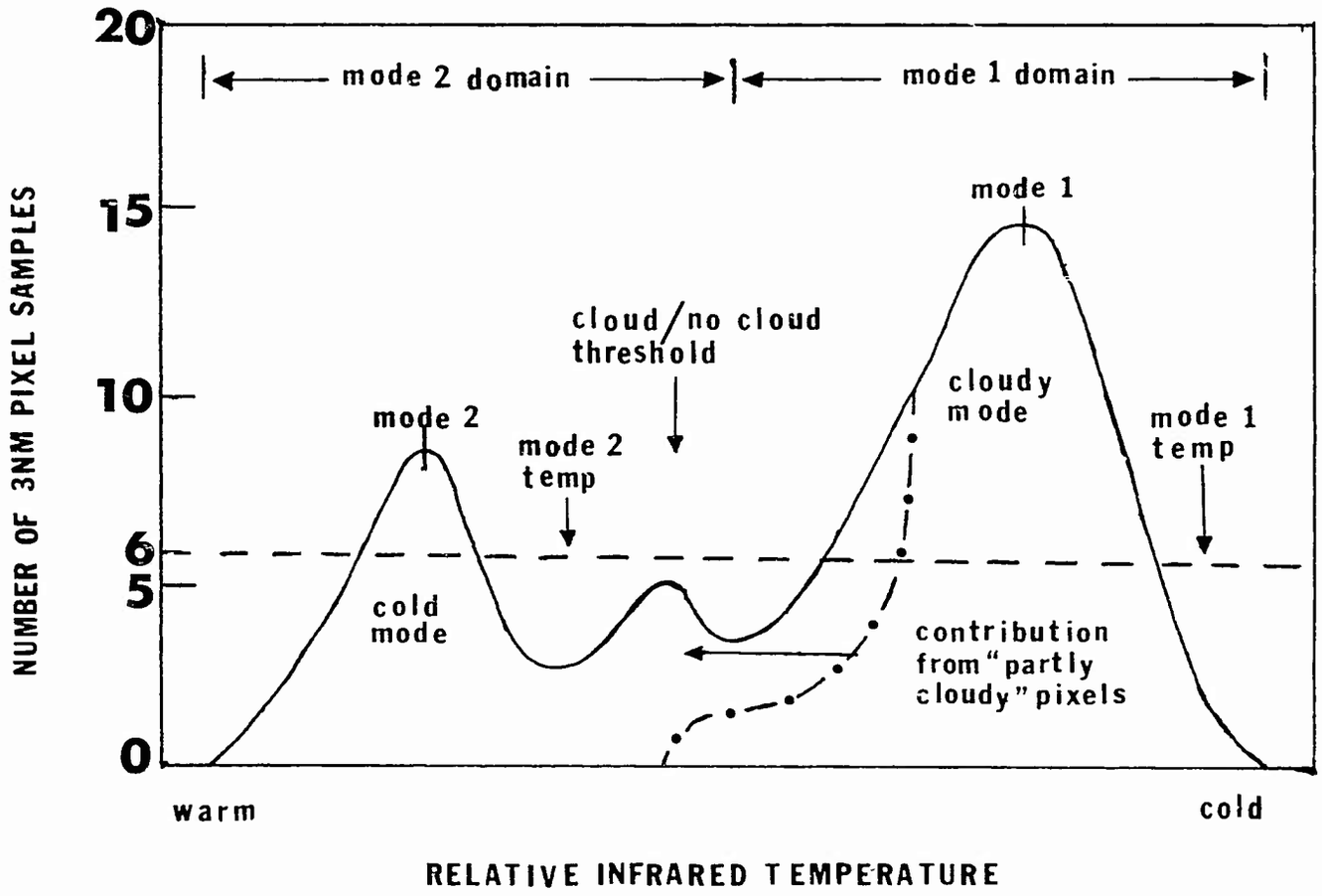

Figure 12. Schematic of an infrared frequency distribution for a single gridpoint. The distribution is constructed for a total of 64 pixel grayshade samples each of which is characterized by a grayshade ranging from 1 to 64. The dash-dot curve is an example of empirical cloud amount reduction as described in the test.

mode was selected. This temperature provides the greatest sensitivity as it is always the coldest with respect to the surface temperature and also corresponds to the temperature associated with pixels containing the greatest amount of cloud. This results in a more representative cloud top temperature.

The modal temperature is compared to the conventionally derived background surface temperature to make a cloud or no-cloud decision for that mode. The surface temperature actually corresponds to the cloud threshold point depicted in Figure 12. It follows intuitively that a modal infrared temperature colder than the surface temperature yields an affirmative cloud decision. The number of pixels in a cloudy mode after resolution compensation, divided by the total number of pixels associated with the 25 nm gridpoint (usually 64), gives the cloud amount in percent.

5.5 Low-cloud limiting. The cloud determination is not yet complete, however, due to unavoidable irregularities in the surface temperature data base which limit the reliability of the cloud or no-cloud decision. A restriction is placed on the amplitude of the surface-modal temperature difference as shown in Figure 13. In effect, the curve of Figure 13 determines the lowest permissable cloud height with respect to the surface and is expressed in Kelvin degrees above (colder than) the surface. This restriction is a function of the visual background brightness data base which indirectly provides information regarding soil type, data sparcity, and aridity of the region. This information thus provides an indication of the local diurnal temperature amplitudes and temperature data reliability. In this way it is possible to determine those areas where temperature data are unreliable without limiting cloud detection sensitivity in other areas of the world. Snow is independently locatable and is assigned a brightness grayshade of 31 for application of the curve in Figure 13. The height limit is relaxed for snow areas as shown. This procedure represents a compromise in the ability to detect low level clouds. However, without this limitation, dry, data-sparse areas would generally be too cloudy or, as the alternative, low clouds would be undetected over most of the earth's surface.

5.6 Height determination. If clouds are indicated as described in the previous paragraph, a cloud height must be determined for the cloudy mode(s). If modal temperature is assumed to represent the temperature of a radiating surface which emits as a blackbody (with some exceptions), it is a straightforward procedure to find an atmospheric height which corresponds to a modal temperature. Height is found by linear (constant lapse rate) interpolation in a macro-scale (200 nm) upper air height/temperature analysis and forecast maintained in the AFGWC data base. Reported heights used in the interpolation are the surface, 850 mb, 700 mb, 500 mb, 300 mb, and 200 mb. Sources of the temperature analysis data are conventional atmospheric soundings and vertical temperature radiative profiles obtained from satellite data (when available). Forecast temperatures and pressure heights are also available from the AFGWC primitive equation forecast model when the current analysis is too old or unavailable. A standard atmospheric temperature profile is used in tropical areas where gridded temperature fields are unavailable. Clouds and cloud fields which do not act as blackbody emitters may result in erroneous

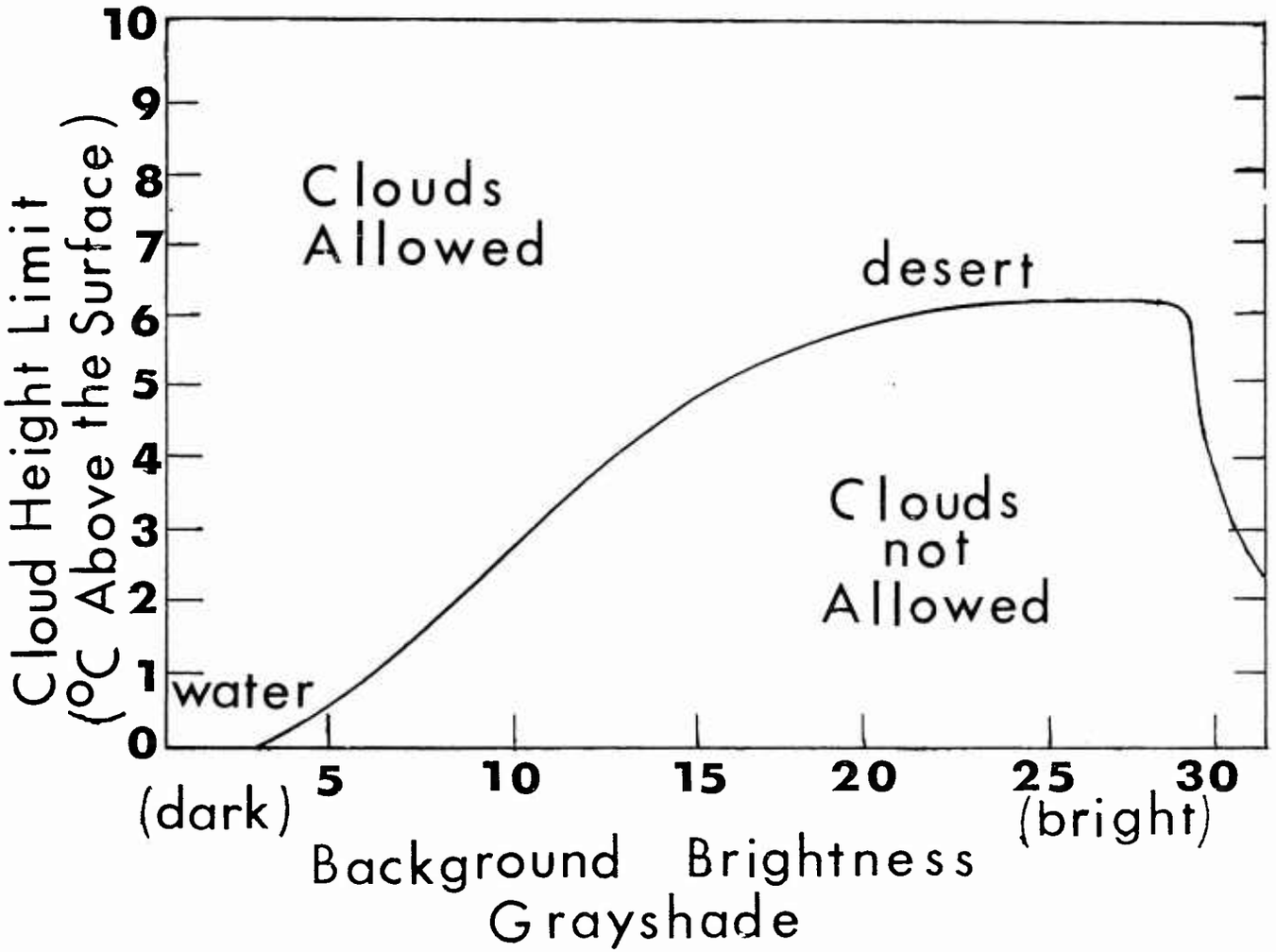

Figure 13. Schematic of the cloud cut-off curve used to limit low clouds over bright areas of the earth where the infrared processor is more likely to make errors.

cloud top temperatures and heights. Such is the case for semi-transparent cirrus clouds and scattered cloud fields where cloud elements are below the pixel resolution. Infrared temperatures are warmer than the true cloudtop temperatures resulting in a cloudtop height lower than it actually is. The magnitude of this error is unknown, but may be large in the case of thin cirrus.

No restrictions are placed on the infrared height with respect to proximity of the earth's surface other than those described in the section about low-cloud limiting. Inversions restrict stratus detection when cloud top temperatures are greater (warmer) than the underlying surface temperature.

6. VISUAL DATA PROCESSOR

The visual data processor of the 3DNEPH incorporates raw pixel imagery from the SGDB and grayshade values from the background brightness (albedo) data base in the production of a total cloud amount for each 25 nm gridpoint. (Figure 14 shows the overall processing procedure). The processor makes 64 independent cloud/no cloud decisions for each 25 nm gridpoint. Each decision is made by comparing a raw imagery pixel grayshade to a 25 nm background brightness grayshade. The total number of affirmative cloud decisions divided by the number of available pixels yields the percentage of total cloud.

6.1 Background brightness. The background brightness is an independent data base which provides an up-to-date grayshade value for every 25 nm gridpoint. This value represents the brightness of the earth's surface and is proportional to albedo. Separate values are maintained for each operational satellite so that the brightness is normalized for sensor characteristics. Details of the background brightness data base are provided in the appendices.

The background brightness is specified at 25 nm and not at the 3 nm resolution because of computer storage requirements and limitations in the gridding accuracy of the raw satellite data.

6.2 Cloud decision. The cloud decision procedure requires special considerations because of the resolution difference between the background brightness and the pixel grayshade sample. The 25 nm resolution background brightness represents an average of 64 pixel grayshades while the 3 nm pixel grayshades may range far above and below the 25 nm average. This variation may be expressed as the absolute value of the statistical variability or mean variance of the 3 nm samples about the average. It follows that the brightness for a single pixel grayshade must exceed the background brightness grayshade plus a grayshade quantity which accounts for this variance before an affirmative cloud decision can be made. Expansion of this rationale to many 25 nm gridpoints representing a cross section of terrestrial features yields a large variance spectrum which is a function of the terrain and illumination anomalies for the satellite at hand. Furthermore, variability is linked to the 25 nm average background brightness such that dark and very bright areas have low variabilities and areas of intermediate brightness have high variabilities. This relationship is depicted in Figure 15. Water is dark and homogeneous

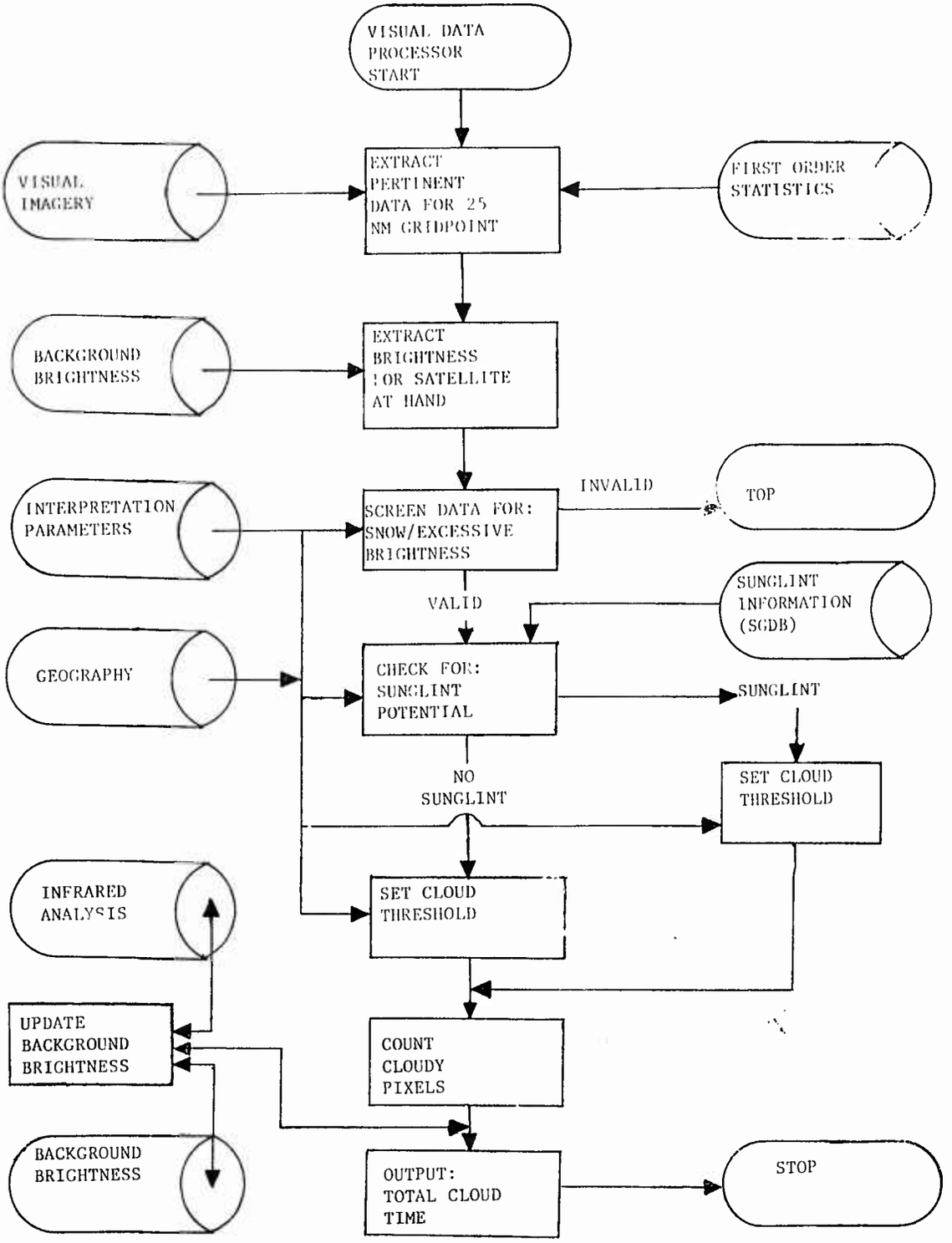

Figure 14. Flow chart of the major steps in processing visual satellite imagery.

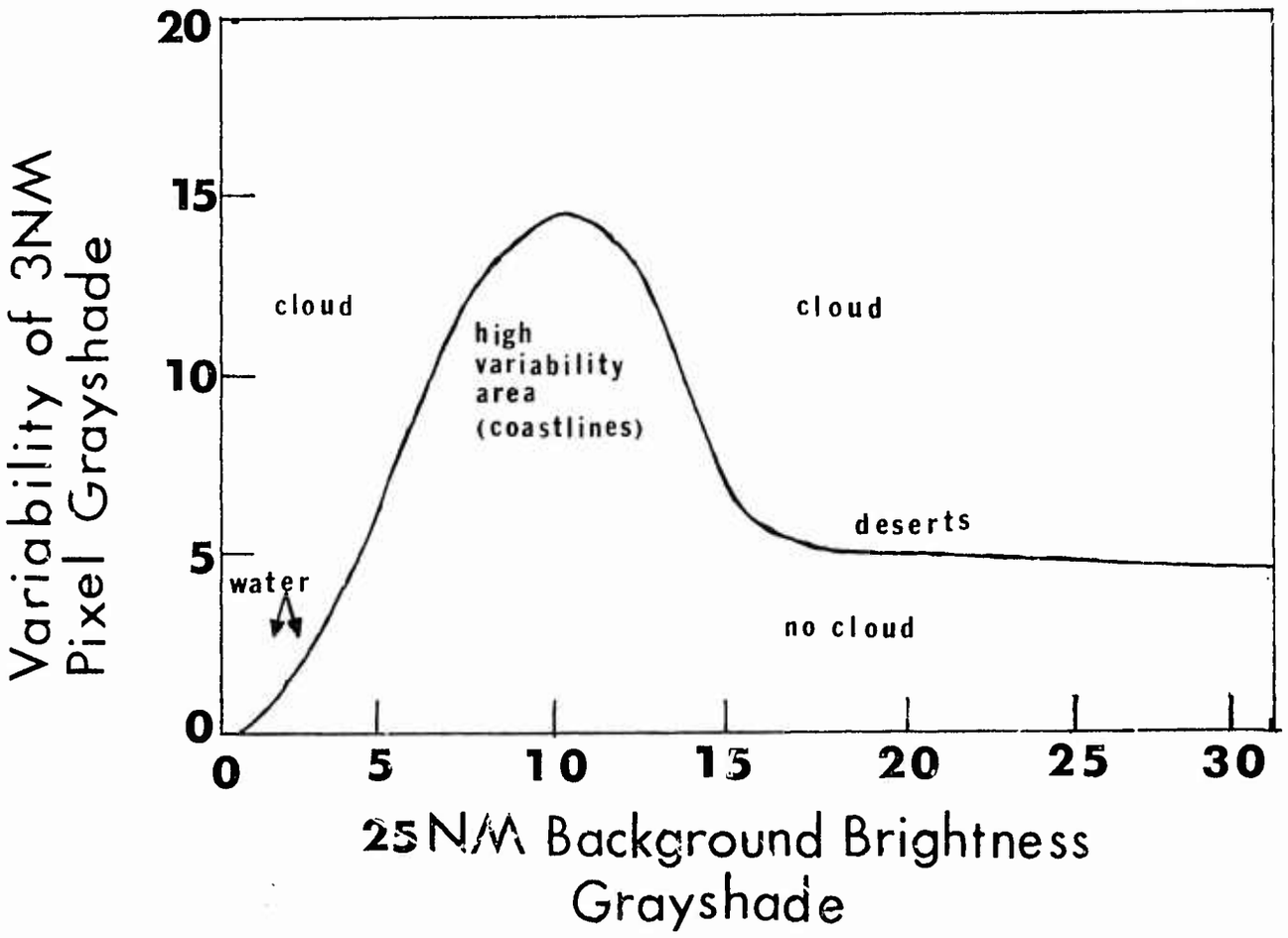

Figure 15. Generalized variability curve of 3 nm pixel grayshade as a function of 25 nm background brightness grayshades. This curve is the basis of the cloud/no-cloud decisions made in the visual data processor. The high amplitude area corresponds to coastal and other high variability terrain features. Approximately 95 percent of all 25 nm gridpoints are found in the background brightness range of 1 to 6.

(low variability) and is represented in the lower left portion of Figure 15. The center portion of the variance curve is indicative of high variability terrain such as coast lines and mountainous areas. In extremely bright desert areas the variance again decreases as seen to the right of Figure 15. This variance curve provides a cloud/no cloud threshold grayshade value and is applied operationally as follows:

$$C_T = B_i + V_G$$

where C_T is the brightness threshold for clouds, B_i is the 25 nm background brightness average grayshade for gridpoint i, and V_G is the typical variability of 3 nm pixel grayshades about the background brightness and is obtained from Figure 15. A pixel with a grayshade brighter than C_T is considered cloudy.

The cloud decision procedure is not without some limitations. Small cloud elements over high variability backgrounds are essentially undetectable, but this is a reasonable compromise considering the small portion of the earth's surface with highly variable albedos (with respect to 25 nm gridpoint areas) and the tendency toward clear skies in arid, high albedo areas. The procedure works very well in darker areas which comprise about 99 percent of the earth's surface.

6.3 Special considerations. The cloud decision procedure already described provides accurate and reliable results. Certain anomalies in the solar illumination and surface reflectivity, however, can result in erroneous analyses unless the anomalies are properly identified or treated.

6.3.1 Snow. The presence of snow at a gridpoint renders a visual analysis useless. Present techniques cannot discern clouds from a bright background caused by snow or ice. This limitation dictates an accurate determination of snow and ice areas. Snow cover data are available to the visual data processor at the 25 nm resolution from the AFGWC Snow Analysis Program (SNODEP, Luces, 1975). The snow data base is updated daily and provides a reasonable indication of snow presence. Sea ice information is also available from the 3DNEPH geography data base and is updated weekly from data provided by the Navy. See the appendices for details. Whenever snow or ice is present at a gridpoint, the visual data processor does not make a cloud amount calculation and defaults to storage of a missing indicator in the output data. The impact of this limitation is shown graphically in Figure 16. It must be noted, however, that a wintertime hemisphere (with an abundance of snow) has poor solar illumination in polar latitudes resulting in rejection of large areas independent of snow presence or absence.

6.3.2 Sunglint. Sunglint is a very bright area resulting from reflection of the sun from the earth's surface into the satellite's visual sensor. This is a highly variable process with the degree of brightness depending on time of day, time of year, location, surface conditions, and sensor sensitivity. The impact of sunglint on the 3DNEPH visual satellite data processor can be an erroneous analysis of clouds over a clear sunglint area. Techniques have been developed which minimize the

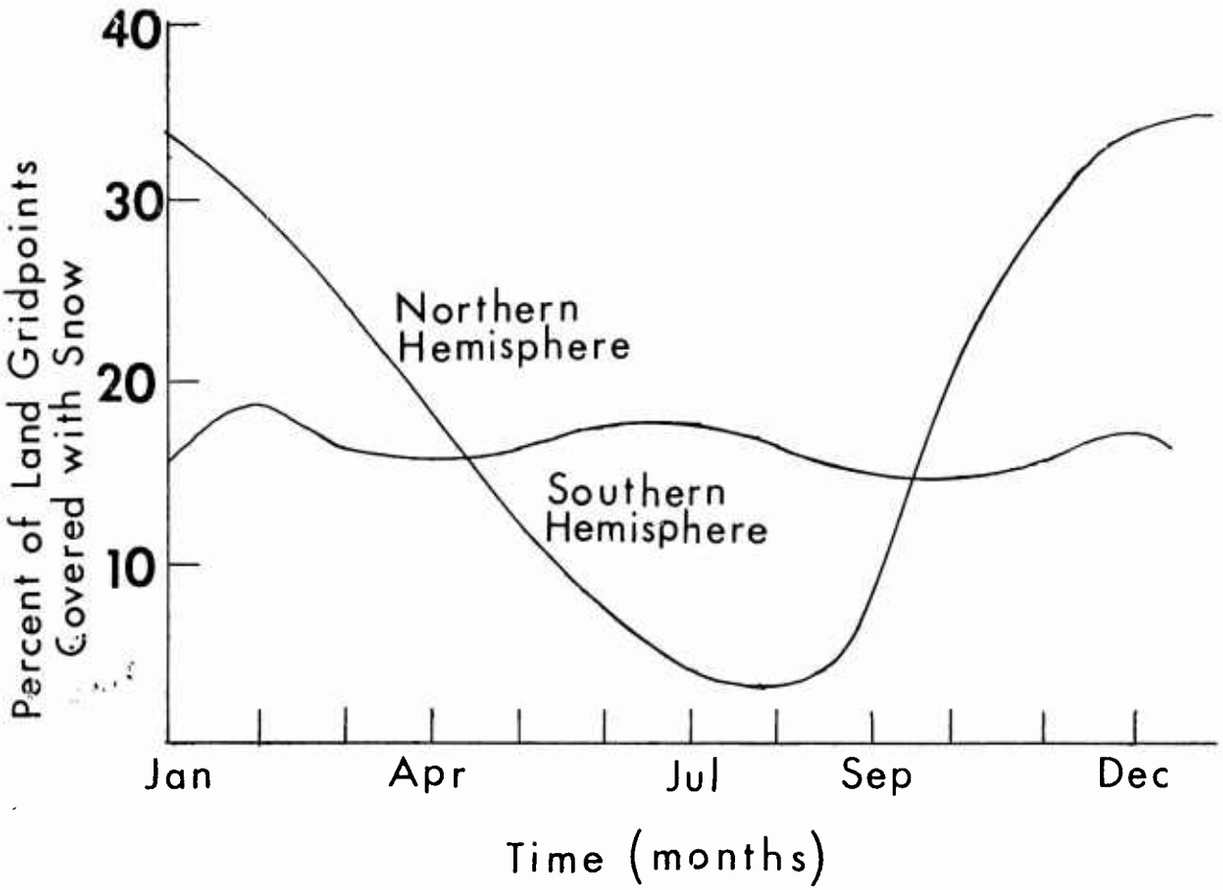

Figure 16. Frequency distributions of the percent of snow-covered 25 nm gridpoints as a function of time of year and hemisphere. Snow-covered gridpoints are not analyzed by the visual satellite data processor.

effects of sunglint. Treatment of sunglint consists of trimming and discarding intensely bright sunglint areas or substitution of a cloud threshold grayshade for the threshold otherwise available from equation 5. Both procedures require knowledge of various angular relationships among the satellite, sun, and local point on the surface. These angles are available or can be derived from data stored in the Satellite Global Data Base. Definitions of the angles are given in the appendices.

6.3.2.1 Trimming. The trimming procedure involves specification of zenith and/or scan (look) angles and discarding all gridpoints which exceed these angular threshold limits. Trimming is often necessary for satellites with early morning sun-synchronous orbits. Sunglint becomes severe on the east (sunward) side of the orbital data strip and may require deletion of data strips several hundred nautical miles wide (up to 20 percent of the data). Trimming is also employed in the vicinity of the terminator to exclude excessively dark areas.

6.3.2.2 Grayshade substitution. Grayshade threshold substitution is applied in areas of sunglint potential as determined from sunglint "cones." Sunglint cones are derived from the scan and zenith angles and represent the sensor's angle from perfect reflection. (see the appendix). A critical cone angle is manually identified for each satellite and is used as a yes/no threshold for implementation of the cloud threshold substitution. The cloud threshold used within the critical cone area is obtained manually and represents the brightest grayshade observed in clear areas. This procedure limits the sensitivity to small-scale clouds or other clouds exhibiting darker pixel grayshades.

7. CONVENTIONAL DATA PROCESSOR

The conventional data processor takes surface, aircraft, and upper air reports from the AFGWC data base; sorts, screens, and combines reports to produce a gridded eighth-mesh data base of cloud information. This data base, known as the best reports file, contains only gridpoints for which data are available and is in 3DNEPH format - including the vertical levels. Figure 17 shows the overall flow of the process. Table 4 provides an idea of the quantity of data processed.

7.1 Surface data processor. The surface data processor determines cloud amounts for the 15 layers of 3DNEPH from several sources of validated surface reports.

7.1.1 Data types and time considerations. Cloud data are extracted from synoptic, METAR, and Airways coded reports. If more than one type of report is available at a given time, all unique information from both reports is used to produce a composite report. Conflicting information is resolved with consideration for data timeliness and implicit data quality. Layered cloud data from Airways and METAR reports are given a

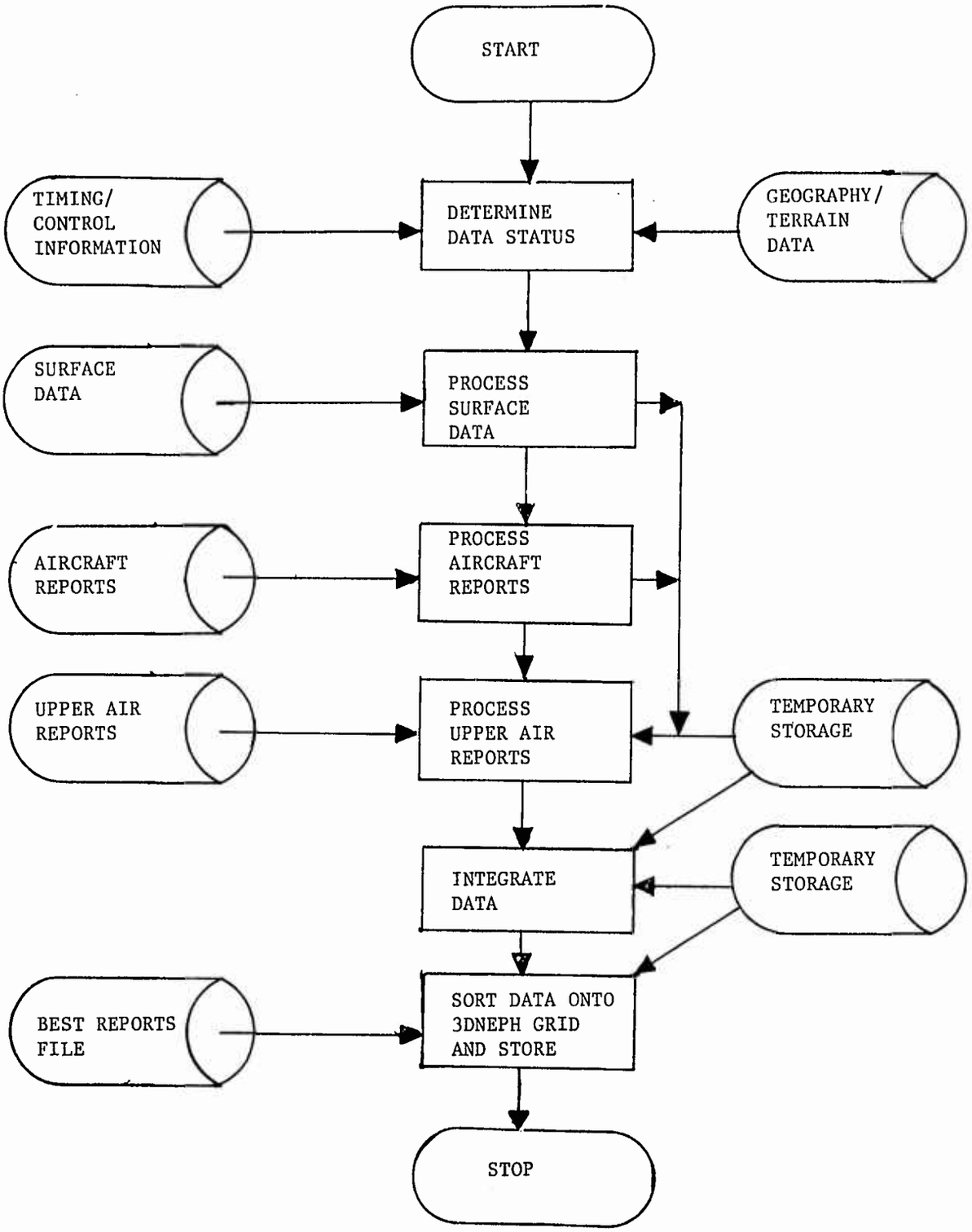

Figure 17. Functional flow chart of the conventional data processor.

TABLE 4. TYPICAL NUMBERS OF CONVENTIONAL REPORTS RECEIVED BY 3DNEPH, BY 3DNEPH BOX, TIME, AND HEMISPHERE. THESE REPORTS ARE INTEGRATED TO PRODUCE "BEST REPORTS."

	N.H. VALID TIMES								S.H. VALID TIMES			
BOX	0Z	3Z	6Z	9Z	12Z	15Z	18Z	21Z	03Z	09Z	15Z	21Z
2	0	0	0	0	0	0	0	0	0	0	0	0
3	10	12	17	18	15	14	3	2	0	0	0	1
4	37	50	49	48	45	45	21	22	7	1	9	7
5	14	19	19	22	18	23	5	2	35	11	33	41
6	6	13	13	14	12	21	10	11	11	2	8	14
7	0	0	0	0	0	0	0	0	2	0	2	2
9	1	1	0	1	1	1	0	0	0	0	0	0
10	18	21	14	16	11	11	4	6	1	1	0	1
11	44	51	50	54	42	38	12	14	2	2	1	2
12	337	340	315	336	308	237	198	284	2	0	2	2
13	70	101	124	100	82	118	59	58	76	41	98	100
14	28	36	21	27	40	83	28	29	56	20	76	79
15	0	0	3	6	4	5	5	6	19	10	26	24
16	0	0	0	0	0	0	0	0	0	0	0	0
17	7	7	6	6	4	3	3	3	0	0	0	0
18	10	12	11	9	7	7	3	3	9	6	5	8
19	234	251	250	242	163	157	120	124	1	0	0	0
20	515	547	537	563	570	518	498	532	0	0	0	0
21	384	282	364	364	448	446	418	396	58	38	66	68
22	145	146	157	174	181	191	156	147	5	1	9	7
23	6	6	22	28	18	20	8	5	0	0	1	1
24	5	6	5	14	15	19	9	9	0	3	2	2
25	0	0	0	0	0	0	0	1	4	4	1	4
26	8	13	9	8	5	4	1	5	10	8	4	10
27	76	90	83	86	48	59	32	41	0	0	0	0
28	175	133	146	185	204	210	205	201	0	0	0	0
29	344	287	352	371	402	401	394	396	7	0	8	11
30	770	798	896	857	794	869	868	841	0	1	1	2
31	24	18	19	38	31	32	31	29	1	4	3	3
32	0	4	25	42	39	44	39	34	3	5	3	2
33	1	2	1	2	0	0	0	0	12	7	6	13
34	26	26	14	16	13	14	21	27	13	20	17	24
35	55	79	50	52	35	40	41	63	18	32	24	30
36	133	128	105	101	100	113	131	134	2	0	1	1
37	71	67	70	83	94	102	99	99	3	3	3	3
38	423	395	514	564	566	624	572	598	0	4	2	2
39	35	38	50	56	51	52	49	50	24	124	92	107
40	18	39	40	46	47	62	55	54	8	20	16	12
41	0	0	0	0	0	0	0	1	2	1	0	2
42	3	2	0	0	2	2	4	8	17	23	17	26
43	166	167	141	115	109	158	164	177	50	51	46	39
44	448	435	387	353	426	459	459	455	3	10	7	4
45	242	236	192	187	250	267	233	258	2	2	0	0
46	15	16	8	12	21	38	21	30	4	8	4	4
47	13	19	21	35	39	46	43	49	19	60	42	16
48	0	0	4	15	11	16	16	15	21	25	19	17
49	0	0	0	0	0	0	0	0	0	0	0	0
50	0	0	0	0	0	1	0	1	12	8	6	7
51	20	22	16	11	13	21	25	32	24	26	14	14
52	213	217	168	155	203	228	221	221	14	18	11	12
53	75	84	50	47	92	120	87	102	2	3	4	0
54	7	11	3	3	7	13	8	13	3	3	0	0
55	0	0	0	0	0	3	0	2	1	3	5	4
56	0	0	0	0	0	0	0	1	0	0	0	0
58	0	0	0	0	0	0	0	0	3	1	1	1
59	0	1	0	0	0	0	0	0	8	11	7	5
60	24	28	7	6	14	30	25	28	34	33	28	18
61	64	39	11	21	52	71	66	66	1	2	1	0
62	11	8	7	5	11	12	20	15	2	2	1	1
63	0	0	0	0	0	0	0	0	0	0	0	0
TOTAL BEST REPORTS	5331	5303	5366	5514	5663	6068	5490	5700	625	658	732	753
UNCOMBINED REPORTS	12802	12393	12004	12575	13781	14990	13951	13687	1144	1032	1501	1410

higher ranking than synoptic cloud data except when layered data are given in synoptic supplementary data. All surface cloud data are ranked above upper air sounding data. All hourly and special surface reports valid since 3 hours before the analysis valid time are considered (6 hours before the valid time for the Southern Hemisphere). Figure 18 shows the typical flow of data into AFGWC.

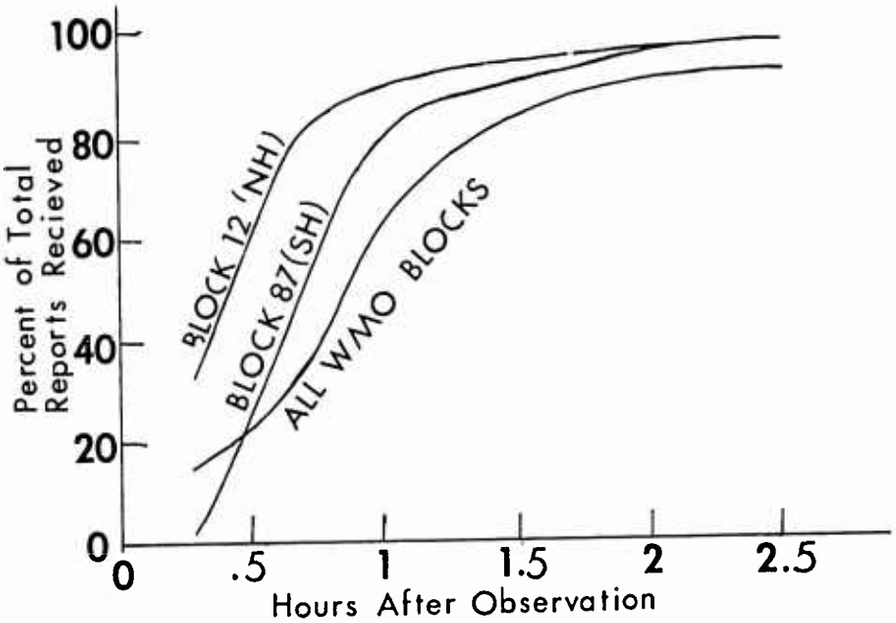

Figure 18. Graphic representation of conventional data flow into AFGWC. Selected areas are shown as typical examples. World Meteorological Organization (WMO) Blocks represent particular areas of the world.

7.1.2 Present weather. Present weather is converted to a weather factor (KWEA) and used to determine cloud layers and types. Table 5 shows the conversion to KWEA. The most significant present weather element is included as an independent parameter in the 3DNEPH data base.

7.1.3 Layered cloud data. These data are stored directly into the corresponding 3DNEPH layer when cloud bases and amounts are specified in the reports. Scattered, broken, and overcast cloud amounts are assigned 25, 75, and 100 percent coverage, respectively. Cloud amounts reported above an overcast layer are set to missing.

7.1.4 Special considerations for synoptic data. Synoptic data contain limited cloud information about layered amounts. The only layered data are the amount of all low or middle clouds and the base of the lowest clouds visible.

If more than one low or middle cloud layer is observed, the synoptic reports do not contain sufficient information to define each layer. The following procedures are used with synoptic reports:

TABLE 5. CONVERSION OF PRESENT WEATHER TO WEATHER FACTOR.

Type of Weather	WW (WMO Code 4617)	KWEA
--	0-9	0
Mist	10	1
--	11-14	0
Precipitation in sight	15	1
Precipitation in sight	16	2
Thunder	17	2
Squalls	18	2
Funnel clouds	19	3
Drizzle, past hour	20	1
Rain/Snow, past hour	21-22	1
Rain/Snow, past hour	23	2
Freezing drizzle/rain, past hour	24	1
Rain/Snow showers, past hour	25-26	2
Showers (hail/rain/snow), past hour	27	2
Ice fog, past hour	28	0
Thunderstorm, past hour	29	2
--	30-49	0
Drizzle	50-59	1
Rain	60-69	2
Snow	70-79	2
Showers	80-89	2
Thundershowers	90-99	3

7.1.4.1 Layered amounts. Only cloud height categories are determined from synoptic data. These categories are low (surface to 6500 ft above the ground), middle (6500 to 22000 ft MSL), and high (above 22000 ft MSL). Cloud amount probabilities are assigned to height categories based on the lowest cloud reported and the types of clouds.

(a) If a cloud type is not observed, zero percent probability is assigned to the corresponding height category.
(b) When a valid cloud type is given, 100 percent probability is assigned.
(c) For a missing cloud type, 50 percent probability is assigned.

Actual layered cloud amounts are then computer based on the total sky cover, if available, using the assumption that clouds are randomly distributed. If sky cover, low and middle cloud amounts are missing, synoptic data are discarded.

7.1.4.2 Cloud bases. The base of clouds in the three height categories may be calculated as follows:

(a) Base of low clouds (H_L) in feet AGL:

$$H_L = 2200 - (300 \times KWEA) \quad (6)$$

(b) Base of middle clouds is set at 10000 feet AGL.
(c) Base of high clouds (H_H) in feet AGL:

$$H_H = 35000 - 13000(Latitude/90) \quad (7)$$

7.1.5 Surface obscurations. Clouds are assigned to the first 3DNEPH layer with cloud base at terrain level if a report indicates fog and/or visibility less than one mile (1600 meters). The cloud amount is determined from the type of fog and layer depth is determined from the horizontal visibility. Higher clouds are allowed if no obscuration (-x or x) is reported. For a total obscuration, 100 percent coverage is assumed with the base equal to the vertical visibility. If the vertical visibility is missing, the cloud base is computed as a function of the present weather.

7.1.6 Thin clouds. Thin clouds may be reported in the Airways code. Such information is stored in the Best Reports File and is useful in computing cloud thickness.

7.1.7 Vertically developed clouds. Cumulonimbus clouds and thunderstorm phenomena result in cloud placements of the reported amount in the low category, 80 percent of the low amount in the middle category, and 64 percent of the low amount in the high category. For towering cumulus and rainshowers, clouds are assigned to the middle category at 80 percent of the amount reported in the low category.

7.1.8 Total sky cover. When specified in a report, the total sky cover is stored and retained through all subsequent processing. When unavailable, statistical summing (using a randomness summing method) of cloud layer amounts is used to arrive at a total cloud amount.

7.1.9 Cloud tops. The height of cloud tops is obtained empirically from equation 8:

$$T_1 = B_1 + D_k + S_k(B_1 + H) + A\ (D_{k+1}) + S_{k+1}(B_1 + H) \quad (8)$$

Where T_1 is the cloud top height of layer 1 in feet above MSL, B_1 is the reported base of the cloud above terrain, D_k is a cloud thickness factor (from Table 6), S_k is a cloud coefficient related to KWEA, H is the local terrain height in feet, A is the layer cloud amount in tenths, and the index, k, is a function of the weather factor (KWEA) and cloud amount. The relationship between k, D_k, and S_k is given in Table 6. Cloud tops are routinely computed by an alternate method and the final cloud top is chosen from the maximum height of the two methods. The alternate method is based exclusively on KWEA. If KWEA = 1, tops are 9,000 feet. If KWEA = 2, tops are 14,000 feet. If KWEA = 3, tops are computed as follows:

$$T = 40000 - 10000(\text{Latitude}/90) \quad (9)$$

where the latitude is in degrees and T in feet.

7.2 Upper air data processor. Upper air data are provided in an integrated AFGWC data base containing reports from RAOBs, rawinsondes, dropsondes, rocketsondes, and satellite soundings. These reports are screened and used to locate layered clouds by performing a moisture analysis of the available data. The stepwise procedure for cloud amount determination is described in the following paragraphs.

TABLE 6. RELATIONSHIP BETWEEN EMPIRICAL CLOUD THICKNESS CALCULATION PARAMETERS k, D_k, S_k.

k	D_k	S_k
1	0	0
2	1287	.13108
3	2843	.25523
4	4323	.41947
5	5864	.62827
6	7636	.87444
7	9843	1.11910

7.2.1 Missing data. Where not specified in the data base, heights are computed using the hydrostatic equation. Temperature-dew point spread values are computed when required according to:

$$T - T_d = 0.285(T - 273) + 20.6 \qquad (10)$$

where T is the temperature in Kelvin degrees and T_d is the dew point in Kelvin degrees.

7.2.2 Midpoint values. Pressure, temperature and temperature-dew point spread are computed for the midpoint of a 3DNEPH layer by interpolating between adjacent reported levels. Midpoint values of MSL layers are computed directly and midpoint values for the terrain-following layers are computed by subtracting the station elevation from the report height.

7.2.3 Condensation Pressure Spread (CPS). The CPS, defined as the pressure change required for a parcel to attain saturation, is computed from the pressure, temperature and temperature-dew point spread for each layer and is used to relate atmospheric moisture content to cloud amount. The uncorrected CPS, C_u, is given as an approximation by: (Edson, 1965)

$$C_u = (T - T_d)_1\left(-4.9 - 0.93\left(\frac{P_1}{1000}\right) - 9.0\left(\frac{P_1}{1000}\right)^2\right) \qquad (11)$$

where C_u, T, and T_d were defined previously, and P_1 is the pressure at the midpoint of a layer 1.

7.2.4 Cloud amount from CPS. Finally, the cloud amount is found from a CPS-cloud amount conversion table derived by Edson (1965). Use of the tables requires calculation of an index, I, as follows:

$$I = 0.5\ KC_u + 1.5 \qquad (12)$$

where K is a correction factor based on temperature at the midpoint of a layer. Figure 19 shows the CPS-cloud amount relation described by Edson. Separate curves are provided for the 850, 700, 500, and 300 mb levels.

7.3 Aircraft data processor. The aircraft data processor computes total and layered cloud amounts from various types of validated aircraft reports (RECCO, COMBAR, ICAO, and MAC abbreviated). Three types of coded information are used: flight weather (Table 7), flight condition (Table 8), and explicit cloud layer data. Total and layered cloud amount decisions are described below.

7.3.1 Total cloud amount. The following decisions determine the total cloud cover:

(a) If the flight condition is clear (coded 1), the total cloud amount is set to zero percent.
(b) If the flight condition is coded 5, 9, or 18, the total cloud amount is set to 100 percent.
(c) If flight weather is coded 5, 6, or 7, the total cloud amount is set to 100 percent.

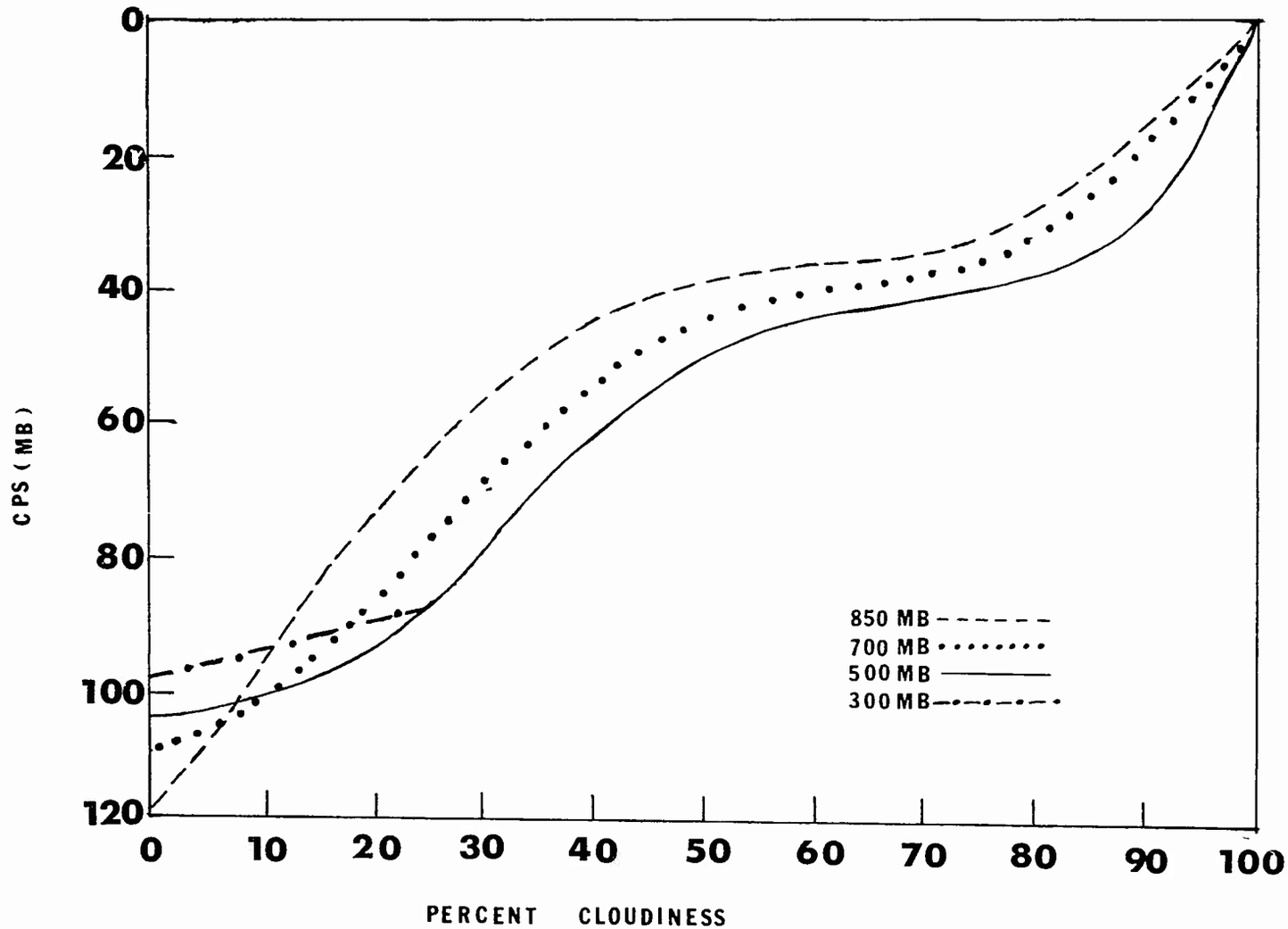

Figure 19. Relationship between Condensation Pressure Spread (CPS) and cloud amount for various levels of the atmosphere.

(d) If the cloud amount in a reported layer is overcast, the total cloud amount is set to 100 percent.
(e) If none of the above are available, the total cloud amount is set to missing.

TABLE 7. AIRCRAFT FLIGHT WEATHER

Code Figure	Weather
0	Clear (no clouds at flight level)
1	Partly cloudy (scattered or broken)
2	Continuous layer(s) of cloud(s)
3	Sandstorm, duststorm, or storm of drifting snow.
4	Fog, thick dust, or haze
5	Drizzle
6	Rain
7	Snow or rain and snow mixed
8	Shower(s)
9	Thunderstorm(s)
10	Lightning
11	Scattered clouds
12	Broken clouds

7.3.2 Layered cloud amounts. Layered cloud data are rather limited in aircraft reports and when available, usually describe only a few layers in the vicinity of the aircraft. The following decisions can be made from the flight condition code:

(a) If coded 11 or 12, all layers above the flight level are set to zero percent.
(b) If coded 15 or 16, all layers below the flight level are set to zero percent.

(c) If clear at flight level, all layers are set to zero percent.

Specific reported cloud layer amounts are assigned directly to the appropriate 3DNEPH layers. If bases or tops are available, but the amount is missing, a cloud amount of 60 percent is assumed. If inconsistencies develop because two or more coded report types are contained in a single aircraft report, specific layered information is given highest priority followed by flight condition reports and flight weather reports.

TABLE 8. AIRCRAFT FLIGHT CONDITION

Code Figure	Flight Condition
0	Total amount of cloud less than 1/8.
1	Total cloud amount at least 1/8, with either 1/8-4/8 above or 1/8-4/8 below, or a combination thereof.
2	Cloud amount more than 4/8 above and 0-4/8 below.
3	Cloud amount 0-4/8 above and more than 4/8 below.
4	Cloud amount more than 4/8 above and more than 4/8 below.
5	Chaotic sky - many undefined layers.
6	In and out of clouds, on instruments 25% of time.
7	In and out of clouds, on instruments 50% of time.
8	In and out of clouds, on instruments 75% of time.
9	In clouds all of the time, continuous instrument flight.
10	Clear (no clouds at any level).
11	Above clouds (tops less than 10000 ft).
12	Above clouds (tops 10000-18000 ft).
13	Above clouds (tops above 18000 ft).
14	Below clouds (bases less than 10000 ft).
15	Below clouds (bases 10000-18000 ft).
16	Below clouds (bases above 18000 ft).
17	Between broken or overcast layers.
18	In clouds.
19	In and out of clouds.

7.4 Decision tree processor. The decision tree processor integrates surface, upper air, and aircraft data such that only one report, containing the best information from possible multiple reports, is given per gridpoint. When two or more conventional reports are within a 15 nm radius of an eighth-mesh gridpoint, a single report must be selected or the reports must be integrated to produce a single best report. A final module of this processor sorts the integrated reports to produce an ordered data base in 3DNEPH eighth-mesh format.

7.4.1 Best surface report selection. A single report may be selected using the following decision criteria:

(a) The report with the largest total cloud amount is used.
(b) If the reports have identical total cloud amounts, the report with the lowest cloud layer is used.
(c) If total cloud cover for the lowest cloud layer are the same the report received last by 3DNEPH is used.

7.4.2 Merging surface reports. The most recent report is used and if an overcast layer is reported, any available reports up to 3 hours old (6 hours in the S.H.) are searched for additional cloud information above the overcast layer. Multiple overcast layers are allowed.

7.4.3 Integration of all conventional data. The following decisions are made when two or more conventional reports influence a single gridpoint (Table 9 illustrates the process).

TABLE 9. ILLUSTRATION OF CONVENTIONAL DATA INTEGRATION BY THE 3DNEPH. (THE RAOB DATA HAD NO INFLUENCE IN THIS CASE)

3DNEPH Parameters	Surface Data	Aircraft Data	RAOB Data	Integrated Report
Total Coverage	100%	100%	-	100%
Lyr 15 Amount	-	0	-	0
Lyr 14 Amount	-	0	-	0
Lyr 13 Amount	-	0	-	0
Lyr 12 Amount	-	0	-	0
Lyr 11 Amount	100	0	0%	0
Lyr 10 Amount	100	100	0	100
Lyr 9 Amount	0	-	20	0
Lyr 8 Amount	0	-	20	0
Lyr 7 Amount	0	-	C	0
Lyr 6 Amount	0	-	0	0
Lyr 5 Amount	45	-	80	45
Lyr 4 Amount	45	-	80	45
Lyr 3 Amount	0	-	0	0
Lyr 2 Amount	0	-	0	0
Lyr 1 Amount	10	-	0	10
Low Cloud Type	ST	-	-	ST
Middle Cloud Type	AS	-	-	AS
High Cloud Type	-	0	-	0
Present Weather	FOG	0	-	FOG
Minimum Base	0	-	-	0
Maximum Top	-	13,000 ft	-	13,000 ft

(a) The process begins with the surface report as the initial report. Surface data are ranked highest below 10000 ft MSL.
(b) Data from aircraft reports are integrated into layers above 10000 ft.
(c) Upper air reports are stored for those layers without information.

7.4.4 Best Reports File. The final function of the decision tree processor is the sorting and storage of the reports in the Best Reports File. This file is retained for about 3 hours in the computer and then saved on tape for 24 hours. It is especially useful for quality control and correlation with other data sources. Operationally, the file is used by the data integration processor where it is merged with satellite and continuity data.

8. DATA INTEGRATION PROCESSOR

The data integration processor performs the final processing of cloud information collected to this point in the production cycle. This processor merges visual and infrared satellite data; converts satellite analyses to the 3DNEPH analysis format; merges satellite, conventional and continuity data; and performs meteorological consistency checks.

8.1 Final satellite data processing. Satellite analyses consist of visual and infrared sensed cloud amounts and infrared modal heights. Mutual (visual and infrared) or independent cloud types are also available. Such data must now be converted to specific cloud layer amounts and heights and data conflicts must be resolved. Data up to 4 hours old (7 hours in S.H.) are considered in the following decision process.

8.1.1 Total cloud cover. When both visual and infrared estimates of total cloud cover are available at the same gridpoint, an immediate check of their ages is made. If different, the oldest data are discarded; however, the data are practically always the same age (coincident data from the same satellite). The analysis with the greatest cloud cover is retained when the ages are the same. This decision is made to retain high, thin clouds which are more frequently detected by infrared sensors. Low clouds, which are more easily detected by the visual sensors, are also retained through this decision.

8.1.2 Cloud top height. The modal heights determined by the 3DNEPH infrared data processor are directly usable as cloud top height. In addition, the height of the highest (coldest) mode becomes the maximum cloud top for that gridpoint.

8.1.3 Cloud layer amount. The percent cloud cover in the coldest mode (closest to the satellite) is taken directly as the layer amount. If two modes are identified, the modal amount given in the warmer (lower cloud) mode must be adjusted in consideration of clouds hidden to the satellite's view by the first layer. This adjustment is given by:

$$P_z = 100 \times \frac{A_z}{100-A_1}, \quad A_1 \neq 100 \tag{13}$$

where P_z is the percentage of cloud in the second (warmer) mode, A_1 is the percent cloud in the first mode, and A_z is the uncorrected second mode cloud amount in percent.

8.1.4 Cloud thickness and cloud bases. The cloud bases are computed by subtracting cloud thickness from the cloud top. Cloud thickness is determined as a function of the layer cloud amount and layer cloud top (see Table 10).

TABLE 10. CLOUD LAYER THICKNESS AS DETERMINED FROM INFRARED DATA CONTAINING A SINGLE MODE

Mode Height(ft)	Layer Thickness	Layer Amount(A_1)
Less than or equal to terrain height	0	0
Above terrain but less than 18,000 ft	$3000 \times \frac{A_1}{100}$	A_1
Above 18,000 ft	$4000 \times \frac{A_1}{100}$	A_1

8.2 Data integration. Combined satellite and conventional data are integrated with a continuity field to complete the cloud analysis. The continuity field is nothing more than the previous or latest 3DNEPH analysis available, and is used primarily to fill in for missing data and parameters. As a general rule, timeliness governs the integration process and determines which data type will dominate.

8.2.1 Conventional data spreader. Conventional data in the Best Reports File for a single gridpoint are spread to influence surrounding gridpoints as a prelude to actual integration. The spreading algorithm is a weighting function adapted from Barnes (1964). The weight (W) to be applied at a neighboring gridpoint is given by:

$$W = 1/\left(1 + 48\ (R/R_S)^2\right) \tag{14}$$

where R is the distance of the gridpoint from the report location and R_S is computed from:

$$R_S = 25/D_R \tag{15}$$

where R_S is a scan or search radius and D_R is calculated for each gridpoint containing a report and is a function of the number of reports within a distance of four gridpoints. These weights are used to modify the cloud coverage of the conventional data.

8.2.2 Merging satellite, conventional, and continuity data.

8.2.2.1 Total cloud cover. The satellite data are dominant in the merging process if within two hours of the analysis time and if the total

cloud coverage is 55 percent or greater. Under these circumstances, conventional and continuity data are first combined followed by the dominant satellite data. If the tests of the satellite data are not satisfied, information obtained from conventional data is used as the final total cloud amount. This does not hold if the conventional report contains only high clouds. If conventional data are not available; however, visual satellite cloud amount data will be used only if cloud height data from infrared or continuity data are available within a radius of 6 gridpoints.

8.2.2.2 Cloud height. Cloud heights are used as developed during previous processing. One exception is the height adjustment made when cumulonimbus (Cb) clouds are present. If the Cb's were detected from visual data alone, i.e., infrared data not available, the Cb tops are set at 40,000 feet MSL. When infrared data are available, a check insures the tops are between 22,000 and 55,000 feet. If surface data are unavailable, Cb bases are set at 2,000 feet above the ground.

8.2.3 Meteorological consistency. As a final step before storage in the AFGWC data base, each gridpoint is checked and adjusted, as appropriate, for the following:

(a) Agreement between cloud layer amounts and total cloud cover.
(b) Total cloud cover, present weather, and cloud type agreement.
(c) Agreement among minimum base, maximum top, and cloud layer heights.

9. MANUAL DATA PROCESSOR

The manual data processor of the 3DNEPH takes input provided from a digital encoding table and alters the 3DNEPH data base according to coded instructions in the input. The most important aspect of the procedure is that meteorological consistency can be maintained despite alternations of cloud layers and types over large areas.

9.1 Concept. Human alteration of the 3DNEPH data base is an ultimate form of quality control. Meteorological analysts monitor portions of the 3DNEPH output and provide real time correction whenever errors are detected. This procedure insures the finest overall quality of the cloud analysis for all users and also provides valuable feedback to programmers and managers.

9.2 Procedure. Continuous monitoring of the cloud analysis is usually accomplished with the window mode of operation. These limited area nephanalyses are evaluated by comparing printed displays with corresponding satellite data and surface data (if available). If a correction is desired, the cloud display is placed on a digital encoding table and the erroneous area is delineated with a special cursor. A change instruction is provided via a keyboard and accompanies the area perimeter information to the main computer. Here the 3DNEPH manual data processor interprets the instruction, computes the proper location in the 3DNEPH grid, and finally applies the correction to the window data base. Simultaneously, the instructions and perimeter data are stored for the next

scheduled 3DNEPH hemispheric analysis. The corrections are later applied to the hemispheric data base (with certain restrictions) followed by a purge of all instructions. The cycle is then repeated. Alterations can be made to the 3DNEPH hemispheric data base directly, if desired.

9.3 Change instructions. A special table relating cloud types to specific 3DNEPH layers insures meteorologically consistent adjustments of the data base. The analyst, therefore, does not have the overwhelming task of specifying every layer to be changed. Table 11 shows the relationship between the cloud types specified by the analyst and the affected layers. In addition to the cloud type (and implied layers), the analyst specifies a cloud amount change. If preceded by a "+", that cloud amount is added; if preceded by a "-", that cloud amount is deleted from the pre-existing analysis amount. Without a plus or minus sign the appropriate layers are overwritten by the specified amount. See the examples with the table.

10. QUALITY CONTROL PROCEDURES

10.1 Concept. Quality control of the 3DNEPH is very difficult because of the real time nature of 3DNEPH and its multifaceted auxiliary activities. Large volumes of data and multiple data types also increase the difficulty of the tasks. A quality control program for 3DNEPH must identify (and correct where possible) erroneous analyses as they occur, determine their cause to prevent repetition of the error, and provide documentation which keeps real time as well as archive users informed of problems and efforts to correct them. Long-term problems and analysis biases must also be identified, especially for archive users. The quality control program for 3DNEPH satisfies these objectives with a balanced set of objective (automated) and subjective procedures supported by frequent, timely documentation.

10.2 Objective procedures. Several automated quality control programs operate within the 3DNEPH system to provide meaningful statistical and display output. The programs can be started manually by the programmer/user or automatically by the 3DNEPH. The automated quality control programs are described in the following paragraphs:

10.2.1 Built-in consistency checks. A processor built into the 3DNEPH checks each analysis for meteorological consistency before it is stored in the data base. This is described in section 8.2.3.

10.2.2 Independent consistency checks. An independent program performs the same checks as above. When an error is detected, this program prints all available information about the gridpoint as well as nearby conventional reports from the Best Reports File. It is also capable of restoring the corrected analysis in the data base.

10.2.3 Geography/Terrain checks. The geography/terrain fields are checked periodically by counting gridpoints of certain types and comparing with prespecified numbers. If the numbers do not match, a message is sent to the computer operator followed by a detailed printed explanation.

TABLE 11. RELATION OF ANALYST SPECIFIED CLOUD TYPES AND RESULTANT CHANGES TO 3DNEPH LAYERS

3DNEPH Layers	Cloud Input	Cloud Description	Modification to Layers: Zero Layers	Add x/8	Add x/8	Subtr. x/8
1 SFC-150 ft						
2 151-300	ST	Low ST/Fog	1-8	4,5	4,5	1-8
3 301-600						
4 601-1000	CU	TCU/CB	1-12	7-10	7-10	1-12
5 1001-2000						
6 2001-3500	SC	SC/CU	1-8	6-8	6-8	1-8
7 3501-5000						
8 5001-6500						
9 6501-10000	AS	Thin AS	9-12	10	10	9-12
10 10001-14000						
11 14001-18000	AC	Thick AC	9-12	10,11	10,11	9-12
12 18001-22000						
13 22001-26000	CI	Thin CI	13-15	13	13	13-15
14 26001-35000						
15 35001-55000	CS	Thick CS	13-15	13,14	13,14	13-15

EXAMPLE: Input	Resultant Modification
ST = +3	Add 3/8 cloud to layers 4 and 5.
SC = 5	Zero-out layers 1 to 8 and insert 5/8 cloud in layers 6 to 8.
ST = -1	Subtract 1/8 cloud from layers 1 to 8.

10.2.4 Background brightness checks. The background brightness fields are analyzed statistically and output provided for the programmer which gives minimum, maximum, and average background grayshades for each satellite. A grayshade distribution chart and a count of snow-covered gridpoints are also provided on a box by box basis. This program is run about twice a week and output is saved indefinitely to provide a basis for comparing new statistics.

10.2.5 Analysis evaluation. A correlation program is routinely run to compare 3DNEPH output with conventional surface reports. Various statistics, including a correlation coefficient, are displayed in the output. The comparison is made box by box to isolate regional difficulties. This correlation analysis is not meaningful in assessing the 3DNEPH's validity because the correlated surface reports are a part of the 3DNEPH analysis. However, it does provide valuable insight into the interaction of surface and satellite data and is successful at flagging severe analysis problems, from whatever the cause.

10.2.6 Operational diagnostic output. Each 3DNEPH analysis run produces a diagnostic print containing key statistics about raw data availability and assimilation by 3DNEPH. Many grayshade, temperature, and data count statistics are displayed from satellite data processing including a printed map showing the location and origin of satellite data. Numerous quantitative, gridded displays of virtually all 3DNEPH inputs, outputs, and internal parameters may be selected as desired as part of the diagnostic output.

10.2.7 Satellite data control. An independent program precedes each 3DNEPH to search the SGDB for new satellite data. During the search process, data sources are screened for validity. Unauthorized data (according to a pre-specified list) are eliminated from subsequent 3DNEPH processing and the computer operator is notified. Complete satellite data inventories and charts of data location are provided in printed format.

10.3 Subjective procedures. To a degree, all the objective quality control function described previously require human judgement and action of some type. On the other hand, none of the procedures are entirely subjective. Many programs are used to make displays and effect changes to the data base. The following quality control operations require human input:

10.3.1 Manual correction. The manual data processor described in section 9 is the most important quality control operation as it provides immediate corrective feedback. The limitations of this procedure are the expense in terms of manpower and the fact that not every part of 3DNEPH analyses is checked.

10.3.2 Hemispheric error log. A log of errors as detected by meteorological analysts is maintained for the hemispheric 3DNEPH analyses. The log contains details about the location, extent, and nature of the error. A subjective statement of usability of the data is also given. All hemispheric analyses - Northern and Southern Hemispheres - are evaluated in this log.

10.4 Quality control documentation. A monthly document, the "3DNEPH Archive Journal", is prepared at AFGWC which contains the hemispheric error log, a summary discussion of the errors, and a milestone log describing in detail changes to the production 3DNEPH and anticipated/ actual impact on the output. Information about the status of satellites, satellite data quality, and planned 3DNEPH improvements are also discussed. A copy of the journal is mailed to USAFETAC to support the archived data and a copy is retained at AFGWC. This journal rounds out a comprehensive quality control program.

11. APPLICATIONS

Applications of the 3DNEPH cloud analyses are virtually unlimited. The high resolution, frequency, and global coverage of the analyses are features which satisfy practically any user requirement. There are three principle application areas - automated applications, manual use of displays of the data base, and applications of archived data.

11.1 Content of the output data. The 3DNEPH provides detailed cloud information plus an indication of the present weather. Table 12 describes the output in detail.

11.2 Automated application. Once stored in the AFGWC data base, almost all operational programs at AFGWC have access to the 3DNEPH data base. The various uses by AFGWC programs are too numerous to mention. Some general examples are given below.

(a) The most obvious application of 3DNEPH is a cloud forecast. 3DNEPH data can be compacted to provide an initial and verification cloud field for cloud forecast models of any resolution.
(b) Cloud cover in various levels of the atmosphere can be converted to moisture content and used by numerical forecast models requiring moisture content and used by numerical forecast models requiring moisture data.
(c) Programs which compute solar insolation (as a function of cloud cover) at the surface for crop growth assessment and other applications are satisfied by the frequency and resolution of 3DNEPH.
(d) Analyses and forecasts of rainfall and snow use present weather, cloud type, and the general extent and duration of cloud cover found in 3DNEPH analyses.
(e) Programs supporting flight operations can use 3DNEPH analyses for near real time cloud information.

11.3 Display capabilities for manual applications. Several display programs are used to display 3DNEPH data in a variety of forms. Displays are used within AFGWC to satisfy many operational requirements and to quality control the 3DNEPH. Several of the display program capabilities are described here with sample displays.

TABLE 12. DESCRIPTION OF 3DNEPH OUTPUT DATA. (WMO CODES DEFINED IN AWSM 105-24)

Cloud Parameter	Units
Total Coverage	* Percent
Minimum Base	WMO Code 1677
Maximum Top	WMO Code 1677
Present Weather	WMO Code 4677 (Divided by 10)
Low Cloud Type	3DNEPH Code
Middle Cloud Type	" "
High Cloud Type	" "
Coverage for 15 Layers	* Percent

* To the nearest 5 percent. An additional one percent is a thin cloud indicator, e.g., 51% means 50% thin clouds.

11.3.1 Selective Display Model (SDM). The SDM is a general display model used within AFGWC to display data from most of the AFGWC data bases. The versatility of the program permits selection of varying scales, contours, limiting thresholds, and parameter selection from the 3DNEPH data base. Figure 20 is an example of SDM output.

11.3.2 Vertical cross section display. A special module of the SDM program can produce a vertical cross section of cloud cover through the 3DNEPH data base. The endpoints of the cross section can be arbitrarily requested in terms of latitude/longitude on the 3DNEPH grid system. Vertical and horizontal scales are adjustable. Figure 21 is an example of the vertical cross section.

11.3.3 Photographic display program. The 3DNEPH data base can be displayed by a program which produces a photographic display on an acetate film. The program is versatile and permits overlayment of geography, latitude/ longitude, terrain, contoured meteorological data, and numerical data plots. Varying scales, data scaling, and variable sizes are optional for the user. Figure 22 is an example of the display. A limitation of this display technique is the expense and time required to produce the final copy.

11.3.4 Quantitative high speed printer display. This is the most versatile and frequently used of the display methods. Displays are rapidly and inexpensively produced by the computer's high speed printers. Data

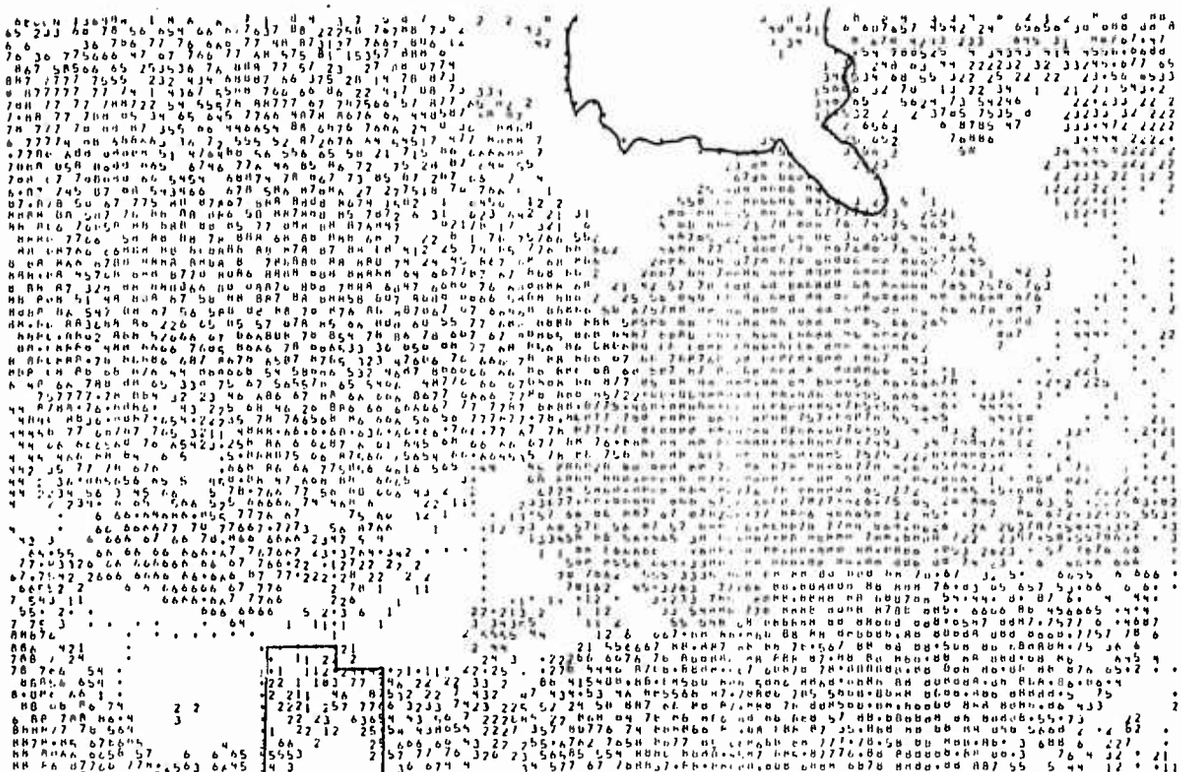

Figure 20. A display of the 3DNEPH data base by the Selective Display Model (SDM). Clouds are shown in eighths over much of North America. Hudson Bay and Utah have been manually outlined to orient the reader. Blank areas are clear, "8" represents overcast, and the dots are geographical outlines and lines of latitude and longitude.

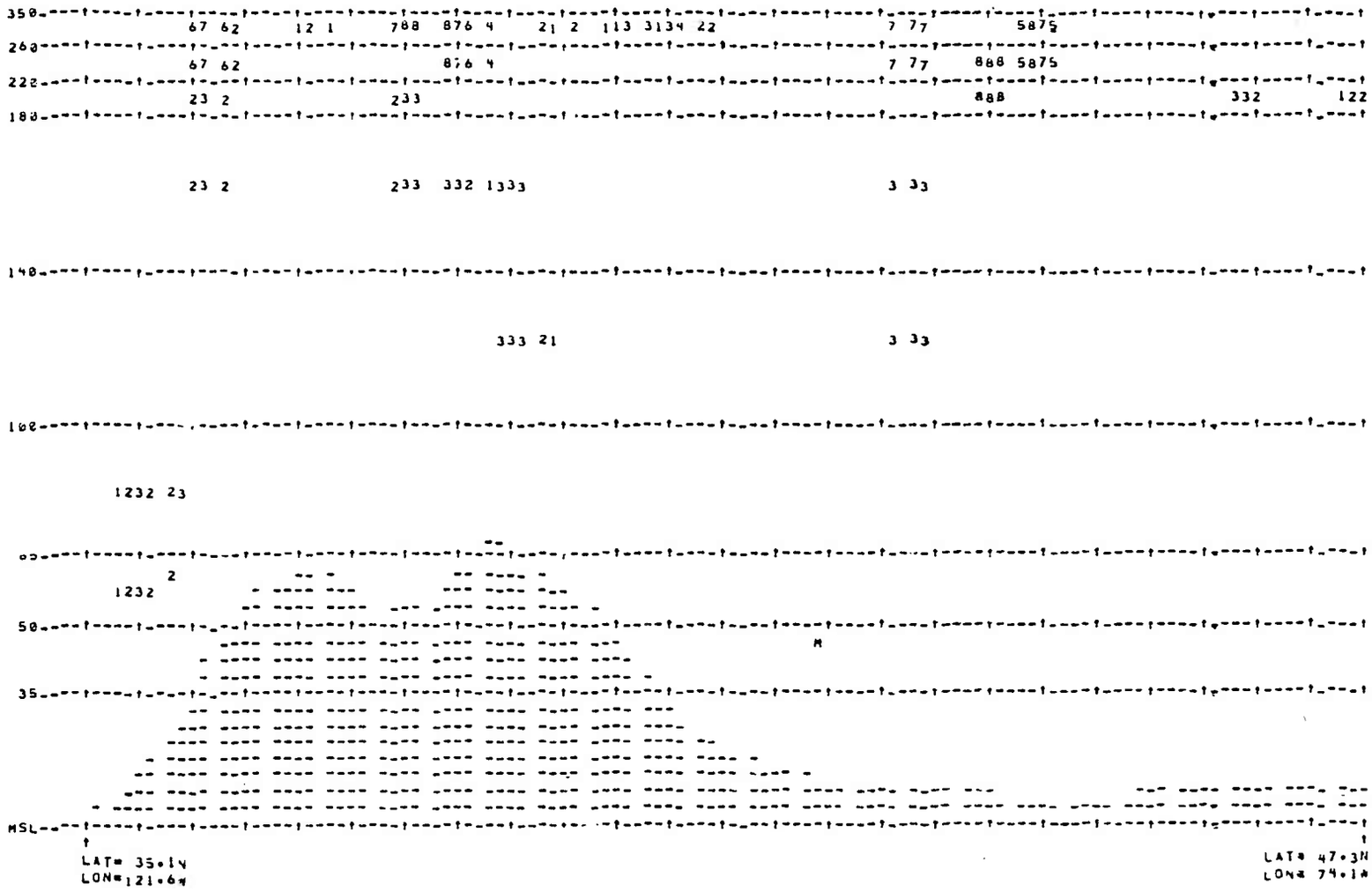

Figure 21. A vertical cross section display through the 3DNEPH data base. Cloud amounts are shown at various levels in eighths of cloud cover (blanks denote clear). The minus signs denote terrain (the Rocky Mountains in this case), and M signifies a missing data point.

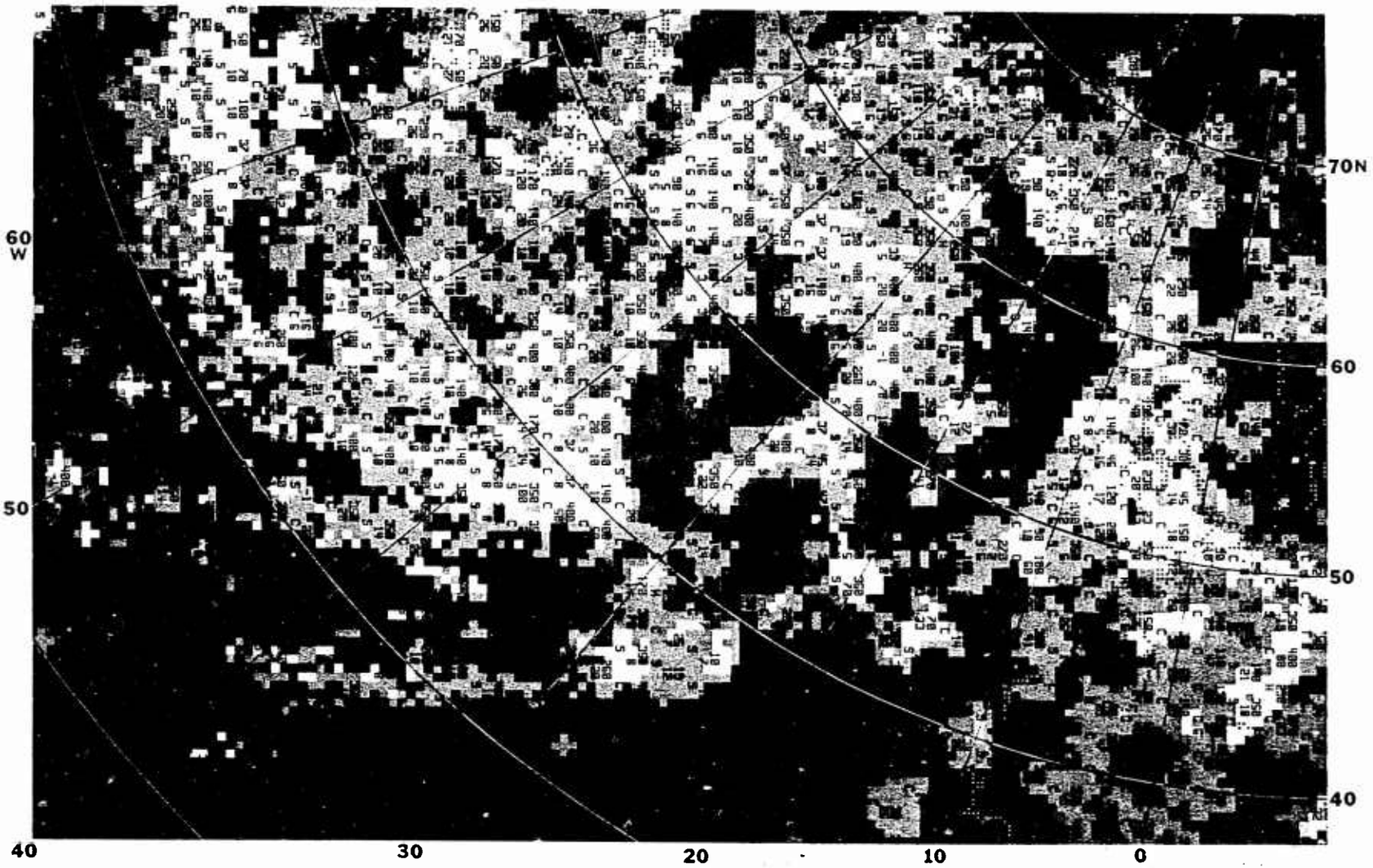

Figure 22. A photographic display of the 3DNEPH data base at the 1 to 15 million scale (reduced for presentation here). Every fourth gridpoint is plotted to show maximum top (hundreds of feet), minimum base, predominant cloud type, and significant weather, if applicable.

are quantitatively displayed in gridded format with optional scales of 1/30, 1/15, and 1/7.5 million. The program is tailored for the 3DNEPH such that 3DNEPH boxes of approximately 70 parameters from the 3DNEPH and auxiliary data bases may be selectively displayed. A particularly useful feature of the displays is that they precisely overlay digital satellite imagery displays. Figure 23 is an example of this display method.

11.3.5 Qualitative high speed printer display. This display program has similar capabilities to its quantitative cousin described above. However, it displays in 16 shades of gray. 3DNEPH data base parameters are scaled to a number from 1 to 16 and by overstriking various characters on the computer's high speed printer, shades of gray are achieved. The program has a full range of options similar to the quantitative display program including selection of the grayshade scaling algorithm and inversion of the grayshades. An example is provided by Figure 24.

11.4 Archival. 3DNEPH has been continuously archived on magnetic tape since January 1971 (May 1974 for the Southern Hemisphere) by the USAF Environmental Technical Applications Center (USAFETAC), Scott AFB, Illinois. USAFETAC handles requests for use of the archive tapes, provides documentation, and reformats or summarizes the raw 3DNEPH data to provide utilitarian data for archive users. Four major components of the 3DNEPH archive procedures are the 3DNEPH Synoptic File, the Box-Time File, the Histogram File, and the documentation/quality control information.

11.4.1 Synoptic File. This is the 3DNEPH data as received at USAFETAC from AFGWC. Data are stored by valid time for an entire hemisphere. Magnetic tapes are physically stored at USAFETAC/OL-A, Asheville, N.C.

11.4.2 Box-Time File. These 3DNEPH data files provide a time sequential set of data for a particular 3DNEPH Box. They are designed to permit rapid retrieval of time sequential information for a gridpoint or set of gridpoints within a small geographical area. Duplicate sets of these files are maintained - one at Scott AFB and one at Asheville.

11.4.3 Histogram File. The Histogram File is a summary of the Box-Time File designed to provide rapid access to 3DNEPH data for certain areas of the world. It consists of cloud frequency distributions or histograms by month for each analysis hour over several years. This is an ongoing project and only selected boxes in the Northern Hemisphere have been summarized to date.

11.4.4 Documentation and quality control information.

11.4.4.1 Synoptic 3DNEPH Quality Control Log. This log provides evaluation of the analyses as provided by AFGWC (described in section 10.4). It is available in hard copy form beginning in January 1976.

Figure 23. Quantitative display of the 3DNEPH data base. This is a portion of the Northern Hemisphere with the United States in the lower center. Cloud amounts are shown in eighths. The original scale was 1 to 30 million and was reduced photographically for display here.

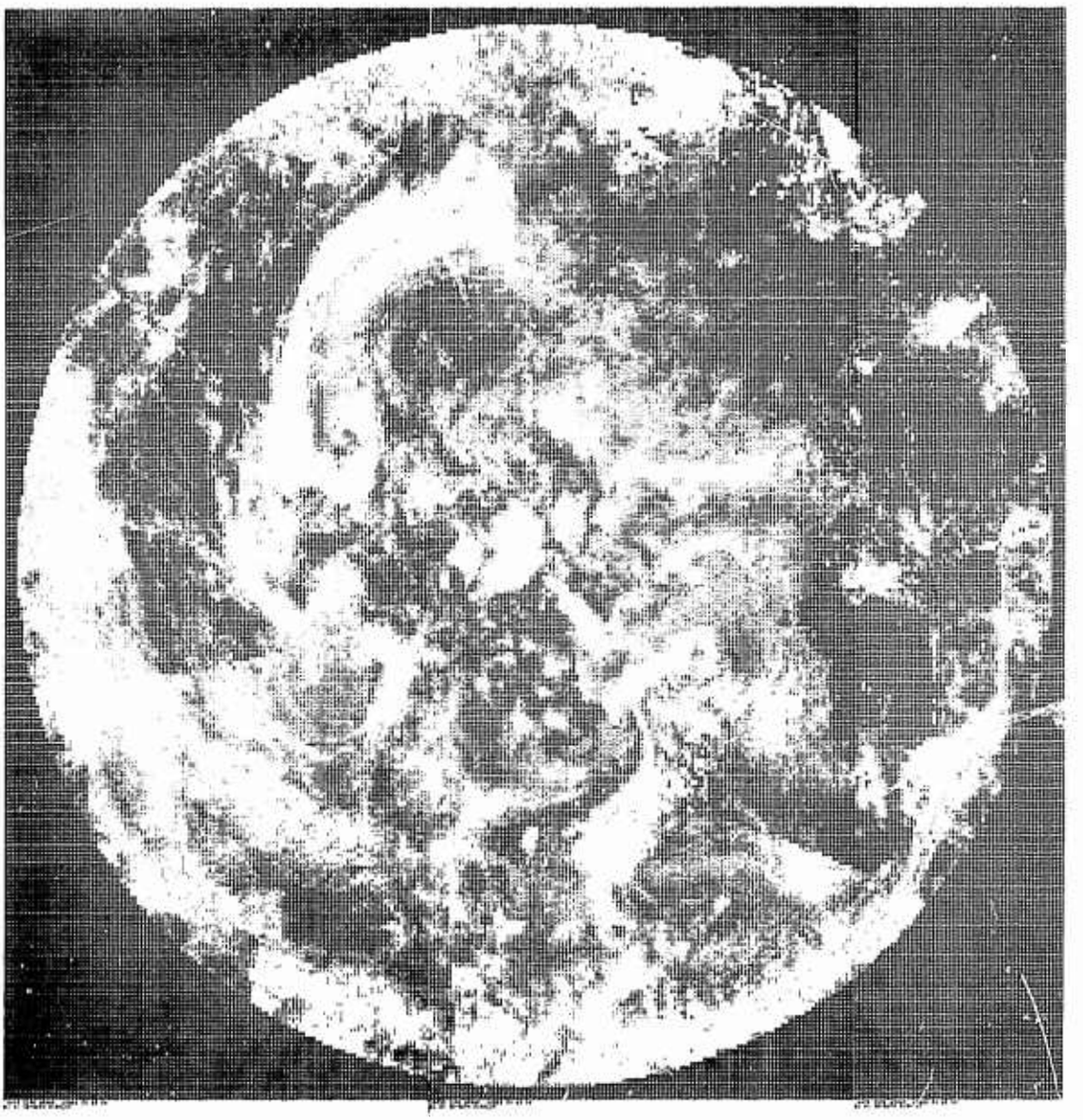

Figure 24. Qualitative display of the 3DNEPH data base produced on a high speed printer. Cloud amounts are depicted by shades of gray (white is overcast, black is clear). The area shown is the Northern Hemisphere and the scale is 1 to 30 million (photographically reduced for display here).

11.4.4.2 The ETAC Information File. This magnetic tape file provides information on the number of gridpoints per box with timely satellite data and the number of conventional reports per box since 29 January 1974.

11.4.4.3 The 3DNEPH Diagnostic Print File. This data file provides enhanced information on the 3DNEPH satellite input data. Satellite identification, quarter orbit number, and 3DNEPH Boxes influenced by the data are provided by this file. A graphic display of data location is also provided. This magnetic tape file begins on 16 August 1977.

12. CONCLUSION

12.1 Summary. The AFGWC automated cloud analysis model, 3DNEPH, is a unique computer model providing rapid, comprehensive cloud analyses over the entire world. The model's primary function is the ingestion and reduction of large volumes of meteorological cloud information to a gridded, formatted data base suitable for use by multiple users. The 3DNEPH is a complex computer operating system with two operating modes and multiple auxiliary operations. Each cloud analysis is completed by a string of functional modular processors as described in this TM. Auxiliary operations, such as background brightness, temperature, temperature forecast, and high resolution geography fields are unique as are their respective updating procedures and origins.

12.2 The future. The 3DNEPH is an evolving model. Innovative ideas, combined with new operational requirements, have driven the evolution of 3DNEPH. As a unique model, guidance from the success and failure of similar models was not forthcoming. 3DNEPH continues to occupy a singular role as a provider of high resolution, real time cloud analyses on a global basis. Evolution of the model will certainly continue as improved satellite imagery and new ideas become available. At this time, plans are underway for a second generation model which will:

(a) Operate entirely in a real time, window mode while providing data into a single, up-to-the-minute data base.
(b) Provide additional and more accurate data.
(c) Externalize all timing and threshold factors for expanded testing and adjustment capabilities.
(d) Introduce self-stabilizing software which can detect and correct for variations in the satellite imagery and erroneous biases in the cloud analysis output.
(e) Cut processing and programmer training times by using simplified, well documented, and more efficient code.
(f) Provide a capability to process satellite imagery of differing resolution.

BIBLIOGRAPHY

1. Barnes, S. L., 1964: A Technique for Maximizing Details in Numerical Weather Map Analysis, Journal of Applied Meteorology, Vol 3, No 4, pp 369-409.

2. Cherne, T. L., 1974: The Scan Plane Method for Locating and Gridding Scanning Radiometer Satellite Data, AFGWC Technical Memorandum 74-1.

3. Coburn, Allen R., 1971: Improved Three Dimensional Nephanalysis, AFGWC Technical Memorandum 71-2.

4. Collins, Ralph W., 1970: AFGWC Multilevel Cloud Model, AFGWC Technical Memorandum 70-10.

5. Edson, H., 1965: Numerical Cloud and Icing Forecasts, 3WW Scientific Services Technical Note 13.

6. Geiger, R., 1966: The Climate Near the Ground, Harvard Univ. Press, Cambridge, Mass., Chap. 2.

7. Fye, F., and G. Logan, 1977: AFGWC Satellite-Based Analysis and Prediction Programs, Proceedings of the 7th Technical Exchange Conference El Paso, Texas, pp 113-121.

8. Luces, S. A., S. Hall and J. Martens, 1975: The AFGWC Snow Cover Analysis Model, AFGWC Technical Memorandum 75-1.

9. _____USAF Headquarters Air Weather Service (MAC), 1974: Defense Meteorological Satellite Program (DMSP) User's Guide, AWS Technical Report 74-250.

10. _____USAF Headquarters Air Weather Service (MAC), 1972: Meteorological Codes, AWS Manual 105-24, Vol III.

11. Valley, S. A., 1965: Handbook of Geophysics and Space Environments, McGraw Hill, New York, Chaps. 2, 3.

12. Zdundkowski, W. G., J. Paegle and F. Fye, 1975: The Short-Term Influence of Various Concentrations of Atmospheric Carbon Dioxide on the Temperature Profile of the Boundary Layer, Pure and Applied Geophysics, Vol 113, pp 331-353.

APPENDIX A

HISTORY OF THE AUTOMATED

CLOUD ANALYSIS MODEL

13. 3DNEPH HISTORY

13.1 General. A history of the 3DNEPH is provided primarily for the benefit of users of 3DNEPH archival data. The operational environment at AFGWC is constantly changing and 3DNEPH has constantly been under modification in response to these environmental changes and to efforts toward improvement of the final product. The history presented here in tabular form is very general and only highlights the major modifications having a major impact on the 3DNEPH output or operational character. Volumes of records describing in detail all changes are maintained at AFGWC. The archival user can use this history to note major changes which may influence his statistical analyses or operational application of archived data.

13.2 Chronological history.

Implementation Month/Year	Description/Significance
Jul 1967	Design phase of the 3DNEPH began.
Sep 1967	Design complete and coding began.
Jan 1970	3DNEPH operational with DMSP (Block IV) visual data and conventional data. Output used primarily for display products. Only the GWC Octagon area of the Northern Hemisphere was analyzed.
Mar 1970	DMSP (Block V) data first used.
May 1970	Background brightness concept first employed.
Jul 1970	Infrared data first used for determining cloud heights.
Jul 1971	Infrared data gross error check to flag grossly erroneous infrared data analyses.
Jan 1972	Analysis area expanded to include 3DNEPH Boxes 3, 4, and 5 in the Northern Hemisphere.

Feb 1972	Analysis area expanded to include 3DNEPH Boxes 17, 25, and 33 in the Northern Hemisphere.
Apr 1972	Analysis area expanded to include 3DNEPH Boxes 50, 59, 60, 61, and 62 in the Northern Hemisphere. New geography field delineating land/water boundaries.
May 1972	Analysis area expanded to include 3DNEPH Boxes 24, 32, 40, and 48 in the Northern Hemisphere.
Nov 1972	Window capability added which permitted off-time analysis over selected areas.
Feb 1973	Analysis area expanded to include all 60 3DNEPH Boxes in the Northern Hemisphere. All 60 Southern Hemisphere boxes activated.
Apr 1973	Satellite data processors removed from 3DNEPH runstream and placed in pre-processor runstreams.
Sep 1974	New visual data processor (described in this TM) provides more accurate detection of scattered clouds and is insensitive to bright desert sands. High contrast coastal areas are analyzed correctly.
Apr 1974	Run time of Southern Hemisphere analysis offset 3 hours to 03Z plus each 6 hours to satisfy local operational needs. Maximized incorporation of conventional data.
Oct 1974	Forecast (PROGER) initialization removed because it could not be favorably supported by verification statistics.
Jan 1975	Land temperature forecast module to minimize time-phase problem between infrared satellite data and conventionally based surface temperature analyses. Reduced occurrences of over analysis of clouds. Permitted detection of more low clouds.
Apr 1975	Snow analyses in Northern Hemisphere from the AFGWC Snow Analysis Program (SNODEP) incorporated into satellite processing in 3DNEPH.
Aug 1975	New operational configuration known as Dual Sprint permitted multiple analyses simultaneously. No effect on the archived synoptic analyses.

	A manual alteration on bogus capability (as described in this TM), was added for changing window analyses only.
Sep 1975	Satellite processor "tuning factors" were externalized and placed in a data base. Permitted real time adjustment and correction of output in response to continuous quality control.
Oct 1975	Snow analyses from the Southern Hemisphere as provided by SNODEP were incorporated into the 3DNEPH satellite data processors.
	Satellite Global Data Base (SGDB) provided satellite imagery in a new format (as described in this TM). 3DNEPH correspondingly modified with satellite processing as part of the main runstream. SGDB greatly expanded capabilities by providing gridded geometric relationships and new quality control and display opportunities.
Nov 1975	High Speed Printer (HSP) display package. Provided new capability for qualitative (grayshade) displays of virtually all 3DNEPH primary and auxiliary data bases. Employs inexpensive overprinting technique on conventional HSP. Enhanced quality control potential and operations.
Jan 1976	Archival package known as "CANNER" capable of capturing and reconstituting virtually all data required by the 3DNEPH satellite processor. Very important as a test and evaluation tool.
Feb 1976	Infrared bias correction curve provided smooth, continuous, temperature-dependent correction of raw input grayshade in the satellite data processor. Improved sensitivity to low and cold weather clouds and cirrus clouds. Minimized erroneous analyses especially over desert and snow-covered areas.
Apr 1976	Variability-dependent tuning factors removed from infrared data processor (described in Coburn, 1971). New developments and capabilities rendered this technique obsolete.
May 1976	New background brightness data base which supports the visual data processor. Eliminated classical problems of persistent cloud cover. Prevents catastrophic

	destruction of data base when degraded satellite data is used. Incorporated and interfaced with SNODEP to minimize erroneous visual analyses over snow areas. Very significant savings in operational cost and storage; enhanced quality control capabilities.
Jun 1976	Satellite data cloud typing. Added capability to type all major generic cloud types from satellite data alone. (Previously, only Cb's were typed.)
	Quality control journal which incorporated daily logs of 3DNEPH analysis problems as well as historical milestones of model changes and changes in available satellite data. Maintained at USAFETAC, provides important input for archive data users.
Aug 1976	New infrared data processor which operates as described in this TM. Greatly improved analyses over cold terrain and provided a more homogeneous analysis, i.e., not plagued with occasional clear gridpoints in an otherwise overcast area.
	Tuning factors were stratified to permit independent adjustment with respect to hemisphere, night/day, land/sea, and satellite. Greatly increased the potential for low cloud detection and accuracy using infrared data.
Sep 1976	A new digital input of ice data into the 3DNEPH geography field replaced an inaccurate manual method. More timely and accurate ice edge analyses permits more accurate temperature and satellite data analyses in these areas.
Dec 1976	A new initialization method for the temperature analysis which supports the infrared data processor improved infrared analyses, especially over high terrain such as the Himalayan Mountains.
Jan 1977	A bogus or manual alteration of the hemispheric 3DNEPH data base was started. While window data were bogused as early as August 1975, hemispheric analyses were not effected until now. Erroneous analyses over the Northern Hemisphere are routinely corrected by direct alteration or as a carryover from recent window analyses.

APPENDIX B

LIMITATIONS OF THE CLOUD

ANALYSIS MODEL

14. ANALYSIS LIMITATIONS

The paragraphs below describe recognized long-term analysis limitations of the 3DNEPH and are often referred to as "class problems." Much of the developmental work on the 3DNEPH has been driven by the existence of these limitations. No attempt is made here to identify short-term errors. Where appropriate, a date is given to indicate when a major model change was implemented which affected the problem.

14.1 Software related limitations.

(a) Excessive cloudiness over desert or high albedo areas by the visual data processor due to the misinterpretation of bright backgrounds as clouds. The basis of this problem was a basic philosophical characteristic of the total cloud algorithm. (Eliminated September 1974)

(b) Excessive cloudiness over desert areas by the infrared data processor due to inaccurate surface temperature analyses over data sparse and large diurnal temperature range areas caused by a phase lag between satellite flyover and temperature data receipt. The impact of the problem was minimized with the implementation of an eighth-mesh temperature forecast model in January 1975. The problem was further minimized in June 1976 with the final tuning of an infrared height threshold which is a function of the background brightness. However, this procedure limits the ability to detect low clouds over high albedo areas.

(c) Excessive cloudiness over high terrain areas, particularly the Tibetan Plateau, due to relatively cold temperatures and no surface data to accurately report these temperatures. The problem was minimized with the implementation of the items discussed in paragraph (b) and a new temperature initialization scheme in December 1976.

(d) Erroneous analyses by the visual data processor over snow and ice areas. This was manifested as overinterpretation of clouds in areas of new snow and in areas where the ice analysis contained too little ice. Underinterpretation or no interpretation of clouds resulted when snow melted rapidly or the ice analysis contained too much ice. These errors were caused by the background brightness data base which reacted to snow changes with a 6 day lag and to ice analysis errors in the ice data base. A new background brightness data base and associated updating logic implemented in May 1976 eliminated the snow problems to the extent of the accuracy of the snow analysis model (SNODEP). A new improved ice analysis method was introduced in September 1976.

(e) Underinterpretation of clouds by the visual data processor in areas of persistent cloudiness was a severe problem. This error was induced by design limitations in the background brightness data base which included a 6 day lag in the updating procedure. This problem was eliminated with the implementation of a new background brightness data base in May 1976.

(f) Inability to detect thin cirrus clouds by the visual or infrared processors. This is an inherent limitation of the raw satellite data. When sufficient opacity renders thin cirrus detectable by the infrared processor, the height attached to the cloud top is in error (too low) to a degree which depends on the opacity of the cirrus. In extreme cases thin cirrus may be analyzed as stratus. This problem heavily depends on how the infrared data are tuned at the moment and on the availability of coincident visual data.

(g) Underinterpretation or total omission of low stratus clouds by the infrared processor, particularly where inversions exist. This problem occurs primarily over polar regions and in areas where visual data are not available. It also depends on how the data are tuned at a particular point in time. The problem was minimized by infrared data processor modifications in October 1975 and a new processor in August 1976. The problem still exists to some degree.

(h) Detection of cumulus clouds has been a consistent problem due to the relatively coarse resolution of satellite imagery compared to the size of cumulus cloud elements. Implementations in September 1974, May 1976, and August 1976 have squeezed all available cumulus intelligence from data at the 3 nm resolution and new constant resolution satellite sensors have also added to the cumulus detection capabilities.

(i) Cumulonimbus (Cb) detection in areas influenced by satellite data was performed only by the visual data processor using a sometimes ineffective algorithm. Cb detection is critical since it results in vertical stacking of clouds in the 3DNEPH layers by the data integration processor. If a Cb is not identified, cirrostratus (Cs) is usually placed in the upper layer(s) and all low/middle clouds are omitted. A new cloud typing module was implemented in May 1976 which provides an improved Cb analysis.

14.2 Satellite data related limitations.

(a) Mislocated satellite data resulting in ambiguous cloud lines along coastlines, particularly high contrast coastlines. This problem occurs almost exclusively with visual data, but has been observed with infrared data. The overinterpretation of clouds persists even after the satellite mapping errors are corrected due to the basic design of the background brightness field. Although mislocated data still occur, the new background brightness data base implemented in May 1976 does not perpetuate this condition. Also, the implementation of the Satellite Global Data Base (SGDB) in October 1975 eliminated the need for many transformation algorithms which contributed to the overall inaccuracy of the mapping process.

(b) Noise in the raw satellite data is a common occurrence and in severe cases results in overcast or clear areas with peculiar shapes. Generally, the 3DNEPH satellite processors can produce a reliable analysis despite the presence of noise.

(c) The DMSP data are unnormalized resulting in anomalous analyses with respect to the source of the data, the readout site, nighttime versus daytime, left side of pass versus right side, and equator versus pole. Overall, these anomalies can be categorized as distinct and identifiable biases and their treatment accounts for most of the complexity in the 3DNEPH satellite processors. Nevertheless, many cloud analyses are probably compromised because of attempts to achieve an optimum analysis in a certain area or portion of a pass at the expense of another area. Some manifestations of this lack of normalization are:

    (1) Nighttime infrared analyses are generally worse than daytime infrared analyses (independent of visual data).
    (2) Tropical areas tend to be excessively cloudy.
    (3) The terminator side of infrared passes tend to be excessively cloudy during the fall and winter.
    (4) Small cloud elements on the sunlit side of visual passes which are normally detectable, are not always analyzed.
    (5) The terminator side of visual data tends to be underinterpreted due to decreased illumination on morning satellites.

    Implementations in January 1975, October 1975, February 1976, August 1976, and December 1976 have reduced these problems to minimal proportions.

14.3 Conventional data related limitations. Some standing limitations of conventional data are described below. Manifestations of these limitations in 3DNEPH analyses are not known precisely; however, the user must be aware of possible error sources.

(a) Inaccurate total cloud estimates, especially when clouds are low and parallax error is the greatest. Cloud amounts are usually overestimated.

(b) Inaccurate nighttime observations with a tendency to underestimate cloud amounts, particularly high clouds.

(c) Variations in the reporting procedures and quality of observing procedures between countries.

(d) Inaccuracy of cloud heights when estimated by observers and pilots and as determined by sounding instrumentation.

(e) Instrumentation inaccuracies and transmission garbling.

APPENDIX C

THE HIGH RESOLUTION SURFACE

TEMPERATURE ANALYSIS

A worldwide, eighth-mesh temperature analysis is a vital part of the infrared data processing methodology. The temperature field serves as a background to be compared with raw satellite data to locate relative cold areas which represent clouds. Low cloud heights are determined by interpolation between the surface and 850 mb temperatures.

15.1 Land temperatures. Surface temperatures for land areas are built every three hours subject to the arrival of conventional surface temperature reports. Approximately one hour after each analysis an update is made using the same data, but added to it are late arriving data. The late data are particularly important because they typically come from data sparse regions of the world such as deserts and mountainous areas. It is in these areas that valid temperatures are most important for successful cloud analyses. Each temperature analysis is developed using the following procedural steps:

(a) Initialization using a gradient level (60 mb above to surface) temperature forecast found in the AFGWC data base. The previous analysis is used when making an update analysis.
(b) Available temperature data from surface reports are superimposed on the gradient level (or previous) analysis. Temperature reports are subjected to an error check for abnormally high or low temperatures.
(c) Surface reports are spread to produce a 100 nm resolution gridded field. The spreading procedure (Barnes, 1964) filters the data and reduces its influence as a function of the distance from the report site. Temperatures are corrected for elevation using a fixed data base of lapse rates obtained from Valley, 1965. The lapse rates have a latitudinal and seasonal dependency.
(d) Finally, the 100 nm data are interpolated to the 25 nm resolution.

To permit processing of all satellite imagery, two cycles of 25 nm temperature data are always available. This permits selection of the analysis time most closely corresponding to the satellite data time. A forecast is also provided.

15.2 Sea temperatures. Sea temperatures arrive at AFGWC every 6 hours from the Fleet Numerical Weather Central (FNWC) in Monterey, Calif. These data are on the 100 nm resolution and are derived from multiple sources including microwave satellite data and ship reports. The 100 nm data are directly interpolated down to 25 nm and stored with the appropriate land temperatures to produce a global, 25 nm grid, temperature data base.

APPENDIX D

THE HIGH RESOLUTION SURFACE

TEMPERATURE FORECAST

16. SURFACE TEMPERATURE FORECASTING

The accurate specification of a temperature background is critical when making a cloud analysis from infrared satellite imagery data. The only independent source of surface temperatures is from Airways, synoptic, METAR, and other types of reports. These observations are usually valid at intervals of three hours and are not available until one or two hours after the valid time. When satellite data derived temperatures, which are essentially real time, are compared to the conventional surface temperature, there is a significant difference in observation times. Satellite data are almost always ahead in time compared to conventional data. It is therefore desirable to use a forecast surface temperature valid a short time into the future relative to the analysis time to offset this temperature lag.

16.1 Concept. A special module of the 3DNEPH provides a three hour radiative temperature forecast at the 25 nm resolution. The forecast is made immediately after every temperature analysis. Thus, the 3DNEPH infrared satellite processor can select a temperature which more closely corresponds in time to the temperature scene observed by the satellite sensor. The temperature forecast module provides fast, accurate, short-range forecasts.

16.2 Forecast Generation. The iterative model which produces the temperature forecasts was developed at the University of Utah and is described in detail by Zdunkowski, et al, 1974. The model forecasts temperature profiles in the planetary boundary layer. It is a one dimensional model with approximately 74 transformed vertical grid levels extending from 1 meter below the surface to the stratosphere. Many physical processes are modeled or parameterized including the following:

(a) Water vapor, carbon dioxide, and ozone radiative transfer.
(b) Atmospheric turbidity and scattering.
(c) Temperature diffusivity.
(d) Soil conduction.
(e) Diurnal insolation variations.
(f) Albedo.
(g) Cloud cover and cloud height.
(h) Absorption of solar radiation by water vapor.

A notable exclusion from this list is temperature advection. However, a short, radiative airmass temperature forecast is all that is necessary for this application. Frontal zones with large temperature gradients are usually cloudy so that accurate surface temperatures are not necessary. Temperatures become critical in areas where low clouds are dominant such as in airmass situations where the forecast model performs very well.

The original model was not directly capable of satisfying the requirement for frequent 25 nm resolution forecasts because of large computation times. Also, the many variables and initial conditions could not be satisfied from existing data resources. Instead of using the model directly, a set of temperature change tables were generated by the model for a carefully selected set of variables. A sensitivity analysis excluded many potential temperature predictors and for the remaining predictors a range of values was defined for which significant temperature changes occurred. Additional simplications reduced the number of independent predictors to seven (7) as described later.

16.2.1 Procedure. The iterative forecast model was used to make 72,000 separate three hour forecasts. Each forecast temperature was a function of unique predictor values and existed as a three-hour temperature change in whole Celsius degrees. Once the temperature change tables were prepared, it was relatively simple and efficient to locate a particular temperature change which satisfied the independent predictor variables for a particular gridpoint. Figure D1 illustrates the overall procedure. The temperature changes were generated in groups of 2,000 with each group corresponding to a particular season and latitude. After an initialization process, each forecast was prepared by iterating out to the desired time and extracting the shelter height temperature (approx. 1.5 meters) from the model's temperature profile. This temperature, subtracted from the initial shelter height temperature, yielded the desired forecast. The procedure was repeated many times with each predictor variable changed in turn while remaining predictors were held constant.

16.2.2 Initialization. The iterative forecast model required satisfaction of its many input variables. In general, these were satisfied by a set of standard atmospheres described by Valley (1965). From these, the model's grid could be initialized by interpolation between atmospheric levels. Soil temperatures were changed and matched to each atmospheric profile based on data available from Geiger (1966). Soil parameters such as density, conductivity, etc., were varied as a function of albedo as described later. The various numerical properties of the model required a preliminary iterative session to achieve a steady state condition in the temperature profile. This insured that all physical processes and numerical simulations were balanced and increased confidence that the forecast was a result of modeled physical processes and not numerical transients.

16.3 Temperature predictors. The operational temperature forecast model uses a preselected set of temperature forecast predictors each of which is broken down into several ranges of values to which an index is assigned. The operational forecast model collects raw data for each gridpoint and selects indices to match the raw data. The indices point to a value in the temperature change tables which is algebraically added to the present temperature to produce the forecast. The iterative forecast model followed a similar procedure, but in reverse. The following paragraphs describe the temperature predictors shared by the iterative and operational models as well as many implicit relationships which tie some of the predictors together.

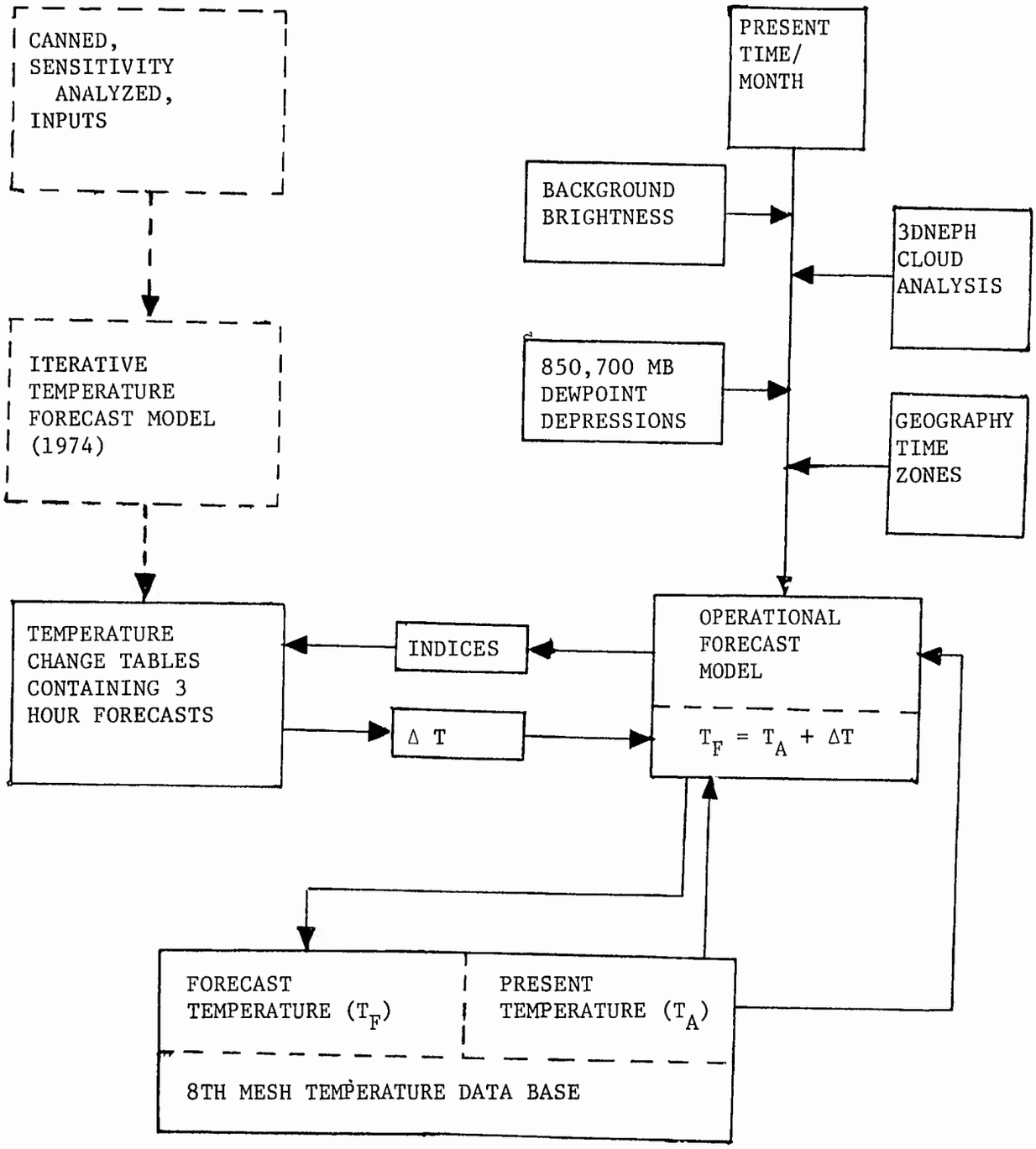

Figure D1. Schematic of the temperature forecast technique. The tables were built in 1974 as indicated by the dashed boxes in the upper left.

16.3.1 Time of year. Seasonal dependency is provided by separate forecasts for each month. Only six months are actually required since solar insolation variations are repeated during the second half of each year. Solar declination and latitude are used in the computation of sunrise, sunset, and solar zenith angles. Atmospheric profiles (Valley, 1965) are provided for each month by interpolation where appropriate.

16.3.2 Latitude. Six latitude zones for each hemisphere account for solar insolation variations. The width of each zone and its location are variable to account for insolation gradients. Table D1 describes these latitude zones.

TABLE D1. LATITUDINAL STRATIFICATION

Month	Latitude(degrees)-Zone Index					
	1	2	3	4	5	6
Jan	0-10	10-20	20-30	30-40	40-60	60-90
Feb	0-15	15-25	25-35	35-45	45-70	70-90
Mar	0-20	20-30	30-40	40-55	55-70	70-90
Apr	0-30	30-40	40-50	50-60	60-70	70-90
May	0-30	30-40	40-55	55-70	70-80	80-90
Jun	0-30	30-45	45-60	60-70	70-80	80-90
Jul	0-30	30-40	40-55	55-70	70-80	80-90
Aug	0-30	30-40	40-50	50-60	60-70	70-90
Sep	0-20	20-30	30-40	40-55	55-70	70-90
Oct	0-15	15-25	25-35	35-45	45-70	70-90
Nov	0-10	10-20	20-30	30-40	40-60	60-90
Dec	0-10	10-20	20-30	30-40	40-60	60-90

16.3.3 Time zone. Each hemisphere is divided into sixteen time zones with each time zone representing a ninety minute time slice. The time zones are defined with respect to the Greenwich Meridian so that local sun time can be determined by a simple calculation using Zulu time. Local sun time provides the critical diurnal solar insolation stratification for the temperature forecast.

16.3.4 Albedo. Albedo is a very important temperature predictor. The AFGWC data base provides worldwide background brightness values as a byproduct of the 3DNEPH visual data processor. Background brightness is stated in terms of grayshades, but is proportional to albedo. The exact

relationship depends on the satellite sensor and local illumination. Only the background brightness from the noontime satellite is used in this application to eliminate some of the brightness anomalies experienced in early morning satellites.

The iterative forecast model required specification of soil conditions for modeling the transfer of heat in the soil. Soil types are not generally available in a digital format, at a high resolution, and on a worldwide scale. To satisfy the soil condition requirement of the model, albedo was subjectively correlated to soil types for which physical properties are known. This method was somewhat crude, but insured consistency between albedo and soil types and provided reasonable results. Table D2 describes the various relationships used and gives the categories or indexes used by the operational forecast model.

TABLE D2. RELATIONSHIP BETWEEN ALBEDO AND SOIL PROPERTIES

Index	Terrain Type	Background Brightness	Albedo	Subjective Soil Type	Density (g/cm^3)	Capacitance (cal/gm^oK)	Conductivity (cm^2sec^oK)
5	Ice Cap	28	.8 - .9	Ice	.9	.8	.005
	Snow Cover	25-28	.6 - .7	Snow	.3	.4	.0006
4	Sand	18-24	.5 - .6	Quartz Sand	1.65	.19	.00063
3	Sand	13-17	.3 - .5	Sandy Clay	1.78	.33	.0022
	Prairie	11-12	.2 - .3	Clayland Pasture	.56	.56	.0012
2	Brush	8-10	.2	Calciferous	1.67	.5	.002
	Farmland	6- 7	.15	Humus	1.7	.3	.003
1	Vegetation	4- 5	.1	Humus	1.5	.5	.005
N/A	Water	1- 3	.07-.09	N/A	-	-	-

16.3.5 Atmospheric moisture. Three categories of atmospheric moisture are used. Each category represents the average dewpoint depression from the surface to 700 mb. Dewpoint depressions of 5, 10, and 15 Celsius degrees are used in each category. Moisture data are not available at the 25 nm resolution, but are interpolated from 200 nm gridded analysis and forecast fields.

16.3.6 Initial temperature. The initial shelter temperature is important in the radiative temperature balance of the model. Two categories of initial temperature are available. To provide improved resolution for this parameter, a table of temperature versus month is used (Table D3). The operational model selects a temperature from the table which most closely corresponds to the analysis temperature and month.

TABLE D3. INITIAL TEMPERATURES (IN DEGREES KELVIN) AS A FUNCTION OF MONTH AND LATITUDE-ZONE INDEX.

Month	Latitude-Zone Index					
	1	2	3	4	5	6
Jan	300	297	288	272	258	240
Feb	300	297	284	275	254	240
Mar	301	294	280	269	252	240
Apr	302	288	276	270	248	240
May	304	296	284	260	252	250
Jun	306	299	291	258	262	260
Jul	308	303	296	278	275	272
Aug	306	300	300	290	268	261
Sep	303	303	298	284	272	250
Oct	301	301	298	286	269	240
Nov	300	300	294	280	268	240
Dec	300	298	290	276	262	240

16.3.7 Nighttime cloud cover. Five categories of "effective" cloud cover height and amount are reduced to a single temperature predicting variable - net flux - to which an index is assigned. This relationship is expressed by:

$$F'_N = F_N (1 - M + M\Omega) \qquad (D1)$$

where F'_N is the corrected net flux at the surface, F_N is the uncorrected (cloud free) net flux, M is the cloud cover in tenths, and Ω is a scale factor which is a function of height. Table D4 shows fluxes for the categories of cloud cover and height used in the forecast model. Indexes are assigned as depicted by the dark jagged lines and actually represent cloud/height combinations of similar effective cloud cover. Index 1 is in the lower left and also includes clear skies (M = Ø) while category 4 is in the upper right. A fifth category (not shown) represents overcast skies for which no forecast is made. That is, a persistent temperature is assumed for the next three hours.

16.3.8 Daytime cloud cover. In the daytime, net flux becomes insignificant as a temperature determiner compared to solar insolation. Cloud amount (and the reflection of solar radiation) becomes an important temperature predictor and leads to a simplification wherein all clouds are assumed to exist at a height of 3 kilometers. Net flux thus becomes a function of cloud amount only as shown in Table D5. Global radiation (solar insolation plus diffuse radiation) is the principle temperature determiner and is corrected for cloud cover according to:

$$G_r' = G_r (1 - .66N) \qquad (D2)$$

where G_r' is the corrected global radiation, G_r is the uncorrected global radiation, and N is the total cloud cover in tenths. Categories of N correspond to the cloud cover and indices shown in Table D5.

TABLE D4. NET FLUX REDUCTION FACTORS AND EFFECTIVE CLOUD COVER INDICES EXPRESSED AS A FUNCTION OF CLOUD AMOUNT AND CLOUD HEIGHT

Height (m)	Cloud Cover (Tenths)									
	.1	.2	.3	.4	.5	.6	.7	.8	.9	
500	.08	.908	.816	.724	.632	.540	.448	.356	.264	.172
1000	.10	.910	.820	.730	.640	.550	.460	.370	.280	.190
1500	.14	.914	.828	.742	.656	.570	.484	.398	.312	.226
2000	.17	.917	.834	.751	.668	.585	.502	.419	.336	.289
2500	.21	.921	.842	.763	.684	.605	.526	.447	.368	.289
3000	.25	.925	.850	.775	.700	.825	.550	.475	.400	.325
3500	.30	.930	.860	.790	.720	.650	.580	.510	.440	.370
4000	.36	.936	.872	.808	.744	.680	.616	.552	.488	.424
5000	.48	.948	.896	.844	.792	.740	.688	.636	.584	.532
6000	.63	.963	.926	.889	.852	.815	.778	.741	.704	.667
7000	.80	.980	.960	.940	.920	.900	.880	.860	.840	.820

TABLE D5. NET FLUX REDUCTION FACTORS AND EFFECTIVE CLOUD COVER INDICES EXPRESSED AS A FUNCTION OF CLOUD AMOUNT (ALL CLOUD HEIGHTS ARE 3 KM.)

Cloud Cover	0	.1	.2	.3	.4	.5	.6	.7	.8	.9	1.
Net Flux Factor	1.	.93	.85	.76	.70	.63	.55	.48	.40	.33	-
Index	1	2	2	2	2	2	3	3	4	4	5

APPENDIX E

PROCEDURES FOR THE MAINTENANCE OF A

BACKGROUND BRIGHTNESS DATA BASE

17. BACKGROUND BRIGHTNESS UPDATING

The background brightness data base is an auxiliary data base of the 3DNEPH and provides a background grayshade against which visual data are compared for cloud determination. It is representative of the brightness of the surface of the earth as seen by a particular visual satellite sensor and is proportional to earth albedo. This global data base is eighth-mesh, corresponds directly with the 3DNEPH grid system, and overlays the Satellite Global Data Base.

17.1 Concept. The background brightness is a dynamic parameter with both rapid and long-term changes resulting from a multitude of factors affecting surface reflectivity and illumination. Additional anomalies may result from satellite sensor and other hardware influences. An updating procedure must be capable of providing representative background grayshade for any point on the earth irrespective of the various time scales of influencing factors. Some of the considerations in the design of the present updating system are:

(a) The operational environment of the 3DNEPH requires the detection of background brightness variations occurring on the order of two or three days. Examples are new snowfall, melting snow, and changing polar ice packs.
(b) Updating procedures must take into account persistent cloud cover with time scales of a week or more.
(c) Seasonal and climatic changes must be detected.
(d) Brightness anomalies of various time scales attributed to satellite hardware and earth-sun-satellite geometry must be incorporated by the updating process.

17.2 Procedure.

(a) Background brightness updating is accomplished real time in conjunction with the visual cloud analyses. A single grayshade value for each eighth-mesh gridpoint is allowed to vary a single grayshade above or below its present value in response to a carefully screened grayshade input for that gridpoint. Fortunately, snow and ice analyses are provided independently of conventional sources. When snow is present, the background brightness is not allowed to change. This also applies in cases of sunglint (sun reflected into the satellite sensor) insufficient illumination (low solar angle), and for cloud covered gridpoints (as determined by visual and infrared analyses). Certain other checks are made before a background grayshade is allowed to change. Figure E1 illustrates the screening procedure.

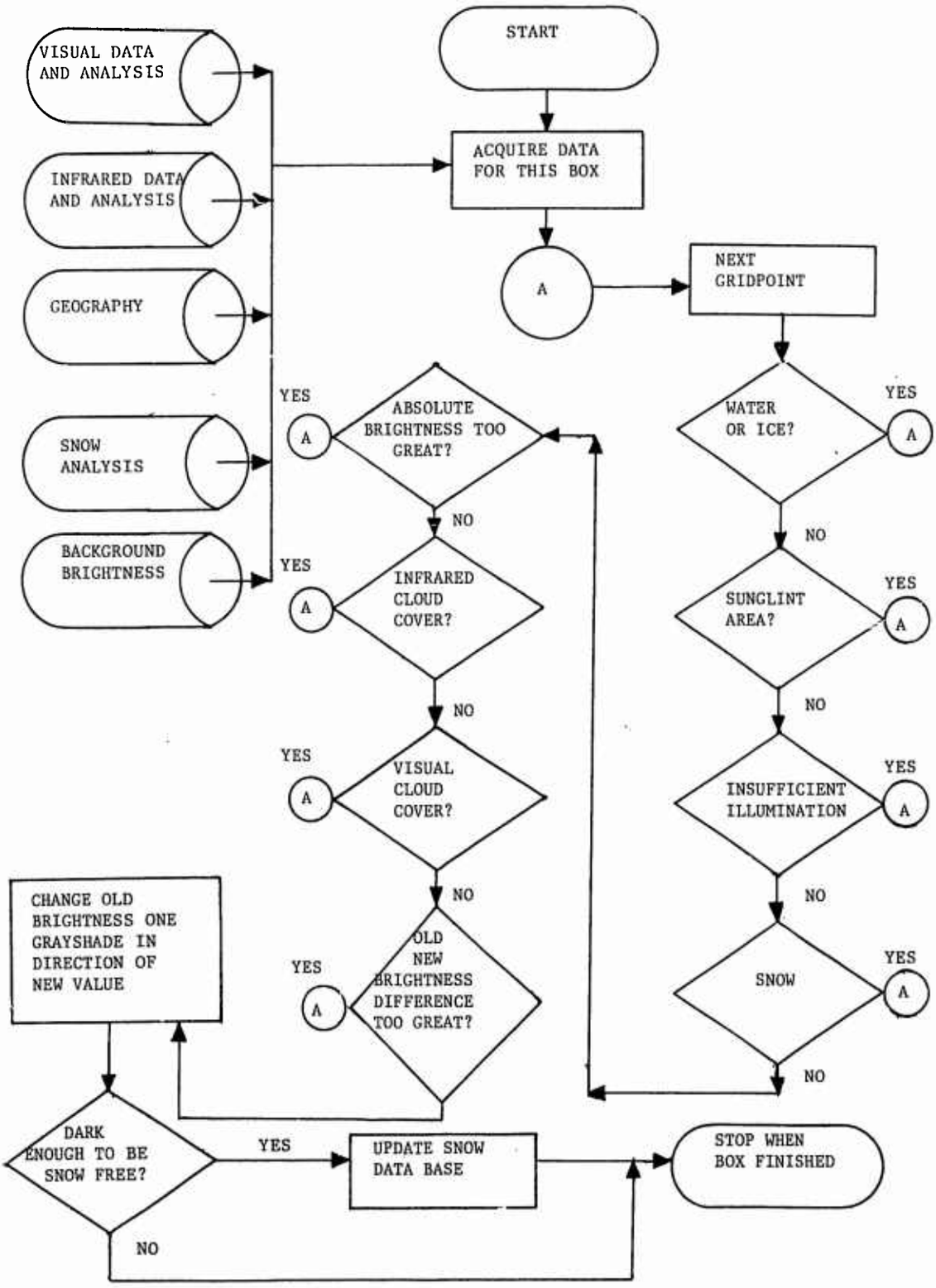

Figure E1. Flow chart of the major decisions made when updating the background brightness field and snow data base.

(b) A final check compares the otherwise "approved" gridpoint grayshade with the existing background brightness value. If they are drastically different, the existing value is not allowed to change. This prevents badly mislocated, noisy, or otherwise degraded data from contaminating the brightness fields. The entire screening procedure results in a slowly changing background brightness field which is not affected by spurious data and persistent cloudiness. It also provides a normalized grayshade for each gridpoint and for each operational satellite.

(c) A simplification in the process is the elimination of water gridpoints identified by the 3DNEPH geography data base. For water gridpoints, a grayshade value can be specified for each satellite and held constant. This saves processing time in the screening procedure as well as storage of brightness for all the world's water areas.

(d) Additional consideration must be given to the selection of screening and change values. If selection is too stringent, a gridpoint may not be able to change resulting in a "stuck" gridpoint. If selection is too liberal, erroneous or spurious information may be introduced into the background brightness fields.

(e) A final feature of the updating process is the memory of a gridpoint's brightness before becoming snow covered. This is accomplished simply by retaining the brightness before snow covers the gridpoint and not allowing it to change until the gridpoint is again snow-free. Figures E2 and E3 are examples of the final product.

17.3 Snow analysis. A spin-off of the background brightness updating procedure is a related determination of snow absence. The snow analysis program, SNODEP (Luces, 1975), builds its analysis from a variety of data inputs including conventional surface reports, Navy sea ice analyses, climatology, and a "no-snow" determination from the 3DNEPH visual data processor.

(a) The no-snow analysis is produced on the 25 nm resolution for gridpoints which received data during the preceding 24 hours from a specified satellite source possessing desirable illumination characteristics. The raw data are screened in the same fashion as described in the background brightness updating procedure to exclude spurious and undesirable data. Once accepted, the 25 nm grayshade is compared to a fixed snow/no-snow grayshade threshold and if numerically less than this grayshade, the gridpoint is flagged as being snow free. For raw data which does not pass the screening, exceeds the threshold, or is obtained from undesirable sources, and for gridpoints not receiving data, an "I don't know" flag is stored at that gridpoint.

(b) The SNODEP program, after processing all conventional data and spreading the analysis to nearby data sparse areas, overlays the satellite no-snow data base and removes snow from the appropriate gridpoints. The analysis, as previously determined, remains in those gridpoints for which the "I don't know" flag is carried.

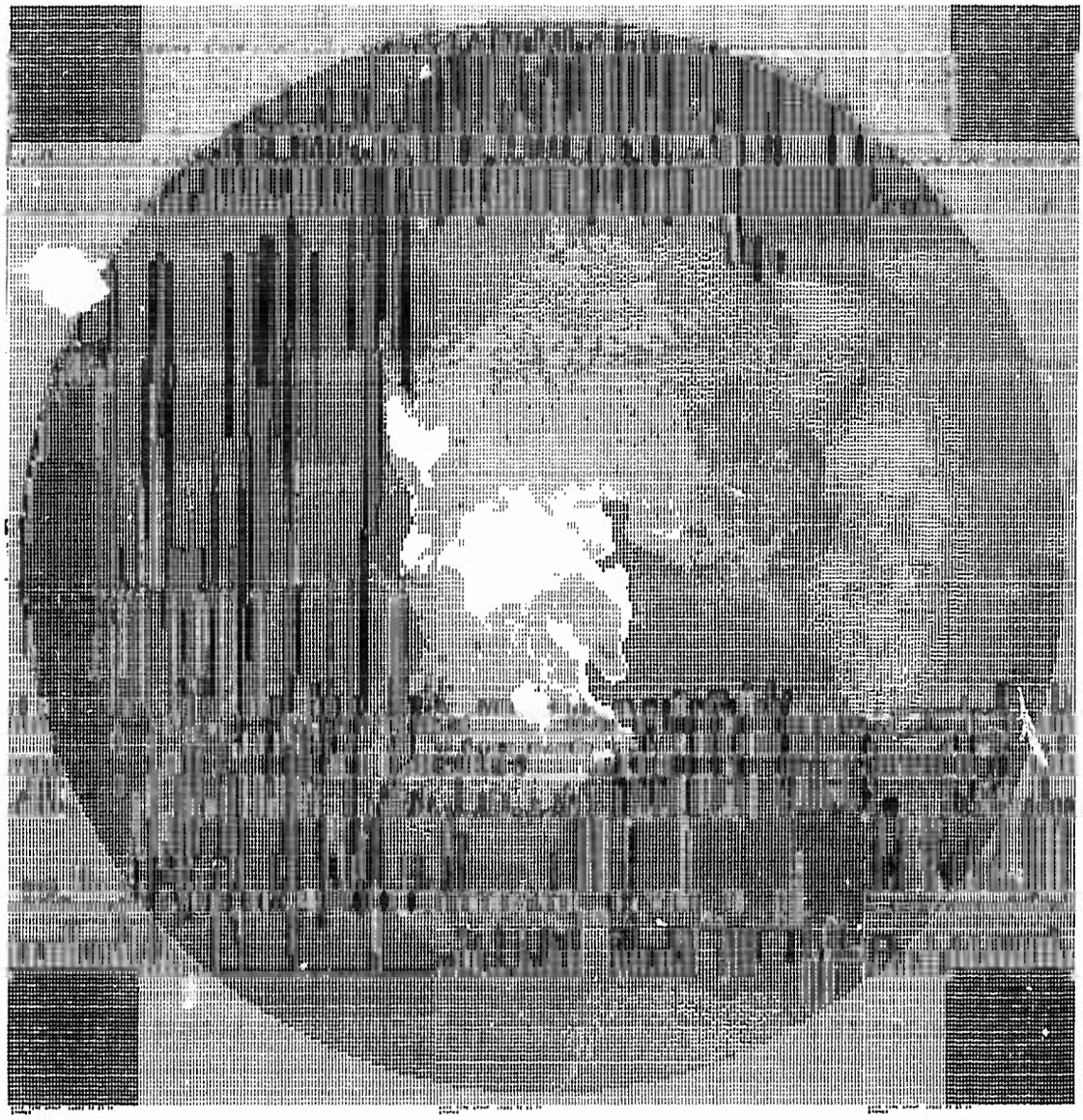

Figure E2. Northern Hemisphere background brightness data base displayed by a high speed printer. Sixteen shades of gray are possible with this technique.

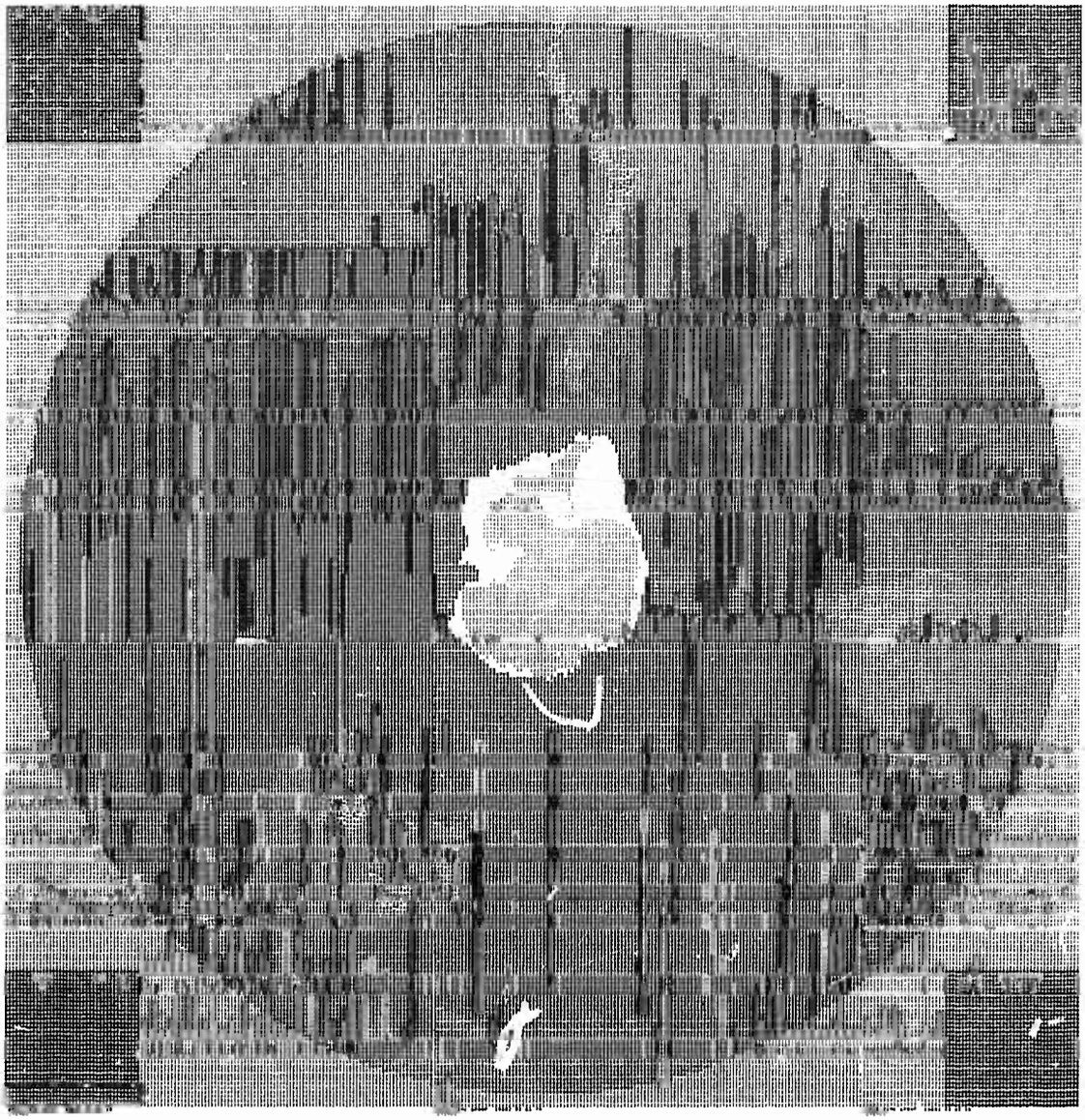

Figure E3. Southern Hemisphere background brightness data base displayed by a high speed printer.

(c) The procedure employed here avoids any undesirable feedback between 3DNEPH and SNODEP since the no-snow determination can generally be considered "truth" once illumination criteria are met. A snow determination by 3DNEPH would not be technically feasible and could lead to feedback which ultimately bars visual processing of large snow free areas.

APPENDIX F

THE HIGH RESOLUTION GEOGRAPHY AND

TERRAIN DATA BASE

18. GEOGRAPHY AND TERRAIN FIELDS

A fixed eighth-mesh data base provides worldwide geographical and terrain height data to several 3DNEPH processors. The role of this data base in 3DNEPH is extremely important since many of the satellite processing decisions are based on the presence of ice, water, or land. Cloud heights and types are also determined in relation to data in the geography/terrain fields. Several figures and a chart are provided in this section to illustrate the density and quality of the data base.

18.1 Structure and content. The geography/terrain digital eighth-mesh data base follows the same grid conventions as all other 3DNEPH gridded data, i.e., the data base is divided into two hemispheres and each hemisphere into 60 boxes. Each computer word represents a single 25 nm gridpoint and contains the following information:

(a) Nature of the terrain - land, water, ice, and land/water (coastline) mixture. A coastal gridpoint may contain any proportion of land to water.
(b) Terrain height expressed to the nearest 10 meters and 100 feet above mean sea level. All ocean gridpoints have zero elevation while positive elevations may exist for large inland water bodies, as appropriate. Negative terrain heights are not used.
(c) Terrain height indicator expressed in terms of the number of 3DNEPH MSL vertical grid levels completely filled by terrain. This is for internal use and optimizes the cloud placement process in 3DNEPH.
(d) A time zone indicator giving one of sixteen time zones numbered counter-clockwise from the Greenwich Meridian. This indicator is used by the temperature forecast model (Appendix D) to calculate local solar time.

18.2 Geography origin. The geography data were extracted from a magnetic tape provided by the Defense Mapping Agency (DMA), previously known as the Aeronautical Chart and Information Center (ACIC). This tape contained latitude and longitude coordinates which traced the coastlines and far exceeded the 25 nm resolution requirement.

18.3 Terrain origin. Terrain elevation was obtained from a 1965 digital tape provided by the Scripps Institution of Oceanography (SIO), La Jolla, California. This tape contained worldwide ocean depths and land elevations in meters averaged over one degree squares of latitude and longitude. Details of the measurement methods and error detection procedures are discussed in SIO Reference Report 65-8. Authors of the digital data are H. W. Menard and Stuart M. Smith. The 3DNEPH terrain

data were developed from the SIO tape by interpolation to the eighth-mesh resolution (ocean depths were omitted). The SIO elevation data were developed from many sources and involved subjective manual averaging over the one degree squares. Several areas of the world were subsequently upgraded at AFGWC using ONC Navigation Charts (from DMA). Elevations were subjectively averaged over 25 nm squares corresponding to the 3DNEPH grid. This has been an ongoing project and will continue. Areas upgraded included India, the Middle East, South America, and portions of Africa.

18.4 Ice-edge analysis. The ice information for the geography field is the only aspect of this data base that is not static. An ice analysis is received weekly from the Naval facilities at Suitland, Maryland. Their ice input consists of hemispheric charts showing ice limits and coverage in eighths. Microwave imagery from Nimbus satellites, DMSP visual imagery, ship reports, climatology, and other information are used in constructing these charts. Once received at AFGWC, the charts are placed on digital encoding tables and the ice limit is traced. Special software enters the ice indicators directly into the 3DNEPH geography data base by changing water indicators to ice indicators and vice versa, as appropriate. The ice-edge is defined as the line separating water with less than 4 eighths of ice from water containing 4 or more eighths of ice. Software "fills in" ice in the areas enclosed by the ice edge. Small ice packs in inland water bodies are frequently resolvable and are entered into the data base also.

TABLE F1. WATER, LAND, COASTAL, AND "OFF WORLD" COUNTS BY 3DNEPH BOX FOR THE NORTHERN HEMISPHERE. COASTAL GRIDPOINTS MAY CONTAIN ANY PROPORTION OF LAND AND WATER.

BOX NO.	WATER	LAND	COASTAL	OFF WORLD
2	349	0	0	3747
3	1699	338	334	1725
4	2207	972	303	614
5	3066	222	202	606
6	2199	121	77	1699
7	371	0	0	3725
9	349	0	0	3747
10	3577	0	7	512
11	3757	82	257	0
12	1457	2420	219	0
13	982	2999	115	0
14	2713	1228	155	0
15	3128	403	86	479
16	174	182	24	3716
17	2349	0	21	1726
18	4087	0	9	0
19	3707	127	262	0
20	473	3346	277	0
21	0	4060	36	0
22	386	3418	292	0
23	482	3355	259	0
24	6	2382	46	1662
25	3481	0	1	614
26	4095	0	1	0
27	3952	57	87	0
28	1602	2064	430	0
29	1190	2364	542	0
30	830	2638	628	0
31	373	3556	167	0
32	11	3512	23	550
33	3482	0	8	606
34	4051	4	41	0
35	3914	31	151	0
36	1267	1889	940	0
37	2600	852	644	0
38	2733	857	506	0
39	160	3885	51	0
40	1291	2074	189	542
41	2397	0	0	1699
42	4096	0	0	0
43	3079	855	162	0
44	245	3608	243	0
45	2521	1125	450	0
46	4082	0	14	0
47	3123	842	131	0
48	1952	451	58	1635
49	371	0	0	3725
50	3617	0	0	479
51	3594	385	117	0
52	1852	1889	356	0
53	3715	117	264	0
54	4091	0	5	0
55	3649	0	0	447
56	403	0	0	3693
58	380	0	0	3716
59	2434	0	0	1662
60	3171	225	150	550
61	998	2327	229	542
62	796	1539	126	1635
63	403	0	0	3693
TOTAL:	123518	62801	9695	49746

TABLE F2. WATER, LAND, COASTAL, AND "OFF WORLD" COUNTS BY 3DNEPH BOX FOR THE SOUTHERN HEMISPHERE.

BOX NO.	WATER	LAND	COASTAL	OFF WORLD
2	346	0	0	3750
3	2361	0	0	1735
4	3357	49	70	620
5	215	3225	44	612
6	33	2289	66	1708
7	178	146	44	3728
9	346	0	0	3750
10	3568	0	0	528
11	4095	0	1	0
12	4096	0	0	0
13	1523	2471	102	0
14	300	3720	76	0
15	2463	1055	83	495
16	377	0	0	3719
17	2361	0	0	1735
18	4074	0	22	0
19	4093	0	3	0
20	4096	0	0	0
21	2794	985	317	0
22	4033	35	28	0
23	4096	0	0	0
24	2424	0	1	1671
25	3472	0	4	620
26	4089	0	7	0
27	4096	0	0	0
28	3286	732	78	0
29	3024	869	203	0
30	4091	0	5	0
31	4095	0	1	0
32	3499	27	14	556
33	3465	0	19	612
34	4058	2	36	0
35	3871	83	142	0
36	2546	1420	130	0
37	2166	1808	122	0
38	4094	0	2	0
39	993	2952	151	0
40	454	3041	53	548
41	2383	0	5	1708
42	3896	21	179	0
43	1763	2121	212	0
44	3967	89	40	0
45	4084	0	12	0
46	4086	1	9	0
47	2163	1647	286	0
48	285	2029	138	1644
49	368	0	0	3728
50	2297	953	351	495
51	1579	2270	247	0
52	3044	966	86	0
53	4096	0	0	0
54	4093	0	3	0
55	3632	0	1	463
56	361	27	12	3696
58	208	91	78	3719
59	1765	258	402	1671
60	2513	732	295	556
61	3534	0	14	548
62	2452	0	0	1644
63	400	0	0	3696
TOTAL:	155497	36114	4194	49955

Figure F1. Northern Hemisphere geography field. Coastal or grid-points containing a mixture of land and water are shown as a "C". Ice gridpoints have been omitted and appear as water. This 1 to 30 million scale display has been photographically reduced for display here. Only one-fourth of the total gridpoints are shown in this display.

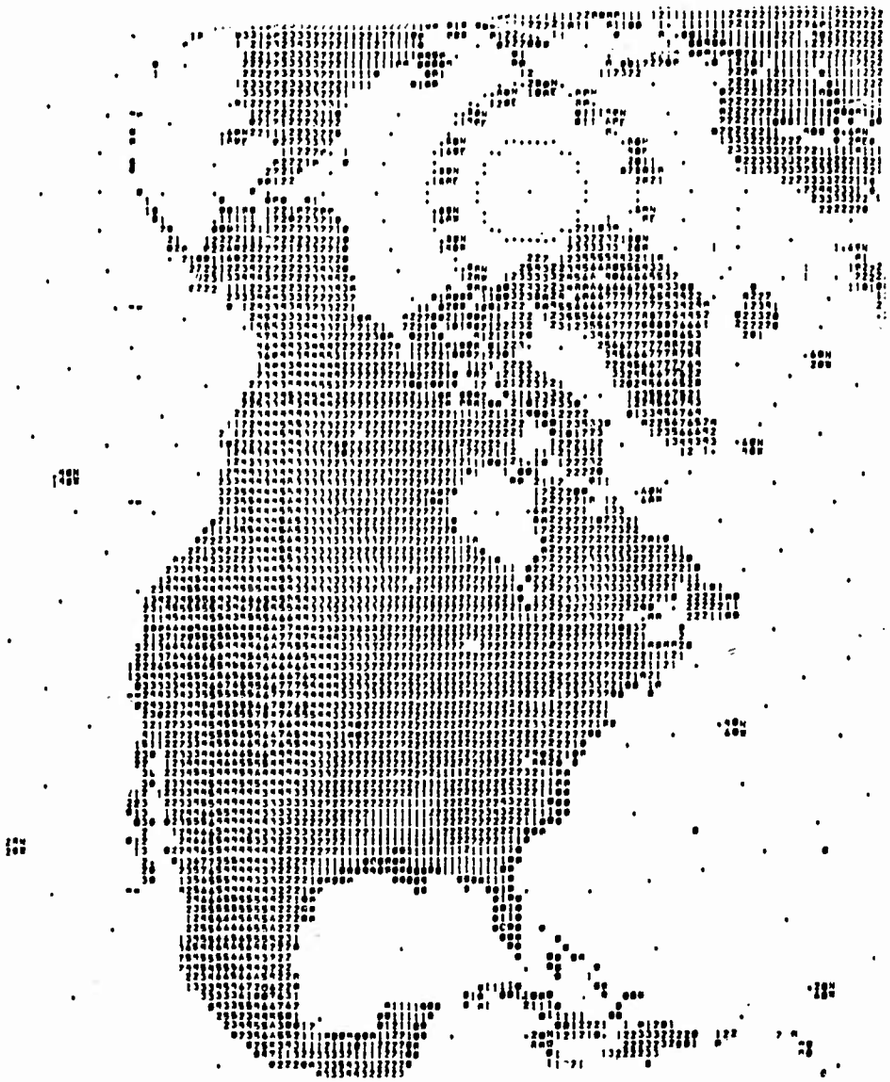

Figure F2. The 3DNEPH terrain field over North America. Heights are coded as follows: 0 = 0 to 10 meters; 1 = 11 to 100 m; 2 = 101 to 500 m; 3 = 501 to 1000 m; 4 = 1000 to 1500 m; 5 = 1501 to 2000 m; 6 = 2001 to 2500 m; 7 = 2501 to 3000 m; 8 = 3001 to 3500 m. Only one-fourth of the gridpoints are shown in this display.

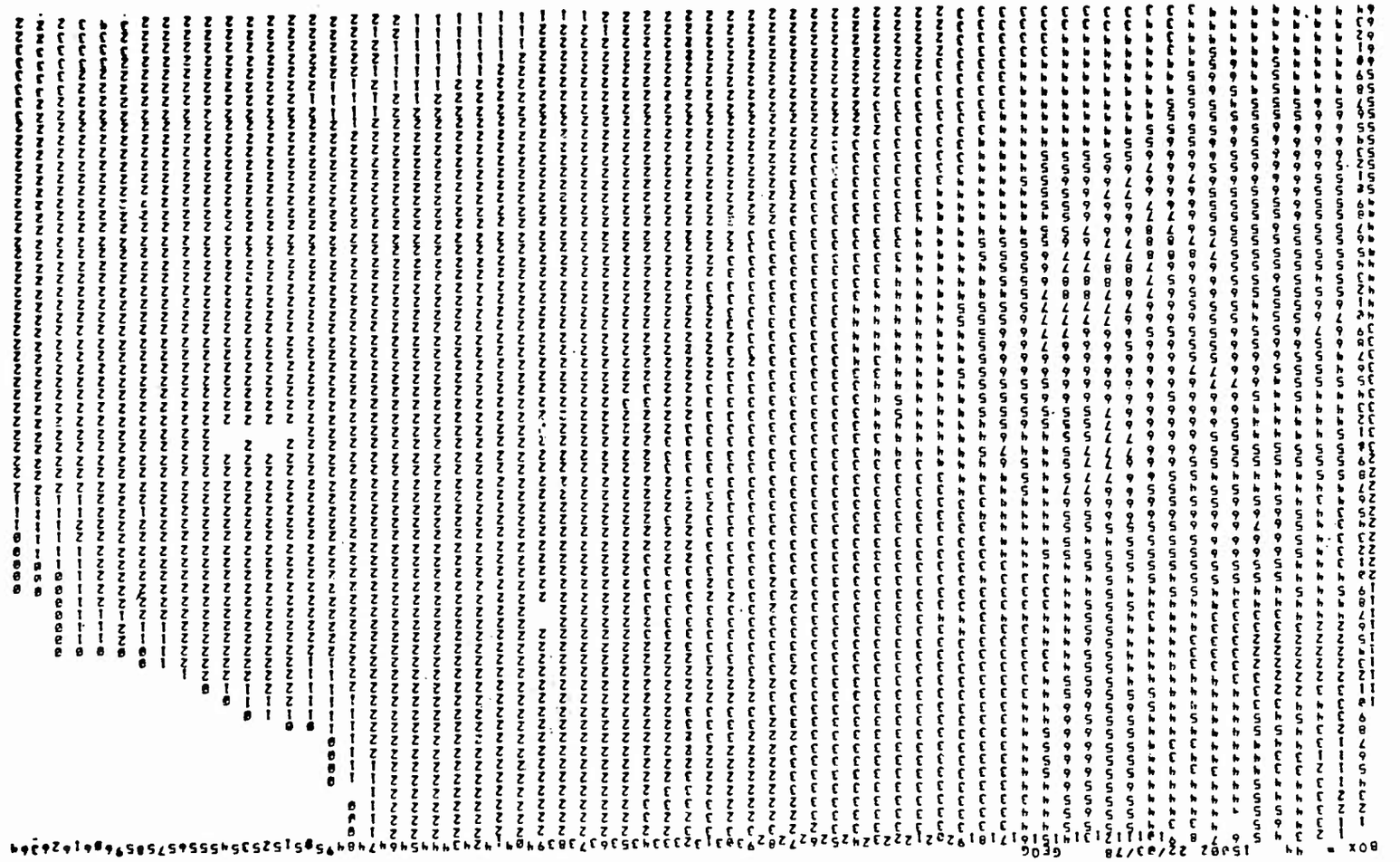

Figure F3. The 3DNEPH terrain field in Box 44 (See Figure 1). Heights are shown using a code described in Figure F2. All eighth-mesh gridpoints are displayed for this box.

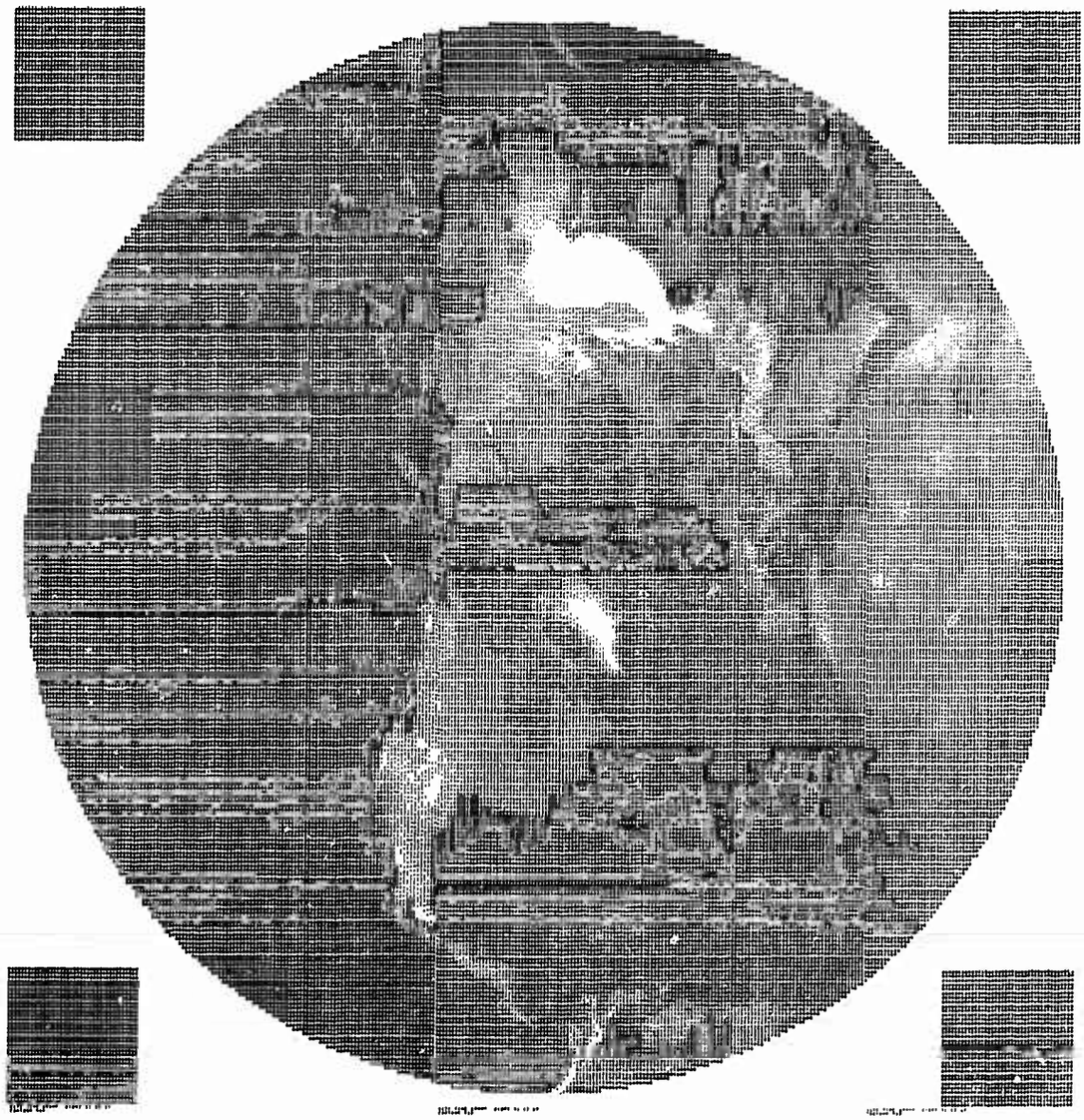

Figure F4. Qualitative grayshade display of the 3DNEPH terrain fields. Highest elevations are shown as white and lowest elevations as black. The area shown is the Northern Hemisphere.

APPENDIX G

CONVENTIONS AND APPLICATIONS OF SATELLITE

GEOMETRIC INFORMATION

19. GEOMETRIC CONSIDERATIONS FOR SATELLITE DATA

The Satellite Global Data Base, in addition to providing high quality imagery, provides user programs with geometric information which is very helpful in visual and infrared analyses of the imagery. Geometric data are provided at the 50 nm resolution. Thus, each group of four eighth-mesh gridpoints is provided a local zenith angle, a scan or look angle, and a left-right indicator for determining if the gridpoint is left of right of the satellite subtrack.

19.1 Trimming. Certain satellite data may be unuseable for several reasons as discussed in satellite processor sections. Generally, the unuseable data are associated with a certain geometric relation among sun, satellite, and gridpoint. A threshold may be stipulated in terms of scan and local zenith angle such that all data outside these thresholds are discarded. Figure G1 defines these angles and Figure G2 is a typical example of the horizontal layout of these angles.

19.2 Sunglint cone. The sunglint angle is the angle between the satellites look angle and the angle of perfect reflection. Figure G3 and G4 define and illustrate the various angles involved. The sunglint cone is an area on the earth's surface, usually elliptically shaped for noontime satellites, which is arbitrarily selected to circumscribe the area from which the sun's reflection will be visible to the satellite visual sensor. The size and shape of the bright sunglint area depends on relative sun and satellite positions as well as surface conditions on the earth. Note that the earth is assumed to be flat in the sunglint geometry. Considering the accuracy needed and that cone angle thresholds are arbitrary, this assumption is permissible. Sunglint angles are computed from the following equations:

$$\theta = Z - \beta \qquad \text{for gridpoints right of the subtrack} \qquad \text{(G1)}$$

$$\theta = Z + \beta \qquad \text{for gridpoint left of the subtrack} \qquad \text{(G2)}$$

where θ is the sunglint angle, Z is the zenith angle, and β is the look (or scan) angle. The zenith angle is a function of season and hemisphere as well as time of day. Thus, once cone or thresholds are established, they continue to provide the desired angular delineations despite changes in Z.

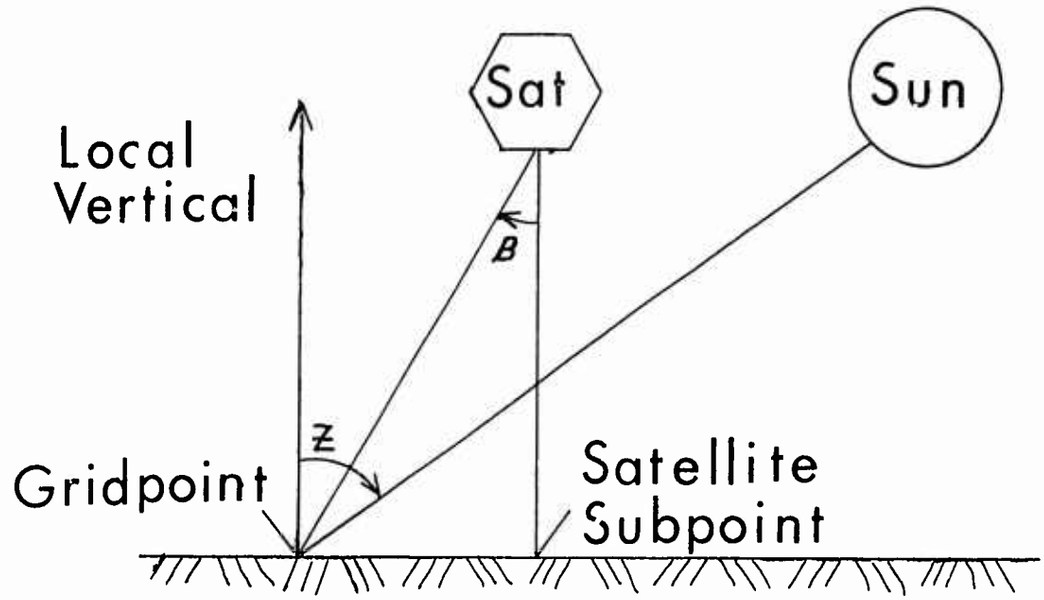

Figure G1. Angular relation of satellite, sun, and local gridpoint in defining the zenith angle (Z) and the look (or scan) angle (β).

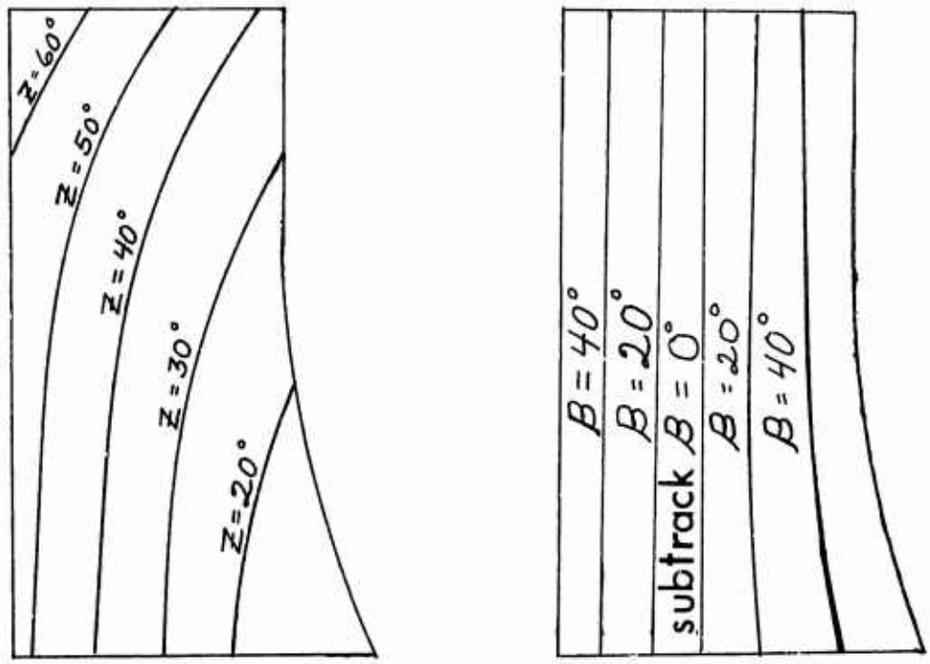

Figure G2. Typical zenith angle (Z) isopleths and look angle (β) isopleths over a quarter orbit swath of satellite data.

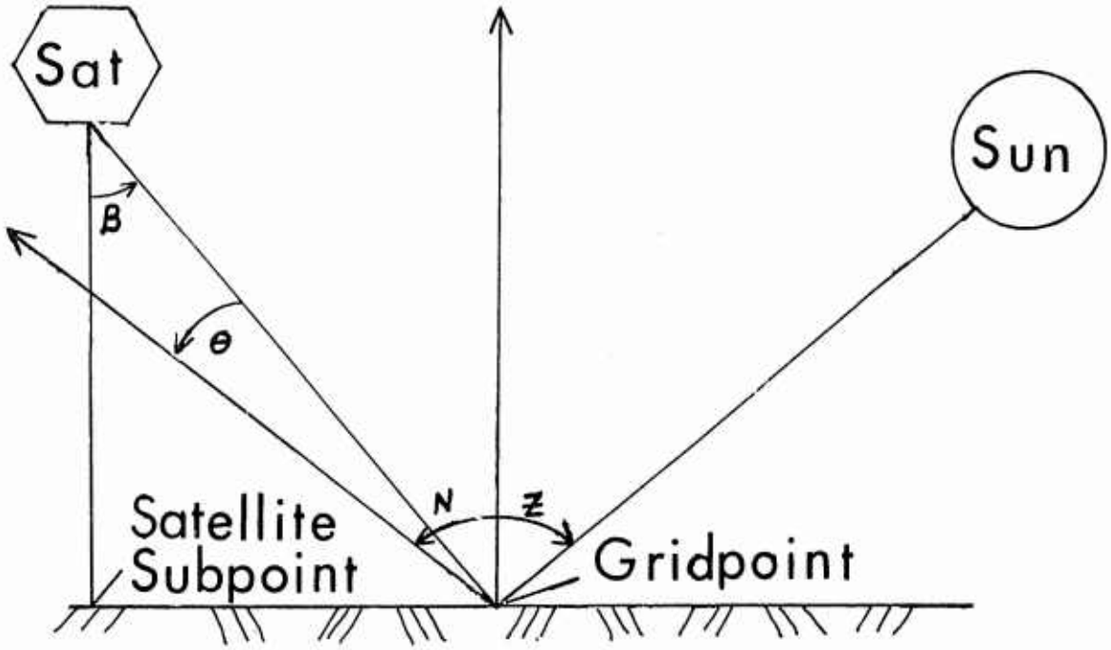

Figure G3. Angular relationships used to define the sunglint angle (θ) β is the look (or scan) angle, Z is the zenith angle, and N is the angle of perfect reflection (N = Z). The angles depicted are typical of a morning satellite.

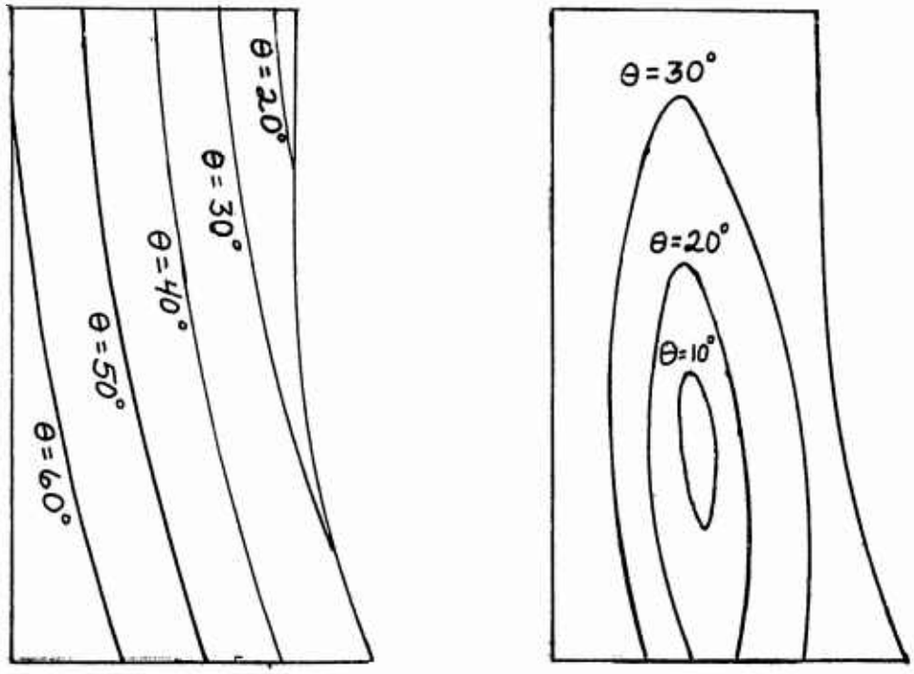

Figure G4. Typical sunglint angles (θ) shown as isopleths (sunglint cones) on a quarter orbit swath of a morning (left) and a noontime (right) satellite.

APPENDIX H

PROCEDURES FOR THE NORMALIZATION/CORRECTION OF

INFRARED SATELLITE DATA IMAGERY

20. INFRARED DATA BIASING

The ability of the infrared satellite data processor to detect clouds depends on a comparison between a satellite data temperature and a surface temperature background. Temperature differences between these sources determine the presence and height of clouds. These temperatures are not directly comparable, however, and must be carefully corrected for a host of biases which are functions of radiative transfer, hardware, software, and measurement methods. The methodology described here attempts to correct or remove these biases and make the surface and infrared temperature directly comparable. Stated another way, the objective of the procedure is to achieve perfect agreement (no temperature difference) between the infrared data temperature and that actually existing at the earth's surface (in the absence of clouds).

20.1 Infrared bias sources. The biases observed in the infrared satellite imagery are described below.

20.1.1 Limb-darkening. This is the depletion of radiation as the satellite sensor "looks" left and right of its subtrack due to the increased atmospheric pathlength at these greater angles. The net effect is increasingly colder temperatures (less radiation) closer to the edge of the satellite's field of view. A correction described in section 5 discusses the basic treatment of this phenomenon. Further corrections which are functions of the "look" angle are applied and discussed subsequently.

20.1.2 Water vapor attenuation. This phenomenon is similar to limb-darkening, but is tied more to the distribution of atmospheric water vapor than angular relationships. Water vapor is the most active atmospheric absorber of infrared radiation and its presence can account for sizeable depletion (or attenuation) of infrared radiation. The net effect is a colder than anticipated temperature in infrared imagery which is proportional to the amount of water vapor present.

20.1.3 Sensor variation/calibration. The sensitivity of the infrared satellite sensor changes with time and while calibration procedures are established, some grayshade variation due to sensor changes occur. This is also true of ground-based equipment which processes the signal. A particularly troublesome variation is sometimes observed between different satellites producing strong temperature discontinuities where orbital paths meet or intersect. As long as sensor sensitivity and processing variations are gradual, the bias may be predictable and adjustments made, but sudden, spurious changes can have disastrous effects on the infrared cloud analysis.

20.1.4 Across track variation. This is a temperature bias which is a function of the local sun angle at various points along the track and in the field of view of the satellite. For an early morning satellite, the problem is most severe. On the dark (terminator) side of the satellite's path, temperatures are relatively cold. On the sunlit side, however, the earth's surface may be quite warm from an early morning sun. The result is a very large and troublesome temperature gradient across the satellite's path.

20.2 Surface data biases. Another set of temperature biases can be found in the surface temperature analyses which have their origin in conventional reports. The biases described below are not intrinsic to the data, but represent areas of concern when trying to compare them with infrared temperatures.

20.2.1 Time phase lag. A rather obvious bias source results from difference between conventional report times and satellite crossings. More specifically, the problem centers around the fact that satellite data are essentially real time while surface temperature analyses may lag several hours behind satellite data. Efforts to correct this problem have resulted in the operational generation of short temperature forecasts as described in another appendix.

20.2.2 Measurement above the radiating surface. The background temperature analysis is based on temperature measurements at the "shelter height" (approximately 1.4 meters above the surface) while the infrared satellite sensor detects the temperature very near the actual surface of the earth. This can result in very large temperature differences (Zdunkowski, 1975) between the two sources especially in arid regions and on hot days in any climate.

20.2.3 Inaccuracies of surface data. Several temperature analysis problems are in the measurement inaccuracy and subsequent perils of transmission. Certain error checks are made on the AFGWC data base which detect and discard obviously erroneous temperature reports. More subtle errors of unknown quantity and magnitude do survive and influence the infrared cloud analysis to varying degrees. A more significant problem lies in the unavailability of temperatures over large areas of the world. In these areas, temperatures are extrapolated from known temperature areas. An additional confidence factor is incorporated into the infrared cloud analysis logic and is described in section 5 as "low-cloud limiting."

20.2.4 Resolution. The resolution difference between surface temperature reports and infrared detected temperatures is large. Surface reports are available, on the average, every 100 nm while satellite imagery provides a 3 nm resolution This means that many terrain features which exhibit temperature anomalies are not visible in conventionally derived temperature analyses, but may appear in infrared data. This implies erroneous cloud analyses whenever these differences are large. The procedure described in Appendix C partially corrects for this bias.

20.3 Correction procedure.

(a) Temperature correction procedures for surface and infrared temperature sources which are not treated entirely or in part by auxiliary operations, are handled in the infrared processor itself. Various temperature corrections are applied directly to the modal temperatures (discussed in section 5) with the objective of achieving agreement between infrared and surface temperatures in cloud-free areas. Reasonable success is achieved by using a stratified correction equation which capitalizes on geometric information provided by the SGDB.

$$T_c = T_o + A_g + CG + A_z + A_l \qquad \text{(H1)}$$

where T_c is the corrected temperature in K^o x 10, A_g is a temperature dependent (grayshade) correction in K^o x 10, C is a multiplication factor for adjustment convenience, G is the equivalent of T_o but expressed in a grayshade, A_z is a zenith angle dependent correction in K^o x 10, and A_l is a look angle dependent correction in K^o x 10.

(b) The critical term in equation H1 is A_g which provides the largest correction. A_g was derived by correlating infrared and surface temperature for known clear areas. A simple scatter diagram and a graphically constructed curve (Figure H1) provides the A_g correction for a particular satellite. Figure H2 shows an actual bias curve. The significance of A_g is its response to not only water vapor attenuation, but the many systematic errors described previously for infrared and surface data.

(c) While A_g provides the basic correction, the remaining terms permit explicit correction as functions of the local gridpoint's zenith angle (measured from vertical to sun) and look angle (measured from satellite subpoint to the gridpoint). The coefficient is arbitrarily selected to permit manual manipulation of the correction equation. Different corrections can be selectively specified depending on satellite, hemisphere, day or night, and water or land.

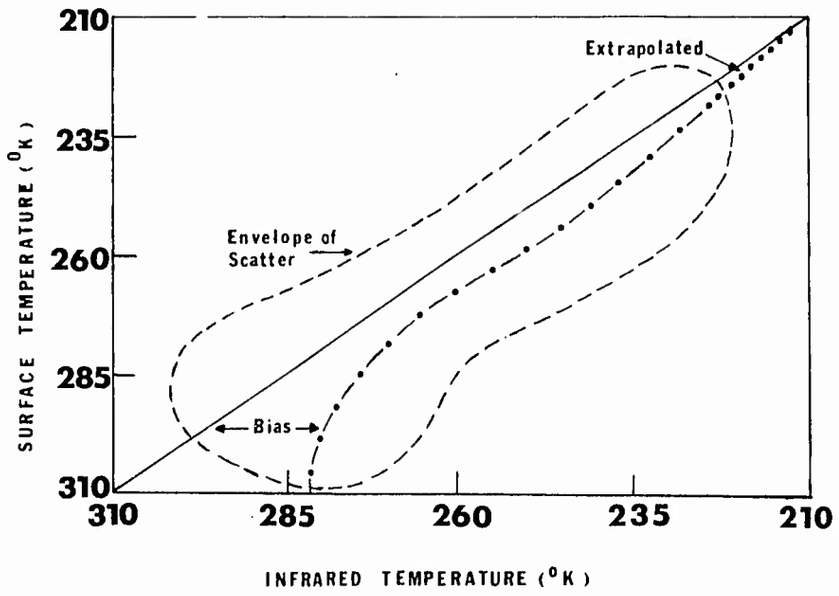

Figure H1. Origin of the infrared bias correction curve. The data count used in constructing this typical scatter diagram was over 100,000 correlated points.

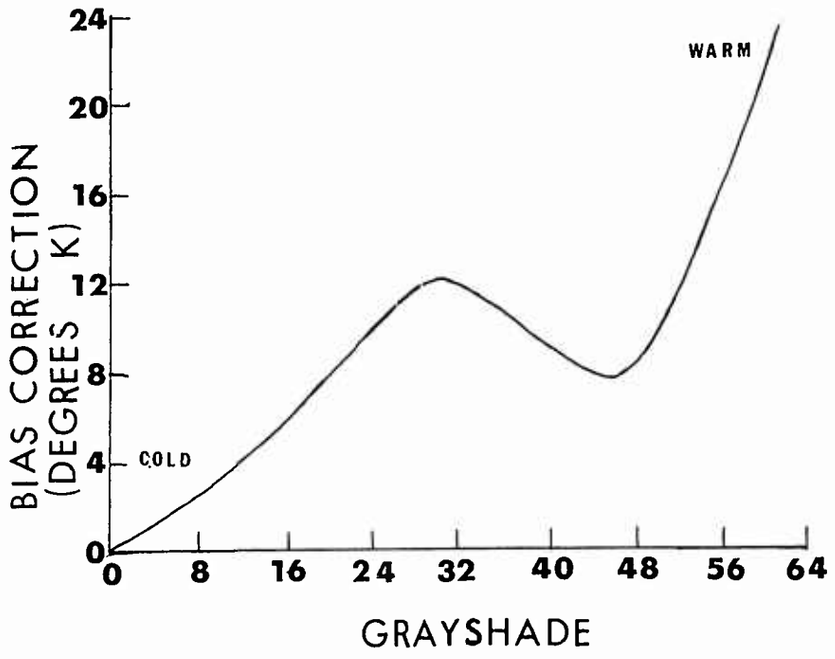

Figure H2. A typical bias correction curve used by the infrared data processor and extracted from the scatter diagram shown in Figure H1. The source of the dip at grayshade 48 is unexplained, but is thought to be associated with the freezing point and phase change of water.

APPENDIX I

DETERMINATION OF CLOUD TYPES FROM INFRARED AND VISUAL SATELLITE IMAGERY

21. SATELLITE DATA CLOUD TYPING

The cloud typing of satellite imagery in the 3DNEPH satellite data processor uses an empirical set of weighted equations and thresholds which are functions of visual and infrared grayshade and variability. The technique described here has been in use since 1976 and provided 80 percent or better reliability in development tests against corresponding cloud types obtained from surface reports.

21.1 Classification scheme. The cloud typing algorithms distinguish between stratiform (smooth texture) and cumuliform (rough texture) clouds and between low, middle, and high clouds. This enables the 3DNEPH to identify the major generic cloud types as shown in Table I1.

TABLE I1. GENERIC CLOUD TYPES IDENTIFIABLE BY THE 3DNEPH SATELLITE PROCESSOR. TYPES ENCLOSED IN PARENTHESIS CANNOT BE DIFFERENTIATED.

	Low	Middle	High
Stratiform	St	(AS/NS)	Cs
Cumuliform	Sc Cu Cb	Ac	(Ci/Cc)

21.2 Algorithm development. The cloud typing algorithms were developed from intuitive visual and infrared relationships as shown in Figures I1 and I2. Infrared grayshade determines the height of clouds and visual grayshade contributes to the stratiform - cumuliform distinction. Variability (Figure I1) is primarily an input for the stratiform/cumuliform distinction. Figures I1 and I2 were subjectively constructed after examination of many numerical grayshade/variability displays overlayed with corresponding satellite imagery and surface data. Operational algorithms were constructed from these figures and subsequently modified to achieve optimum results.

21.3 Procedure. Figure I3 shows the overall input and output of the cloud typing module. Tuning factors consist of weight factors and grayshade/variability thresholds. These were established during development and were used to fine tune the cloud type output to agree with surface reported cloud types. Cloud typing depends on the availability of data. When visual and infrared data are at hand, no restrictions are placed on cloud types. If only visual data are available, only cumulonimbus clouds are typed; and if only infrared data are available, low clouds are excluded from typing. A "missing" is stored in the data base when there is insufficient data of either type available. The cloud typing algorithms reflect the relationships shown in Figures I1 and I2, but certain tendencies can be further amplified:

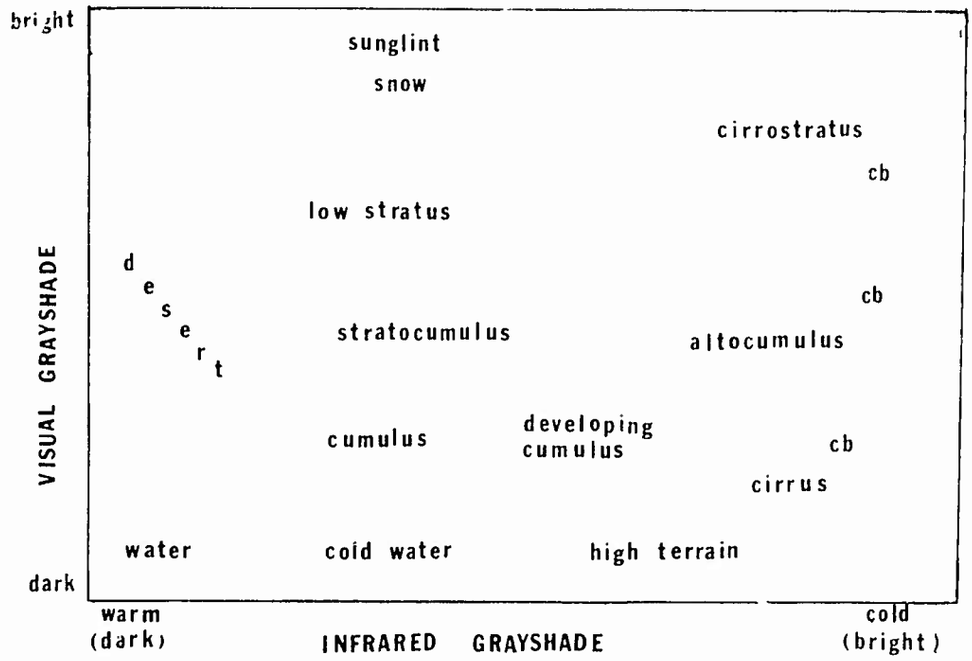

Figure I1. Graphical display of the relationship between infrared and visual grayshade for the typing of clouds.

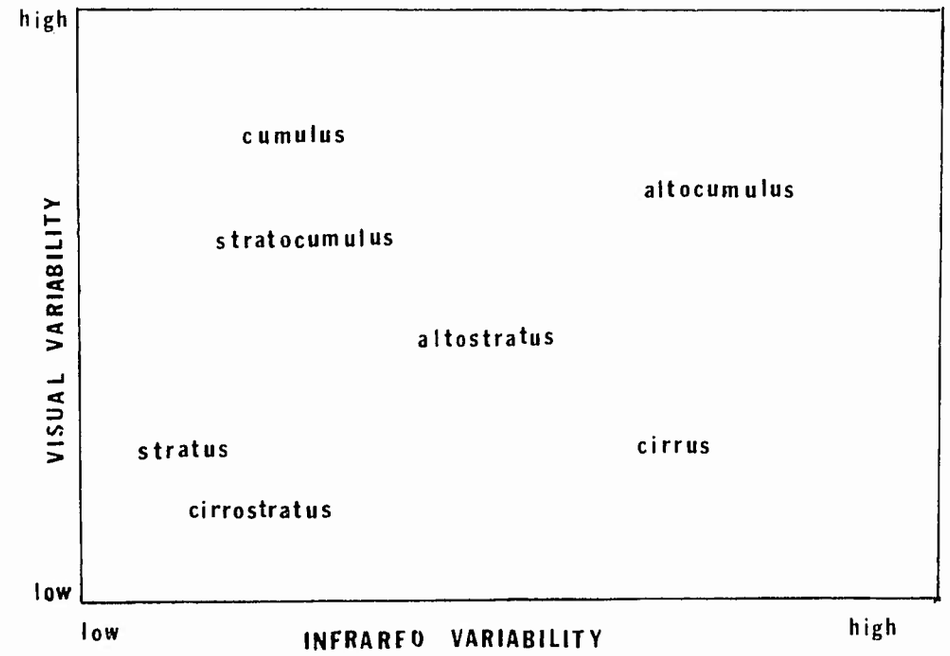

Figure I2. Graphical display of the relationship between infrared and visual variability for the typing of clouds.

(a) Cumulus clouds are more easily detected in infrared data than stratus.
(b) Middle clouds are easily typed with both visual and infrared data.
(c) High clouds are easily detected by infrared data.
(d) Thin clouds (particularly cirrus) are difficult or impossible to detect.
(e) It is difficult to distinguish between cirrostratus and large cumulonimbus tops.

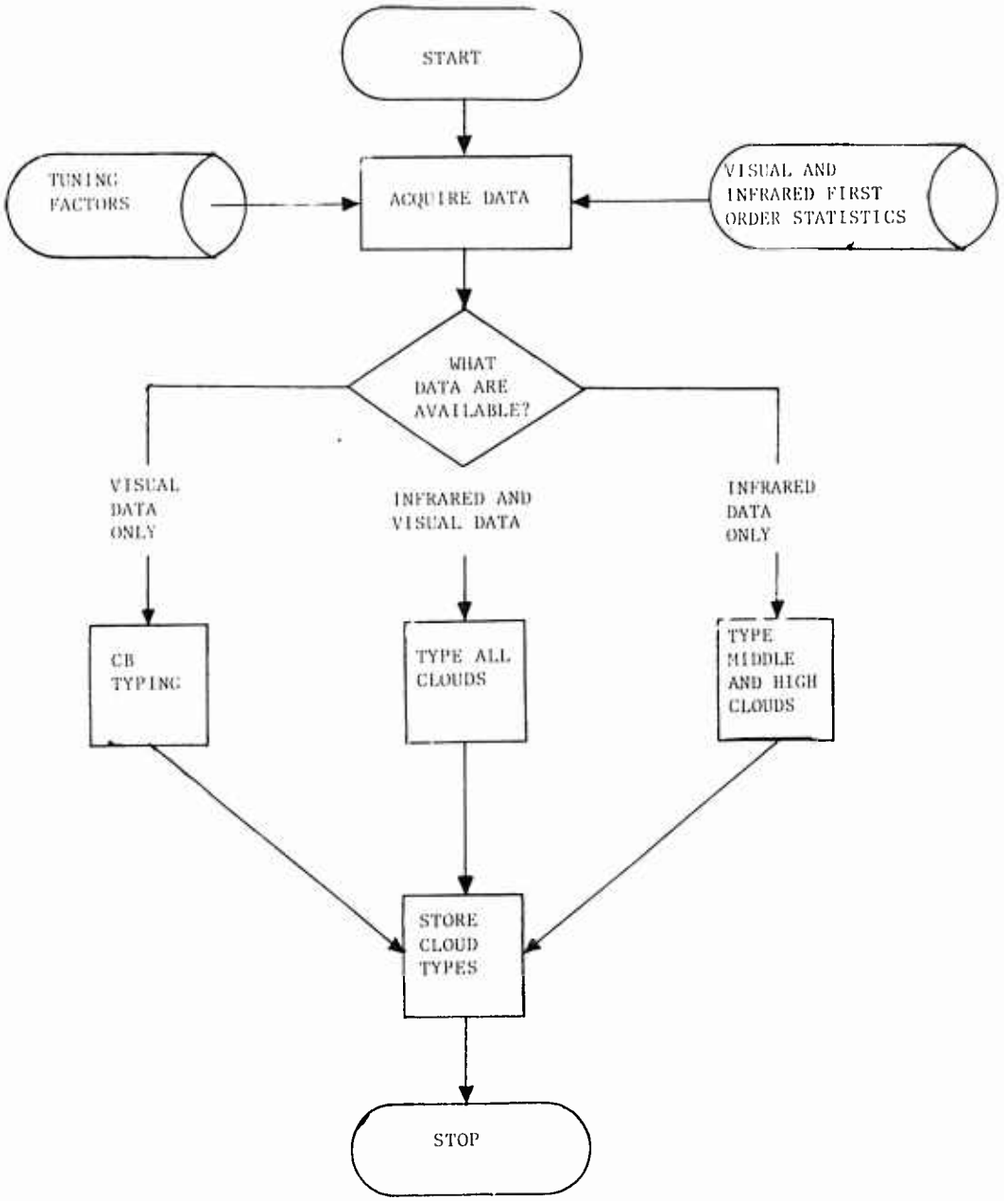

Figure I3. Flow chart of the 3DNEPH cloud typing module showing the decisions relating to data availability.